Simulating irrigation requirements in peatland ecosystems:

Optimizing agricultural water needs in an ecologically sensitive environment

by

Meaghan Kilmartin

Department of Bioresource Engineering

McGill University, Montreal

December 2023

A thesis submitted to McGill University in partial fulfillment of the requirements for the degree of Master of Science

Abstract

Master of Science Meaghan Kilmartin **Bioresource Engineering**

The use of modelling tools to predict the daily soil water balance has become widespread in the development of irrigation management strategies. These predictions provide insights at the field scale and aid regional water resource management. This study is focused on the water needs of irrigators in Lanoraie, Quebec. In this region, there are competing water demands between the irrigated crops, primarily potato, other vegetables, and berries, and an ecologically-sensitive wetland complex. The growing season is expected to be increasingly warmer, drier, and more variable due to climate change. Thus, to balance the agricultural and ecological water needs of the region, it is necessary to optimize irrigation requirements to achieve highest crop yields. This study estimated the net irrigation requirements of the major irrigated crops and soil types in Lanoraie for the historical dry, average, and wet years using the AquaCrop model. AquaCrop was next used to predict the effect of climate change on irrigation requirements. Three irrigation treatments were investigated, comprising a management allowable depletion (MAD) of 20%, 35%, and 50% of plant available water (AW), for potato, squash, strawberry, and cranberry cultivated on sandy and sandy loam soils. The resulting crop water needs were used to present potential water supply scenarios.

The AquaCrop models were calibrated to field measurements of soil moisture in 2022. The model simulated soil moisture under potato with the highest agreement to field sensor measurements (Wilmott index of 0.91). Lowest model efficiency and weaker agreement were observed for the simulation of soil water content in the strawberry field (Wilmott index of 0.65), attributed to atypical growth cycles due to the fact that production was not for the fresh berry market, but for plant distribution. Statistical analysis revealed that both the historical weather (wet, average, or dry growing season) and irrigation treatment (20%, 35%, or 50% depletion of AW) had a significant effect on net irrigation requirement. The MAD of 50% AW demonstrated significant water-saving potential, particularly in dry years where crop-water demand was significantly higher. Under the 50% MAD, the mean net irrigation requirement for potato, squash, strawberry, and cranberry crops in historical dry years were 265 mm, 151 mm, 285 mm, and 161 mm, respectively.

Next, the models were used to predict the impact of climate change on irrigation requirements to the periods 2050 and 2080. The irrigation requirement for potato is predicted to significantly increase by the 2080s compared to the historical period (1997-2021), under the CMIP6 SSP5-8.5 high emissions scenario. Projected irrigation requirements for the other crops remained fairly stable. Irrigation treatment significantly impacted the net irrigation requirement, with an MAD set at 50% AW significantly reducing irrigation requirements across all climate periods.

Finally, the gross water needs of each crop were mapped over the respective field areas and combined into water supply units. The peak volumetric water demand for the month of July was determined in each of the five proposed irrigation sectors of the region. An irrigation pipeline system was proposed to convey water to the five irrigation sectors. Assuming PVC pipe laid on a slope of 0.4%, potential diameters of 67 cm, 82 cm, 65 cm, 75 cm, and 84 cm were calculated for the St-Joseph, St-Thomas, St-Henri, Lavaltrie-Lanoraie, and St-Paul-Lavaltrie-L'Assomption irrigation sectors. A detailed engineering study, as well as a cost-benefit analysis are recommended to determine the optimum pipeline design.

Résumé

Maîtrise en Science Meaghan Kilmartin **Génie des bioressources**

L'utilisation d'outils de modélisation pour prévoir le bilan hydrique journalier du sol s'est généralisée dans le développement de stratégies de gestion de l'irrigation. Ces prévisions fournissent des informations à l'échelle du terrain et facilitent la gestion des ressources en eau au niveau régional. Cette étude se concentre sur les besoins en eau des irrigants de Lanoraie, au Québec. Dans cette région, il existe des demandes d'eau concurrentes entre les cultures irriguées, principalement la pomme de terre, d'autres légumes et les baies, et un complexe de zones humides écologiquement sensibles. La saison de croissance deviendra plus chaude, sèche et variable en raison du changement climatique. Ainsi, pour équilibrer les besoins en eau agricoles et écologiques de la région, il est nécessaire d'optimiser les besoins en irrigation afin d'obtenir les meilleurs rendements. Cette étude a estimé les besoins nets en irrigation des principales cultures irriguées et des principaux types de sol à Lanoraie pour les années historiques sèches, moyennes et humides à l'aide du modèle AquaCrop. AquaCrop a ensuite été utilisé pour prédire l'effet du changement climatique sur les besoins en irrigation. Trois traitements d'irrigation ont été étudiés, comprenant un épuisement admissible de 20 %, 35 % et 50 % de l'eau disponible pour les plantes, pour la pomme de terre, la courge, la fraise et la canneberge cultivées sur des sols sableux et de sable loameux. Les besoins en eau des cultures qui en résultent ont été utilisés pour présenter des scénarios potentiels d'approvisionnement en eau.

Les modèles AquaCrop ont été calibrés sur des mesures de terrain de l'humidité du sol en 2022. Le modèle a simulé l'humidité du sol sous la pomme de terre avec la plus grande concordance avec les mesures des capteurs sur le terrain (indice de Wilmott de 0,91). L'efficacité la plus faible du modèle et une corrélation plus faible ont été observées pour la simulation de la teneur en eau du sol dans le champ de fraises (indice de Wilmott de 0,65), ce qui a été attribué à des cycles de croissance atypiques dus au fait que la production n'était pas destinée au marché des baies fraîches, mais à la distribution des plantes. L'analyse statistique a révélé que les conditions météorologiques historiques (saison de croissance humide, moyenne ou sèche) et le traitement d'irrigation (épuisement de 20 %, 35 % ou 50 % de la FE) ont eu un effet significatif sur les besoins nets en irrigation. L'épuisement de 50 % a démontré un potentiel d'économie d'eau significatif, en particulier au cours des années sèches où la demande en eau des cultures était significativement

plus élevée. Avec un traitement de 50 %, les besoins nets moyens en irrigation pour les pommes de terre, les courges, les fraises et les canneberges au cours des années sèches historiques étaient respectivement de 265 mm, 151 mm, 285 mm et 161 mm.

Ensuite, les modèles ont été utilisés pour prévoir l'impact du changement climatique sur les besoins en irrigation pour les périodes 2050 et 2080. Les besoins en irrigation pour la pomme de terre devraient augmenter de manière significative d'ici les années 2080 par rapport à la période historique (1997-2021), dans le cadre du scénario CMIP6 SSP5-8.5 à fortes émissions. Les besoins d'irrigation prévus pour les autres cultures sont restés relativement stables. Le traitement de l'irrigation a eu un impact significatif sur le besoin net d'irrigation, avec un épuisement maximal fixé à 50 % réduisant de manière significative les besoins d'irrigation à travers toutes les périodes climatiques.

Enfin, les besoins bruts en eau de chaque culture ont été cartographiés sur les superficies respectives des champs et combinés en unités d'approvisionnement en eau. La demande volumétrique maximale en eau pour le mois de juillet a été déterminée dans chacun des cinq secteurs d'irrigation proposés dans la région. Un système de conduites d'irrigation a été proposé pour acheminer l'eau vers les cinq secteurs d'irrigation. En supposant que les tuyaux en PVC soient posés sur une pente de 0,4 %, des diamètres potentiels de 67 cm, 82 cm, 65 cm, 75 cm et 84 cm ont été calculés pour les secteurs d'irrigation de St-Joseph, St-Thomas, St-Henri, Lavaltrie-Lanoraie et St-Paul-Lavaltrie-L'Assomption. Une étude technique détaillée ainsi qu'une analyse coûts-bénéfices sont recommandées afin de déterminer la conception optimale du pipeline.

Acknowledgements

I would like to express my sincere thanks and gratitude to my supervisor, Dr. Chandra A. Madramootoo for his support, guidance, and patience throughout my graduate studies. I am grateful for the opportunity to contribute to this project, as well as the occasions that he provided to present my research at national conferences and to the students of Macdonald Campus. His diligent supervision and wealth of knowledge encouraged me to strive for excellence. I express gratitude to the Mitacs Acceleration program and UPA de Lanaudière for the financial support of this research.

I extend my heartfelt thanks to all the members of Water Innovation Lab at McGill University, for their continuous support and motivation, as well as their helpful insights along the way. Thank you, Aidan De Sena, Calista Brown, Farhan Ahmad, Guia Marie Mortel, Miranda Xiao, Naresh Arumugagounder Thangaraju, Sushree Dash, Shane Sankar, and Shirley Mongeau, you have all had a positive effect on my experience. I am indebted to Farhan, Miranda, and Naresh for their gracious assistance and pleasant companionship during field visits, data collection, and laboratory analyses. Naresh's indispensable contribution, extending from sensor installation to statistical analysis, has been a guiding light and a source of calm amidst my inquiries. His support went beyond the research realm, providing unwavering encouragement and maintaining faith in my abilities during moments of self-doubt. The successful completion of this thesis would not have been possible without his dedicated mentorship and friendship.

I am also thankful to each of the members of the Scelaneau project, whose advice and insights significantly contributed to this work. Additionally, I appreciate the cooperation of the farmers who generously allowed me to collect data from their fields and provided key information and expertise. This research would not have been possible without the collective support and collaboration of these individuals and groups.

Finally, I would like to thank my family and friends for their unwavering support throughout the arduous journey of completing this thesis. Their endless love, encouragement and understanding provided the foundation that allowed me to concurrently pursue this degree alongside my other personal and professional aspirations.

Contribution of Authors

Meaghan Kilmartin is the principal author of this work, which was supervised by Dr. Chandra A. Madramootoo, Distinguished James McGill Professor, Department of Bioresource Engineering, McGill University, Sainte-Anne-de-Bellevue, Quebec, Canada. The objectives and scope of the study were outlined by Madramootoo, in consultation with the Scelaneau project members. Kilmartin conducted the field data collection, model calibration, simulations, relevant statistical and GIS analyses, and wrote the thesis chapters. Professor Madramootoo supervised the study and provided guidance on various aspects of the research. He reviewed the thesis and provided constructive recommendations.

Table of Contents

List of Figures

List of Tables

List of abbreviations

AAFC	Agriculture and Agri-food Canada
APCQ	Association des Producteurs de Canneberges du Québec
ANOVA	One-way analysis of variance
ASTM	American Society for Testing and Materials
AW	Available water
B	Total above ground biomass
BCCA	Bias corrected constructed analogs
CC_o	Initial canopy cover
CC_{max}	Maximum canopy cover
CMIP	Climate Model Intercomparison Project
CN	Curve number
CO_2	Carbon dioxide
CSSC	Canadian System of Soil Classification
CWR	Crop water requirement
ECCC	Environment and Climate Change Canada
EF	Nash-Sutcliffe model efficiency coefficient
ET	Evapotranspiration
ETc	Crop evapotranspiration
ETo	Reference evapotranspiration
FADQ	La Financière Agricole du Québec
FAO	Food and Agricultural Organisation
FC	Field capacity
GCM	Global climate model
GLM	General linear model
GIS	Geographic information system
ha	Hectare
HI_o	Reference harvest index
IPCC	Intergovernmental Panel on Climate Change
IRDA	Institut de recherche et de développement en agroenvironnement
K_c	Crop coefficient

kPa	Kilo Pascals
k_{sat}	Saturated hydraulic conductivity
MAPAQ	Ministère de l'Agriculture, des Pêcheries et de l'Alimentation du Québec
MELCCFP	Ministère de l'Environnement, de la Lutte contre les Changements Climatiques, de la Faune et des Parcs
NASA	National Aeronautics and Space Administration
NRMSE	Normalized root mean square error
OMAFRA	Ontario Ministry of Agricultural, Food and Rural Affairs
POWER	Prediction of Worldwide Energy Resource Project
p	Probability
P	Precipitation
PM	Penman-Monteith
PWP	Permanent wilting point
QDM	Quantile Delta Mapping
RMSE	Root mean square error
SMP	Soil matric potential
SSP	Shared socio-economic pathway
SWC	Soil water content
SWCC	Soil water characteristic curve
TAW	Total available water
TDR	Time domain reflectometry
T_{max}	Maximum temperature
T_{mean}	Mean temperature
T_{min}	Minimum temperature
Tr	Transpiration
UPA	L'union des producteurs agricoles de Lanaudière
UQAM	Université du Québec à Montréal
USDA	United States Department of Agriculture
VWC	Volumetric water content
WP_{ET}	Water productivity based on evapotranspiration

1. Introduction

In many dry regions of the world, water is the major factor limiting agricultural production. The changing weather and climate, increasing population, and groundwater depletion are all factors that exert pressure on limited water supplies (Kisekka et al., 2017). Since agricultural production is a major consumer of water, it is important to use water more efficiently to ensure sustainable crop production (FAO, 2021). Interest in the issue of water limiting agricultural production has been very high in areas with very limited rainfall in the arid and semi-arid zones of the world, where without irrigation, production is almost negligible (Salman, 2021). However, in today's changing climate, optimizing crop water productivity is increasingly important to the world's semi-humid and humid zones as well. There exists a growing uncertainty and variability of rainfall amount and distribution. This is augmenting concerns for farmers, experts, and governments regarding water allocation and the timing and quantities of supplemental irrigation (e.g. Anapalli et al., 2016; Danielescu et al., 2022; Paz et al., 2007). Meanwhile, maximizing the economic yield through optimizing irrigation practices is paramount to feeding a growing global population (Bhatia et al., 2008; Licker et al., 2010; van Ittersum and Cassman, 2013). Predicting crop-water requirements to improve water use efficiency is thus essential in all climatic regions.

In addition to climate change, water resources are impacted by conflicts between different users, such as between the agricultural sector and wetland services (Mirzaei and Zibaei, 2021; Zou et al., 2018). Expanding irrigated areas or intensifying irrigation to increase crop production may increase the rate of environmental degradation (Kang et al., 2009). This study is focused on an agricultural region located in Lanoraie, Quebec, in which there are competing water demands between an ecologically sensitive wetland complex and the major irrigated crops. The major irrigated crops are potatoes, other vegetables, and small fruit, which compose a large portion of the total cropped area of Lanoraie. Water for irrigation is mainly sourced from excavated reservoirs and ponds adjacent to streams, as well as by 12 small dams operated by the municipalities. Irrigators are investing in more efficient and mechanized irrigation technologies. However, they are increasingly conscious of limited water resources and concerned about meeting future market demands. The irrigated region is near a peatland known as the Lanoraie peatland complex. Peatlands are valuable terrestrial wetland ecosystems that supply and filter water, contribute to biodiversity, mitigate flooding, recycle nutrients, store and sequester carbon, and provide habitat

to many endangered and threatened species (Mitsch and Gosselink, 2015). However, wetlands are vulnerable to anthropogenic disturbances, such as urban expansion, agriculture, and climate change (IUCN, 2017). Environmental degradation is prevalent in the Lanoraie peatland complex, evident from tree encroachment and water table lowering. Meanwhile, the growing season weather conditions are increasingly drier and more variable due to climate change, with 2021 being the driest and second-warmest growing season in the last 25 years. Therefore, irrigation water supply must not be at the detriment of the water levels and water quality of the wetlands. Balancing the agricultural and ecological water needs of the region, and reducing its vulnerability to future climate change, requires integrated and sustainable water resource management.

There are a plethora of methods and devices to estimate crop water requirements and water stress, often integrating combined remote sensing and ground data into crop and soil water models (Cahn and Johnson, 2017; Corbari et al., 2019; Pereira et al., 2020; Tolomio and Casa, 2020). Crop models have a wide range of applications in agricultural water management, from on-farm irrigation scheduling to regional assessments and planning. AquaCrop is a water-driven model developed by the FAO based on crop yield response to water that is particularly suited for water-limited conditions. It requires a relatively low number of input parameters and is well known for its balance of simplicity, robustness, and accuracy (Steduto et al., 2009; Vanuytrecht et al., 2014). AquaCrop can be also applied to a variety of crops (e.g. Battilani et al., 2014; Geerts et al., 2009; Stricevic et al., 2011), which has led to its widespread use around the world. Numerous studies have shown the many applications of the model, such as optimizing irrigation (Paware et al., 2017) and field management strategies (Abrha et al., 2012), and predicting the impacts of climate change on crop yield (Khordadi et el., 2019). Furthermore, recent studies have demonstrated the potential of upscaling crop modeling results using appropriate GIS tools (e.g. Alaya et al., 2019; Guo et al., 2021; Han et al., 2020). This study considers the spatial heterogeneity of crop and soil type to assess the irrigation requirements of the Lanoraie study area, through the combined use of the AquaCrop V7.1 crop water productivity model and ArcMap V10.8 ArcGIS® software by Esri.

1.1 Scelaneau project

The research reported in this thesis was funded under the Mitacs Acceleration program and is part of the SCELANEAU project funded by the Ministère de l'Agriculture, des Pêcheries et de l'Alimentation du Québec (MAPAQ) in collaboration with L'UPA, IRDA, and UQAM. The SCELANEAU project aims to evaluate integrated and sustainable water resource management

scenarios in the Lanoraie peatland complex. The intent of the project is to develop irrigation water supply management scenarios to meet the agricultural demands in the region, without degrading the hydrological functions of the surrounding wetland complex.

1.2 Research objectives

The main objective of this study was to estimate the current and future irrigation water requirements for the agriculture-wetland complex of Lanoraie and propose a water supply scenario.

The specific objectives were to:

a) Evaluate the ability of AquaCrop to simulate soil moisture content for the major irrigated crops in Lanoraie for water resource management and planning.
b) Estimate the net irrigation requirements for the historical dry, average, and wet years of the study area, for the major irrigated crops, soil types, and irrigation methods used.
c) Predict the impact of climate change on the future irrigation requirements of the major irrigated crops.
d) Map the gross irrigation requirements to propose possible pipeline diameters of an irrigation supply system.

1.3 Scope

The research area envelopes the Lanoraie peatland complex and surrounding agriculture. It spans seven municipalities, including Lanoraie, Lavaltrie, Saint-Thomas, and L'Assomption. It borders the Saint-Lawrence River, and five rivers flow through the complex. The extent of the study area comprises 5 main watersheds, 12 000 ha of cropland, and 7 600 ha of wetland, and covers a total area of 32 400 ha. This study is focused on the irrigated cropland of four major crop groups: potatoes; vegetables and gourds; cranberries; and other berries and small fruits. The field data collected is limited to four farms in the study area representing the primary crop groups and soil types of the Lanoraie region. The simulated results of the research are extrapolated to the entire study area to estimate the total irrigation requirements and support water resource management in the Lanoraie agricultural-peatland complex.

1.4 Thesis outline

This thesis is organized into chapters to meet the above-mentioned objectives. The chapters are outlined as follows:

Chapter 1	Introduction, Objectives, Scope
Chapter 2	Literature review on the impacts of agriculture on wetlands, land use and irrigation in Quebec, crop water requirements, soil water content, crop characteristics, crop water modelling, and the impact of climate change on agriculture.
Chapter 3	Detailed Methodology
Chapter 4	Results and Discussion
Chapter 5	Conclusion and Recommendations

2. Literature Review

2.1 Impacts of agriculture on wetlands

2.1.1. Peatland Ecosystems

Peatlands are terrestrial wetland ecosystems characterized by a positive water balance and net peat accumulation (Mitsch and Gosselink, 2015). Peatlands perform valuable ecosystem functions and provide many benefits in the form of ecosystem services. They supply and filter water, contribute to biodiversity, mitigate flooding, recycle nutrients, and provide habitat to many endangered and threatened species (Brander et al., 2013; Hefting et al., 2013; Mitsch and Gosselink, 2015). Arguably, in the current climate crisis, the most notable ecosystem service provided by peatlands is their ability to store and sequester large quantities of carbon due to peat accumulation (Yu, 2012; Mitsch and Gosselink, 2015). Although peatlands only occupy 3% the global land area (Xu et al., 2018), they store approximately 600 Gt of carbon, equivalent to one third of the global soil carbon stocks (Post et al., 1982; Yu, 2012). However, if the peat deposits are disturbed, that carbon can be released and significantly contribute to atmospheric CO_2 (Hemes et al., 2019; Mitsch and Gosselink, 2015).

Peatlands are often degraded due to anthropogenic activities, such as agriculture. Over the last few hundred years, it is estimated that more than half of the world's wetlands have been lost because of changes in land use (Davidson, 2014; Mitsch and Gosselink, 2015; Zedler and Kercher, 2005). The use wetlands for agriculture is driven by economic and social incentives, to meet the demands for food, fiber, and fuel production (Nguyen et al., 2017; Wood and Halsema, 2008). Furthermore, the conversion of wetlands to agricultural land is often facilitated by government policies and subsidies and a lack of effective regulatory protections (Finlayson et al., 2005). Wetland drainage in Canada has been incited by private benefits occurring from tax incentives and subsidies; While these programs satisfy public and private policy over the short-term, it can be at the expense of both nature and the economy over the long-term (Finlayson et al., 2005). Many studies have highlighted the competition for water resources between agriculture and wetlands (Jia et al., 2013; Joy and Paranjape, 2007; Zou et al., 2018). There are growing concerns for wetland ecosystems and restoration, and increased awareness of the beneficial services they provide (Chimner et al., 2017; Finlayson et al., 2005; Zedler and Kercher, 2005). Research has shown that the economic valuation of natural wetlands is greater than the profits earned from the conversion or exploitation of wetlands (de Groot et al., 2012; ten Brink et al., 2013).

2.1.2. In situ/direct impacts of agriculture on peatlands

The Millennium Ecosystem Assessment (Finlayson et al., 2005) reports with high certainty that conversion or drainage for agricultural development has been the main cause of global loss of inland wetlands. In the FAO's report on agriculture wetland interactions, they define *in situ* interactions as those where there is a direct agricultural intervention in a wetland (Wood and Halsema, 2008). For peatlands, *in situ* or direct intervention of agriculture includes peat harvesting (Daigle and Gautreau-Daigle, 2001), as well as drainage and conversion for crop cultivation or pasture (Mitsch and Gosselink, 2015; Sica et al., 2016; Verhoeven et al., 2006). Organic matter production in peatlands coupled with low decomposition rates due to the waterlogged conditions, results in a net accumulation of peat and a carbon sink; However, the oxidation of peat, either from direct burning as fuel or drying of a peatland, releases important sources of carbon, contributing to atmospheric carbon dioxide (CO_2) levels (Hemes et al., 2019; Mitsch and Gosselink, 2015). Disturbed peatlands are known to emit more than 10% of global CO_2 emissions (Lunt et al., 2010). Efforts to restore degraded agricultural peat soils showed that it can take restored wetlands over a century to become net sinks from atmospheric greenhouse gases (Hemes et al., 2019). Thus, emphasizing the need to conserve existing peatlands. Furthermore, draining peatlands for agriculture degrades the soil and water resources they depend on, altering ecosystem functions and therefore the services they provide. It results in land subsidence, decreased biodiversity, habitat loss, conditions that favor invasive species, water quality degradation, and increased flood risk (Chimner et al., 2017; Millennium Ecosystem Assessment, 2005; Mitsch and Gosselink, 2015).

2.1.3. Ex situ/indirect impacts of agriculture on peatland ecosystems

Wetlands are also affected by surrounding or *ex situ* agricultural activities, which can alter ecosystem functions and structure (Wood and Halsema, 2008). They are vulnerable to the intensification of agriculture, which can be related to water withdrawals for irrigation, water diversion by dams, soil erosion and sedimentation, and runoff of excess nutrients or pesticides from cropland (Finlayson et al., 2005; Wood and Halsema, 2008). In turn, these interactions have environmental impacts, such as changes in water table levels and streamflow, as well as decreased water quality and biodiversity (Wood and Halsema, 2008).

Drainage is one of the main indirect disturbances to peatlands in an agricultural landscape. Many articles report bog or fen drainage as a result of surrounding land use (Hurkuck et al., 2015; Pellerin et al., 2016; Favreau et al., 2019; Pinceloup et al., 2020). In addition, since water is the

main nutrient solvent and transport agent in wetlands, nutrient cycling in a wetland also depends on hydrology (Mitsch and Gosselink, 2015). Nitrogen inputs have shown to alter vegetation composition and growth, and significantly impact carbon loss in bogs due to higher rates of decomposition (Bubier et al., 2007; Currey et al., 2009; Bragazza et al., 2012).

In disturbed peatlands, the combined stresses of altered hydrologic regime and nutrient inputs may impose vegetation changes (McClymont et al., 2008; Navrátilová et al., 2017). Several studies have shown severe and rapid species composition changes due to anthropogenic disturbances on water and nutrient availability (Pellerin and Lavoie, 2003; Kapfer et al., 2011; Talbot et al., 2014). As opposed to their natural flooded state that inhibits aerobic respiration, peat soils that are drained expose the organic-rich soils to oxidation, releasing large amounts of CO_2 emissions (Hemes et al., 2019). Restoration studies show that maintenance of the high water table year round could significantly reduce carbon losses and potentially allow the return of native wetland species (Knox et al., 2015; Peacock et al., 2014). Therefore, monitoring and conservation techniques are increasingly important for retaining peat carbon stocks disturbed by agriculture.

2.2 Land use and irrigation in Quebec

Quebec is the largest province in Canada and holds 3% of the world's renewable freshwater reserves (MELCCFP, 2023). A large proportion of this resource is in the North, while the majority of the population is concentrated in the south. The province's land is largely covered by forests, wetlands, and water bodies, with the urban and agricultural lands located in south-western Quebec (AAFC, 2015). The south-western region has a humid continental climate, with a historical mean annual precipitation between 750 to 1000 mm of combined snow and rainfall and a reference evapotranspiration between 480 and 740 mm (Nand and Qi, 2023).

Quebec's agricultural expanse covers 3.45 million hectares, with field crops occupying 54.5%, hay 40.5%, vegetables 2%, and fruit crops 2.1% (Statistics Canada, 2017). The majority of field crops, such as corn and soybean, depend on growing-season rainfall, while irrigation is primarily for vegetable and fruit crops (Elmi et al., 2010; Gallichand et al., 1991). Alterations in rainfall patterns and depth, and rising temperatures can limit rainfed crop production. In the past decade, suboptimal spatial and temporal distribution of growing-season rainfall negatively impacted field crop yields in the region (AAFC, 2020). Although the total precipitation over the growing season is sufficient for overall crop development, the region experiences frequent short drought events in May, June, July, and August. These periods are problematic for shallow root zone crops, notably

vegetables that are susceptible to soil moisture deficits, which can result in significant crop yield reductions (Gallichand et al., 1991). Consequently, irrigation is commonly employed for these crops to attain their potential yields and generate higher revenues. For instance, potatoes are shallow rooted and sensitive to droughts. Recently, enhanced marketable yields of potatoes, leading to increased net profits, have been realized through the implementation of supplementary irrigation during dry periods (Létourneau and Caron, 2019; Matteau, 2019). Consequently, farmers have embraced investments in center-pivot sprinkler irrigation, drip irrigation, and sub-irrigation systems specifically for potato cultivation, reaping desired advantages in response to the growing demand for marketable potatoes. Similar irrigation management is essential to achieve potential yield for drought-sensitive fruit crops, such as strawberry and cranberry (Létourneau and Caron, 2019; Pelletier et al., 2015a). Between 2010 and 2020, the area of irrigated land has progressively risen from 14,340 to 20,790 hectares (Statistics Canada, 2023). The economic viability of irrigation in south-western Quebec is particularly evident for high value crops due to their greater returns (Nand and Qi, 2023).

In numerous catchments with a concentration of irrigated agriculture, the increasing water demand across various sectors combined with diminished allocations to fulfill environmental flow requirements has led to less dependable and more costly irrigation allocations. This predicament is aggravated in instances where irrigated agriculture is identified as the predominant contributor to environmental harm and excessive water extraction, particularly during the summer months when river and groundwater levels reach their lowest, coinciding with peak irrigation demands (Hedley et al., 2014).

In southern Quebec, particularly in the densely populated lowlands along the St. Lawrence River, there are conflicting interests between the preservation of natural environments and their conversion for other purposes (He et al., 2017). Urbanization, infrastructure expansion, and agricultural activities have contributed to land use changes and fragmentation (Paquette et al., 2003; Jean and Létourneau 2011). However, this region also boasts the highest biodiversity and the fertile agricultural land in Quebec, creating tensions among various stakeholders. Over the past four decades, the St. Lawrence River Lowlands have lost 45% of their wetlands, with the remaining 65% of the areas impacted by human activities (Joly et al., 2008). Despite these adverse effects, the conversion of wetlands into agricultural land persists in Quebec due to economic incentives and the absence of regulatory safeguards for wetlands.

2.2.1. Agricultural-wetland complex in Lanoraie, Quebec

Drainage and vegetation changes in ombrotrophic peatlands isolated in agricultural landscapes have been thoroughly studied in eastern Canada. While bogs are typically described as resilient ecosystems that undergo important composition changes over centuries or millenia (Gunnarsson et al., 2002), several studies have shown severe and rapid species composition changes due to anthropogenic disturbances on water and nutrient availability (Pellerin and Lavoie, 2003; Kapfer et al., 2011; Talbot et al., 2014).

In the Lanoraie wetland complex, which is part of a vast hydrosystem, the surface and groundwater are intensively used for irrigation and drinking water (Bourgault et al., 2014). Drainage in the region, along with other anthropogenic disturbances, negatively impacted peatland species composition (Tousignant et al., 2010). For example, human-induced drainage, eutrophication and a drier climatic conditions have been shown to intensify shrub and tree encroachment, inhibit *Shpagnum* growth, and enable the establishment of introduced and generalist species (Pellerin and Lavoie, 2003; Pasquet et al., 2015) Two large peatlands (1115 ha) isolated in the agricultural landscape showed a 35% floristic dissimilarity, a 280 ha increase in forest, and a 5-15 times greater abundance of non-peatland species than specialist bog species (Pasquet et al., 2015). Pellerin et al. (2016) revealed that the recent tree encroachment of the Lanoraie peatland complex was triggered by drying of the peat surface. Furthermore, the water table drawdown coincided with the onset of encroachment and the peak of surrounding agricultural activities. More recently, a study investigated the effects of tree encroachment on plant richness and diversity of bogs isolated in an intensive agricultural landscape in southern Quebec, including in Lanoraie (Favreau et al., 2019). The authors found biotic differentiation within sites due to the introduction of non-peatland species and shade-tolerant vascular plants. Such compositional changes are expected to increase the similarity between bog and upland vegetation, resulting in decreased regional diversity (Favreau et al., 2019). A subsequent study conducted in different bogs in the same area, by Pinceloup et al (2020), highlights the potential of the introduced terrestrial species to decrease species diversity at the regional scale (Olden, 2008; Pinceloup et al., 2020). The observed changes are likely due to a combination of regional drainage, nutrient enrichment, and climate warming (Pinceloup et al., 2020). Overall, the studies show evidence of water table drawdown, altered species composition, rapid vegetation succession, and loss of diversity.

The maintenance of a wetland's hydrological regime and its natural variability is essential to maintain its ecological characteristics, such as biodiversity, and the key regulatory and provisioning ecosystem services it provides to humans (Finlayson et al., 2005). Hydrological low flows are sensitive to increasing temperatures associated with various climate change scenarios (Marx et al., 2017). These impacts of climate change are also affected by other factors, such as land use. Thus, it is important to consider the combined effects of climate change and land use on water yield and flow characteristics for water resource management (Zhang et al., 2018). Assani et al. (2022) studied the spatio-temporal variability of seasonal daily minimum flows from 1930-2019, due to the impacts of climate, agriculture, and wetlands, in 17 watersheds in the Saint-Lawrence Lowlands of southern Quebec. They found that agricultural area was the main factor in the spatial variability of seasonal daily minimum flows. The increased runoff resulting from agricultural soils causes a significant decrease in the seasonal daily minimum flows in the spring, summer, and fall. (Assani et al., 2022). The loss and degradation of wetland ecosystems is expected to be exacerbated by climate change, which will in turn reduce their ability to mitigate impacts and provide ecosystem services (Finlayson et al., 2005).

2.3 Crop water requirements

While the essential role of water in crop production has been acknowledged since the inception of agricultural practices, the potential of greater yields through increased water application grew as new crops were introduced and farming became more market-oriented (Pereira and Allen, 1999). The concept of crop water requirements emerged with evidence of the correlation between yields and water application and gained importance with the initiation of large-scale engineering projects to establish water supply for new irrigation areas, necessitating precise estimation of required water volumes. Doorenbos and Pruitt (1977) defined crop water requirement (CWR) as the depth of water (mm) needed to meet the water loss through evapotranspiration from a disease-free crop, growing in large fields under non-restricting soil water and fertility, and achieving full production potential under the given growing environment. The CWR depends on the type of crop, the growing stage, and the climate (Battisti et al., 2018; Surendran et al., 2015).

For irrigated crops, the concept of CWR is complemented by the net irrigation requirement (I_{net}), representing the net depth of water needed to fully meet a specific crop's water needs, by accounting for the portion of CWR not fulfilled by rainfall, soil-water storage, and groundwater. In practical terms, I_{net} is converted to gross irrigation requirements, considering the efficiency of

the irrigation systems in use (Pereira and Alves, 2005). Thus, CWR is the basis of irrigation planning, scheduling, water delivery, and resource management (Pereira and Allen, 1999).

2.3.1. Climate

Climate is the most critical and variable factor determining the planet's distribution of primary ecosystem types (Zhou and Wang, 2000), and thus the crops that may be cultivated in each region. Climate can be considered as the overarching patterns of temperature, precipitation, humidity, wind, and radiation that characterize a region (Chen and Chen, 2013). However, many climate classification systems primarily rely on near-surface air temperature and precipitation as the key variables for characterizing energy and water balance, as exemplified by Thorthwaite (1948).

The climate of any location on Earth is characterized by significant variability across different time scales. Various climatic parameters exhibit distinct magnitudes of variation; for instance, hourly solar radiation fluctuates widely within a day, while average radiation remains relatively stable from year to year. Rainfall, among all weather parameters, stands out as the most variable across temporal scales, profoundly impacting agriculture (Salman et al., 2021). The distribution of rainfall at any location varies significantly with the season. Annual precipitation alone is not an effective indicator of the amount of water available for plant growth, as factors like evaporation, seasonal distribution, and soil water-holding capacity vary based on geographical location (Huffman et al., 2013). The major climatic factors affecting daily evapotranspiration, besides rainfall and temperature, are sunshine, humidity, and wind speed. Sunny environments with low humidity and high windspeeds exhibit greater daily evapotranspiration rates. The ratio of rainfall to evapotranspiration provides a general classification of climates: desert; arid; semi-arid; dry; sub-humid; humid; and cold (Spinoni et al., 2015).

In many dry regions of the world, water is the major factor limiting agricultural production, leading to crop failure during extended dry spells. Droughts, both predictable and unpredictable, pose significant challenges to various human activities, particularly agriculture and food security, Interest in the issue of water limiting agricultural production has been very high in areas with very limited rainfall in the arid and semi-arid zones of the world, where without irrigation, production is almost negligible. The scarcity of water in drought-prone regions is how the notion of using it efficiently emerged in water-limited agriculture (Hillel, 1990; Salman, 2021). While irrigation expansion was initially concentrated in arid regions, it has extended to humid areas to enhance crop production (Huffman et al., 2013). The changing weather and climate, increasing population,

and groundwater depletion are all factors that exert pressure on limited water supplies (Kisekka et al., 2017). Since agricultural production is a major consumer of water, it is important to use water more efficiently to ensure sustainable crop production (FAO, 2021). In today's climate crisis, optimizing crop water productivity is increasingly important to the world's semi-humid and humid zones as well.

2.3.2. Reference evapotranspiration

Defined separately, evaporation is the physical conversion of a liquid into a gas and transpiration is the evaporation of liquid water within a plant, occurring through the stomata and plant surfaces into the air. Evapotranspiration (ET) is the amalgamation of these processes through which water is transferred from vegetation and soil to the atmosphere, through both transpiration from plants and evaporation from the soil, from dew and intercepted water on plant surfaces (Jensen and Allen, 2016).

The rate of evapotranspiration of a reference crop (ETo) expresses the evaporative power of the atmosphere at a specific location and time (Allen et al., 1998) and therefore represents the climate-influenced component of the CWR. ETo is the rate at which water would be taken from the soil and plant surfaces if readily available. It is expressed as the rate of latent heat transfer per unit area or as the depth of water evaporated and transpired from a reference crop, such as grass (Jensen and Allen, 2016). Any efforts to enhance irrigation water use efficiency requires accurate estimates of ETo (Hanson, 1991).

There are a multitude of methods for estimating ETo. Physically based, analytical methods, such as lysimeters, the Bowen ratio, eddy covariance systems, and scintillometers require instrument installation across catchment areas and are often not economically feasible (Wanniarachchi and Sarukkalige, 2022). Various equations, including pan evaporation-based, temperature-based, radiation-based, mass transfer-based, and combination-type, have been developed for estimating ETo, with varied performances across different environments (Gocic and Trajkovic 2010). The pan evaporation method relies on field measurements of evaporation multiplied by the respective pan coefficient (Doorenbos and Pruitt, 1977; Huffman et al., 2013). Caution is recommended in interpreting pan evaporation data, due the significant disparities in energy balance between pans and various environmental conditions (Jensen and Allen, 2016). Weather data can support the use of empirical and mechanistic ETo models. The Baier–Roberston, Blaney–Criddle, Priestley–Taylor, and Hargreaves–Samani models have shown to provide

acceptable estimations of ETo when detailed meteorological data are limited or unavailable (Droogers and Allen, 2002; Maulé et al., 2006; Priestley and Taylor, 1972; Tabari et al., 2013). However, the FAO-56 Penman–Monteith (PM) energy-based equation is acknowledged as the sole method for determining ETo (Allen et al., 1998; Allen et al., 2006), consistently providing reliable ETo estimates in comparison to other methods (Cai et al., 2007). It is globally recommended as a universal standard method to calculate ETo and calibrate other ETo models due to its accuracy under various climatic conditions (Gao et al., 2017; Djaman et al., 2018; Zhao et al., 2019).

The FAO-56 PM equation for a daily time step is defined as follows for a grass reference crop (Allen et al., 1998; Pereira et al., 2005; Raes et al., 2009):

$$\mathrm{ETo} = \frac{0.408\Delta(R_n - G) + \gamma\frac{900}{T+273}u_2(e_s - e_a)}{\Delta + \gamma(1 + 0.34u_2)} \quad \textbf{(1)}$$

where R_n is the net radiation (MJ/m^2/day); G is the soil heat flux (MJ/m^2/day); T is the average daily temperature at 2 m height (°C); u_2 is the wind speed at 2 m height (m/s); e_s is the saturation vapor pressure (kPa); e_a is the actual vapor pressure (kPa); Δ is the slope of the saturated vapor pressure curve (kPa °C^{-1}); γ is the psychrometric constant (kPa °C^{-1}).

The accurate estimation of ETo is difficult if long-term historical climatic data are missing or recent data are incomplete. In situations of missing observed data, ETo can still be determined using estimated meteorological variables in the FAO-56 PM equation (Djaman et al., 2018; Sentelhas et al., 2010). In evaluating the sensitivity of key climatic variables for Penman-Monteith ETo, Koudahe et al. (2018) found that the sensitivity coefficient of solar radiation was very high in humid environments, while that of windspeed as well as maximum temperature were greatest in semi-arid environments. Thus, the authors recommend accurate measuring of these variables in estimating ETo using PM. When data are missing at a weather station of interest, it is common practice to supplement data from adjacent stations when estimating ETo (Lu et al., 2018; Shiri et al., 2019). This has led to development of various machine models trained with local or external data to improve ETo estimation, with various levels of performance in different climates (Feng et al., 2017; Lu et al., 2018; Mehdizadeh, 2018; Shiri et al., 2019). Yan et al. (2021) proposed a novel extreme gradient boosting model with the whale optimization algorithm to estimate daily ETo with local and external data. Their trained models that were tested locally outperformed their respective

FAO56-PM models. Like Koudahe et al. (2018), their sensitivity analysis revealed that sunshine duration and windspeed were the critical variables for daily ETo estimation in humid and arid regions respectively (Yan et al, 2021). It is also important to note that the selection of an ETo method is more critical when modeling short-term irrigation requirements, such as daily or weekly values for irrigation scheduling, as opposed to long-term irrigation requirements, such as seasonal or annual (Satti et al., 2004).

2.3.3. Crop evapotranspiration

Based on the crop type and estimated ETo, crop evapotranspiration (ETc) is then computed using the crop coefficient (Kc), which considers the crop variety, the crop growth stages, and the type of climate (Allen et al., 1998; Huffman et al., 2013; Pereira and Alves, 2005):

$$\mathrm{ETc} = \mathrm{Kc}\,\mathrm{ETo} \qquad \textbf{(2)}$$

Crop coefficients vary based on crop type, climate, and soil evaporation. Kc is at its minimum at planting, progressively increases as plants develop, peaks mid-season when the canopy cover reaches its maximum and declines as plants senesce towards the end of the season. To simplify, the crop coefficient curve is segmented into four straight-line sections corresponding to different growth stages (initial, crop development, mid-season, and late season). These segments are defined by three coefficients—Kc_{ini}, Kc_{mid}, and Kc_{end}—along with the duration of each stage measured in days. As ETo serves as an indicator of climatic demand, Kc varies primarily with specific crop characteristics, and only slightly with climate (Allen et al., 1998). This allows for the transfer of standard Kc values across various locations and climates (Pereira and Alves, 2005). While local crop coefficients are preferred (Huffman et al., 2013), reference values for common crops are widely available. Pereira et al. (2021) recently revised the tabulated standard Kc values for vegetable and field crops, via a thorough analysis of the accuracy of the reviewed studies. Local observations of the duration of crop growth stages should be used to account for plant variety, climate and cultural practices (Pereira and Alves, 2005).

In summary, for irrigated crops, I_{net} is defined as the net depth of water (mm) needed to fully satisfy the specific CWR, considering ETc, effective rainfall, soil-water storage, and groundwater contribution (Allen et al., 1998; Pereira et al., 2005). ETc is a critical parameter in determining

CWR, and thus crucial for irrigation scheduling and efficient agricultural water resource management (Koudahe et al., 2018; Wu and Fan, 2019).

2.4 Soil water

2.4.1. Soil water content

Soil water content, or soil moisture, is a measure of the amount of water held in soil. It is an important factor in soil quality, as it affects the availability of water and nutrients to plants, as well as the physical, chemical, and biological properties of soil (Hillel, 2003). Soil moisture content plays a major role in plant growth and essentially dictates the timing and application of irrigation for optimal crop production (Pan, 2012; Susha Lekshmi et al., 2014). Soil moisture is typically expressed as a ratio or a percentage on a mass or volume basis of the soil, with dry soil having a low soil-water content and wet soil having a high soil-water content. Since water applied to a field as rainfall or irrigation is often reported as a depth of water, volumetric water content (VWC) can be converted to a depth (e.g., in mm or cm) of soil water content (SWC) by assuming a unit area. The amount of water that soil can hold depends on factors such as the soil texture, structure, and organic matter content, as well as the climate, weather, and vegetation type (Gardner, 1986).

2.4.2. Plant available water

For irrigation management and planning, the soil's ability to retain water has significant implications for its role as soil water reservoir. The amount of water in the soil that is accessible for plant root uptake is the available water (AW) and is referred to as the soil water-holding capacity (Huffman et al., 2013; King et al., 2020; USDA, 2005). The field capacity (FC) is defined as the residual amount of water held by the soil after the excess has drained following a saturating rainfall or irrigation event. It represents the upper limit of water available to plants. The bottom limit of plant available water is the permanent wilting point (PWP). Below PWP, plants cannot obtain sufficient water to allow plant growth and generally wilt beyond recovery (Huffman et al., 2013; OFA, 2004). The AW depends on the soil type. It can be estimated as the difference between FC and PWP, multiplied by the effective root zone depth (Huffman et al, 2013):

$$AW = (\theta_{FC} - \theta_{PWP})z_r \quad \textbf{(3)}$$

where, AW is the depth of water available to plants (mm); θ_{FC} is the volumetric water content at field capacity (cm^3/cm^3); θ_{PWP} is the volumetric water content at wilting point (cm^3/cm^3); and z_r is the depth of the effective root zone (mm). As AW depletes, it becomes harder for the plant to uptake soil water, which may result in plant water stress before PWP is reached (Allen et al., 1998). Therefore, to account for the fraction of AW that is readily available to plants, a management allowed depletion (MAD) threshold is defined as the soil-water deficit at which irrigation is applied to minimize plant water stress that could affect yield and quality (USDA, 2005). These concepts are summarized in Figure 1 below.

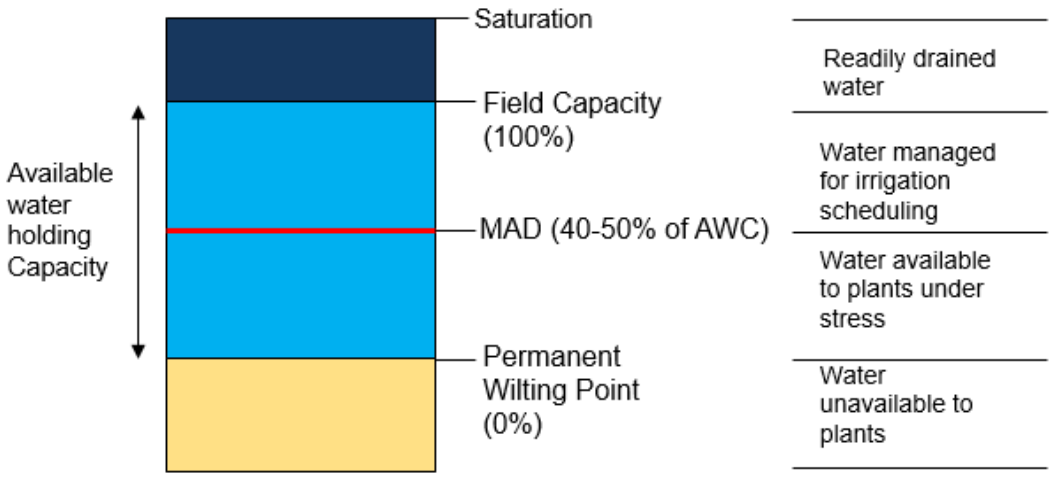

Figure 1. Plant available water and thresholds of the soil water reservoir (source: Sharma, 2019)

2.4.3. Measuring soil moisture

Soil moisture can be measured using direct measurement methods, such as gravimetric (ASTM, 2019; Hillel, 2003; Robinson et al., 2008), or indirect measurement methods, including resistivity (Sreedeep et al., 2004), neutron scattering (Fityus et al., 2011), and dielectric techniques (Mittelbach et al., 2012; Selig and Mansukhani, 1975). These methods help provide information on the total amount of water in the soil, as well as the distribution of water between the different soil layers and the availability of water to plants (Gardner, 1986; Hillel, 2003).

The traditional approach to direct measurement of soil moisture is the gravimetric method. It involves collecting a soil sample, drying it to a constant weight in an oven, and weighing the sample to determine the moisture content. Approximately 100 g of soil is dried in an oven at a temperature of 105°C-110°C for at least 24 hours (ASTM D2216-19). Water content on a volume

basis can be determined by collecting the sample in a known volume, such as a metal soil core, and dividing the dry mass by the volume to obtain bulk density. While it is simple and inexpensive, this method is time-consuming, disruptive to the soil, and can be affected by factors such as soil compaction and bulk density (ASTM, 2019; Gardner, 1986; Hillel, 2003).

An indirect method of measuring soil moisture is by using capacity resistance sensors, which can be placed at various depths of the soil. Capacitance sensors consist of an oscillating circuit and a pair of electrodes, which is embedded in the soil and forms a capacitor with the soil as the dielectric. Changes in soil moisture content are measured by the changes in the operating frequency, which depends on the dielectric permittivity of the soil (Robinson and Dean, 1993; Whalley et al., 1992). These sensors are reliable, cost-effective, user-friendly, and can provide accurate real-time measurements, but require soil-specific calibration (Cobos and Chambers, 2010; Kinzli et al., 2012; Susha Lekshmi et al., 2014). These sensors are popular due to their ability to measure soil moisture at various depths of the soil profile. However, volumetric water content measurements are sensitive to salinity and clay content (Mehata et al., 2023; Ojo et al., 2015; Parvin and Degré, 2016; Tedeschi et al., 2014). Mehata et al. (2023) found that among six manufacturer calibrations for capacitance probe sensors, the largest errors were associated with the default calibration. In addition, laboratory calibration can introduce errors associated to incorrect soil compaction (Souza et al., 2020) Field specific calibration is essential to reduce errors and bias (Rowlandson et al., 2013). The gravimetric method is a robust and widely accepted reference method for sensor calibration (Robinson et al., 2008; Songara and Patel, 2022).

Time domain reflectometry (TDR) is a widely accepted technique that measures the dielectric constant, and empirically determines the volumetric water content (Robinson et al., 2008; Rohini and Singh, 2004; Susha Lekshmi et al., 2014; Topp et al., 2000). TDR measures the time delay of electromagnetic pulses, which is dependent on the volumetric soil water content of the soil (Selig and Mansukhani, 1975; Topp et al., 2000). Advantages of TDR are rapid data acquisition, high temporal resolution, and the repeatability of measurements. It is non-destructive, can be used for long-term *in situ* measurements, and is independent of the soil texture and temperature (Noborio, 2001). However, TDR can have a high initial cost (Susha Lekshmi et al., 2014), and it is very time-consuming to do repetitive measurements (Robinson et al., 2008). It can also be difficult to carry out with high accuracy in the field; Site-specific calibration is essential (Hillel, 2003; Kelleners et al., 2004; Mittelbach et al., 2012).

A more advanced method of measuring soil moisture is the neutron scattering technique. A neutron moisture meter consists of a cylindrical probe (that contains a source of fast neutrons and a detector of slow neutrons), and a rate meter to measure the amount of energy scattered by the water molecules in the soil (Hillel, 2003; Jayawardane et al., 1984) This method is has a fast response time, high accuracy and is non-destructive. It is also possible to scan multiple depths of soil to create a moisture distribution profile (Hillel, 2003; Susha Lekshmi et al., 2014) However, there is a high initial cost, low spatial resolution, and potential health hazards in terms of radiation exposure (Jarvis and Leeds-Harrison, 1987). The instrument can also be difficult to move from one site to another and insensitive in shallow soil depths (Hillel, 2003; Zazueta and Xin, 1994).

In summary, soil moisture can be measured using a variety of methods, including gravimetric, dielectric, and neutron scattering techniques. Each method has its own strengths and limitations, and the appropriate method will depend on the specific goals and constraints of the measurement.

2.4.4. Soil composition and texture

The water-holding capacity of soils depends on the soil mineral particles, as well as the organic matter content, compaction, and soil salinity (Huffman et al., 2013; Saxton, 2005). The pore spaces between soil particles are filled with air, and water. The porosity is described as the ratio of the volume of the pore spaces to the total volume of the soil. The bulk density of an undisturbed soil sample is defined by (Eisenhauer et al., 2021):

$$\rho_b = \frac{M_{s\,dry}}{V_b} \quad \textbf{(4)}$$

where ρ_b is the soil bulk density (g/cm^3); M_s is the mass of dry soil (g); and V_b is the volume of the bulk soil sample (cm^3).

Soil mineral particles are sized based on their diameter and classified according to a classification system, such as *The Canadian System of Soil Classification* (CSSC) (Soil Classification Working Group, 1998) Textural classifications define sand, silt, and clay particles, and sometimes subdivide these classes by fine, medium, and coarse fractions. They are often visually represented by a textural triangle (Yudina et al., 2018). The distribution of particle size determines the soil texture (eg. clay, silty loam, sandy, loam, etc.) as well as the soil-water characteristics of a soil (eg. water-holding capacity, aeration, hydraulic conductivity, etc.) (Kroetsch and Wang, 2008).

The method of determining the proportions of mineral particles in each size class is called particle size analysis and typically consists of two parts. First, the proportion of the larger particles, or coarse fractions, is determined by the sieve method. The soil is first grinded to break up soil aggregates, and then passed through a stack of sieves loaded in a mechanical shaker. What remains on each sieve is weighed and its proportion to the total sample mass is calculated. The fraction of gravel, as well as coarse, medium, and fine sand are separated in this way (ASTM C136-06).

The silt and clay fractions cannot be separated by sieving. They are separated by sedimentation, which is based on Stoke's Law. Stoke's Law states that the amount that a particle sinks, depends on the density of the particle, ie., larger particles fall more quickly than smaller particles when suspended in a liquid. Common sedimentation methods, used to analyze the finer fraction of soil, are the pipette method and the hydrometer method (Gee and Or, 2002; Kroetsch and Wang, 2008). In the hydrometer method, the density of soil suspension is determined using the Bouyoucos hydrometer, with measurements executed at specific time intervals contingent on particle size. In the pipette method, clay particles are extracted with a pipette at a certain time, while sand particles are separated with a 270-mesh screen (53.3 μm), and both clay and sand are quantified through gravimetric analysis (Gee and Bauder, 1986). Depending on the goal of the study, a soil pretreatment may precede particle-size distribution analyses, including various chemical pretreatments, a combination of chemical and physical pretreatment, or only physical methods (Gee and Or, 2002). To classify soils through particle-size distribution data, a simple pretreatment method should be used to increase the efficiency of the analysis (Vaasma, 2008).

New methods of the analysis of particle-size distribution and soil morphology have been developed in recent decades, such as, laser diffractometry, X-ray microtomography, scanning electron microscopy, and mass-spectrometry of secondary ions (Yudina et al., 2018). The most common way to present part size analysis data is with a cumulative particle size distribution curve (Gee and Or, 2002). The percentage of particles finer than a given size is plotted against the logarithm of the particle diameter.

2.4.5. Soil matric potential

Soil moisture can also be expressed as soil matric potential (SMP) or soil water tension. While VWC indicates the quantity of water in the soil, it does not directly relate how that water is available to plants. The SMP is the potential energy per unit quantity of water. It describes the relative availability of water to plants and the driving forces of water movement in the soil

(Campbell and Mulla, 1990; Irmak, 2019). It is often expressed as energy per unit volume (pressure) or energy per unit weight (hydraulic head), recorded in kilopascals (kPa) or cm of water, respectively (Hillel, 2003; Eisenhauer et al., 2021). Plants draw accessible water molecules initially, progressing to more tightly bound ones as soil moisture decreases. Consequently, SMP gradually rises with soil dryness, reaching a maximum of zero in saturated conditions. As soil moisture decreases further, SMP becomes increasingly negative (ie. more negative tension). The negative sign is typically disregarded in practical applications (Irmak, 2019).

SMP can be assessed through various methods, with the tensiometer being one of the oldest and most widely used tools (Cambell and Mulla, 1990). The tensiometer comprises a water-filled tube, a porous cup at one end of the tube, and a vacuum gauge at the other. Installed in the field at the desired soil depth, the tensiometer's porous cup must be in direct contact with the surrounding soil. As the soil dries, water is drawn out of the tensiometer, creating a vacuum indicated by the gauge. This process continues until equilibrium is reached between the water in the tensiometer and the soil water, providing a direct measure of soil water tension (Eisenhauer et al., 2021). The VWC can be determined from SMP, and vice versa, through soil water characteristics curves developed for specific soil types (Campbell and Mulla, 1990; Irmak, 2019).

2.4.6. Soil water characteristic curve

The soil water characteristic curve (SWCC), also referred as the soil water retention curve, is the relationship between soil water content and soil matric potential, unique to each soil (King et al., 2020; Tarboton, 2003). These curves can either be determined experimentally through drainage experiments for a specific soil or derived from basic soil properties by using pedotransfer functions (Bittelli and Flury, 2009; Ghanbarian-Alavijeh and Liaghat, 2009). Although the experimental approach of using a pressure plate apparatus is reliable and precise, it can be quite costly, difficult, and time consuming (Pan et al., 2019). Bittelli and Flury (2009) found significant errors in SWCC derived from pressure plate experiments indicating an overestimation of soil water at wilting point, which would be problematic for CWR estimation.

Pedotransfer functions (PTFs) serve as predictive tools for soil properties that are challenging to obtain through easily, routinely, or inexpensively measured parameters (Van Looy et al., 2017). Soil survey data, including field morphology, texture, structure, and pH, often provide readily available information (Wadoux et al., 2023). To fit discrete measured data and facilitate practical applications, various mathematical and empirical representations have been proposed and revised.

Many models, such as the Brooks and Corey (1966), Van Genuchten (1980), Clapp and Hornberger (1978), and Campbell models, have demonstrated their applicability across a range of soils (Ghanbarian-alavijeh et al., 2010; Nasta et al., 2013; Sommer and Stöckle, 2010). The van Genuchten Mualem model equation and parameters are described as follows (Mualem 1976; Van Genuchten, 1980):

$$\theta(h) = \theta_r + \frac{\theta_s - \theta_r}{[1+|\alpha h|^n]^m} \quad \textbf{(5)}$$

where: θ is the volumetric soil water content (cm^3/cm^3); h is the soil matric potential (kPa); θr is the residual water content; θs is the saturated water content; α is an empirical parameter (kPa^{-1}); n is the van Genuchten parameter related to the pore-size distribution; and m is another van Genuchten parameter related to the slope of the curve (m = 1–1/n).

Regrettably, the estimation of coefficients in various empirical models remains challenging and time-consuming. To address this, numerous studies have explored predicting coefficients through PTFs (Cosby et al., 1984; Rawls et al., 2001; Saxton et al., 1986). Schaap et al. (2001) developed the Rosetta computer program employing five PTFs for hierarchical estimation of soil water retention and hydraulic conductivity. The program, based on neural network analyses and the bootstrap method, offers uncertainty estimates for predicted hydraulic parameters (Schaap et al., 2001). Saxton and Rawls (2006) developed PTFs using the extensive USDA soil database to estimate soil water characteristics from readily available soil variables such as texture and organic matter. The equations were integrated with previously documented correlations for tensions and conductivities, along with considerations for density, gravel, and salinity, creating a comprehensive predictive framework for SWCC tailored for agricultural water management and hydrologic analyses. Validation was conducted using distinct datasets encompassing a broad spectrum of soil textures. The predictive system was implemented in a graphical computerized model, SPAW, for convenience and efficiency (Saxton and Rawls, 2006).

2.5 General crop characteristics and production

2.5.1. Potato

Potatoes (*Solanum tuberosum*) are the fourth most important food crop worldwide, after maize, rice, and wheat (Montoya et al., 2016). The potato is a herbaceous annual that produces a starch-rich tuber composed of 75% water (FAO, 2008). Recently, the cultivated area and yield of potato

have increased annually (FAO, 2022) due to its broad adaptability, nutritional richness, processing versatility, and potential for enhancing both production and income (Wang et al., 2023). Quebec is the fifth-largest producer of potatoes in Canada, standing out from other provinces by allocating a larger portion (over 50%) of its production to the fresh market, compared to other provinces turning towards the processed market (Déziel et al., 2019).

Potato is a shallow-rooted crop, commonly grown on medium to coarse soils. It is one of the most sensitive crops to water stress, either as an excess or as a deficit in soil water (King et al., 2020; Stark et al., 2020). The recommended SWC for potatoes varies but is typically optimal when kept between 60 and 85% of AW at different stages of the growth cycle (Allen et al., 1998; King et al., 2020). In Quebec, Dubé and Rochette (1985) suggest a minimum of 50% AW for all growth stages, a level also used by Boisvert et al. (1992) in Ottawa for irrigated potato production experiments. A recent Quebec study of potatoes grown on sandy soils, found that a SMP threshold of –24 kPa optimizes yield and water productivity, while decreasing irrigation water use (Matteau et al., 2022). Further, it was found that potato plants in sandy soils can recover their physiological activities if irrigation is applied after a 1-day stress period at –40 kPa SMP, whereas they cannot revive if irrigation applied after a 7-day stress period at −20 kPa SMP (Jacques et al., 2020).

Tuber growth is inhibited at temperatures below 10°C and above 30°C, with optimum yields produced at a mean daily temperature of 18-20°C (FAO, 2008). In temperate climates and with good agricultural practices, a potato crop can produce 40 tonnes/ha of fresh tuber yield within four months of planting. Growth stages include sprout development, vegetative growth, tuber initiation, tuber bulking, and senescence and tuber maturation (Pavlista, 1995). From the updated FAO guidelines, the standardized mid-season basal crop coefficient and maximum rooting depth for potatoes are 1.10 and 0.4–0.6 m respectively (Pereira et al., 2021). The effective rooting depth is approximately 70% of a crop's maximum rooting depth (Driessen and Konijn, 1992). Studying supplemental irrigation of major crops grown in southern Quebec, Gallichand et al. (1991) determined potato Kc values of 0.51, 1.05 and 0.70 at initial, mid-season, and end of maturity stages, respectively, and a maximum root depth of 0.4 m.

2.5.2. Squash

The common terms "pumpkin", "squash", "gourd", etc. are frequently used interchangeably without distinction for various cultivated species within the genus *Cucurbita* L. (*Cucurbitaceae*): *C. pepo* L., *C. maxima* and *C. moschata*. *Cucurbita* species rank collectively among the 10 leading

vegetable crops globally (Ferriol and Picó, 2008). They are warm season crops that grow best during hot weather and cannot tolerate frost (OMAFRA, 2022). Quebec and Ontario are the two largest producers of fresh vegetables in Canada, accounting for 40% and 42% of Canadian acreages, respectively. Winter squash is one the most rapidly expanding fresh vegetables in the Quebec market (Déziel et al., 2017). In 2015, squash and zucchini in Quebec achieved an average yield of 14.4 ton/ha, representing a 20% increase from 2006 yields (Déziel et al., 2017).

Squash is a shallow-rooted crop (Amer, 2011) best grown on fertile, well-drained soil containing organic matter (Amer, 2011; OMAFRA; 2022). Squash is sensitive to excess soil water from seeding to maturity. Given the relatively shallow depth of roots, in the top 40-50 cm of soil, it is crucial to maintain SWC above 50% of AW to prevent detrimental water deficits (Allen et al., 1998; Hess et al., 1997). According to Ells et al., (1994), more than 60% of *C. pepo* roots are found in the top 15 cm of soil throughout the season. Rapid root development requires a well-managed irrigation schedule to avoid both excess and deficit soil water stress. This ensures proper fruit formation and mitigates the risk of root and stem rot diseases. (Hess et al., 1997; OMAFRA, 2022; Richard et al., 2002).

Pumpkins and squashes grow best at temperatures of 23-29°C during the day and 15°C-21°C at night. Plant growth halts at temperatures below 10°C (OMAFRA, 2022). Crop coefficients for initial, mid-season, and end stages derived from field observations range between 0.2–0.6, 0.85–1.0, and 0.56–0.74, respectively (Amer, 2011; Darouich et al., 2020; Yavuz et al., 2015). The updated standard value for winter squash is Kc = 0.91 (Pereira et al., 2021). Nyathi et al. (2019), reported a harvest index of 85% for pumpkin squash.

2.5.3. Cranberry

Cranberry (*Vaccininium macrocarpon*) is a perennial temperate wetland species native to North America that grows best on sandy and peat soils (Eck et al., 1976; Sandler and DeMoranville, 2008). Cranberries are predominantly grown in the USA and Canada (FAOSTAT, 2022), with a high proportion of production concentrated in three regions: Wisconsin, Québec, and Massachusetts (Caron et al., 2017). The industry has grown rapidly: cultivated cranberry area in Quebec has increased by 440% in the last 20 years (APCQ, 2021). Ample research has been conducted on cranberry production in Quebec.

Cranberries require a moist, well-oxygenated rootzone and crop yield is very sensitive variations in soil water. While their fine and fibrous roots span to maximum depths from 0.15 to

0.30 m, the bulk of cranberry roots is concentrated in the uppermost 0.1 to 0.15 m of the soil surface (Sandler and DeMoranville, 2008). For optimal cranberry yield without excessive water, irrigation should be implemented when the root zone SMP ranges between –7.5 and −4 kPa (Caron et al., 2016; Pelletier et al., 2015a) Values outside this range leading to wet anaerobic conditions or dry conditions limiting capillary rise (Caron et al., 2017). In their study on water requirements and sub-irrigation design for cranberry production, Elmi et al. (2010) concluded that a depletion level of 25-50%. AW could be used to determine irrigation requirements in Quebec conditions without compromising the yield. The period from mid-June to early September, particularly July (flowering) and August (fruit formation), is identified as the most critical for hydric stress sensitivity in cranberry crop growth (Pelletier et al., 2015a, 2015b; Jeranyama, 2017).

Cranberry production requires an abundant supply of water for irrigation, frost protection, cooling, as well as harvest flooding (Eck, 1976; Elmi et al. ,2010). Although harvest flooding accounts for most water applied, that water is typically recycled field by field in a closed loop system, whereas irrigation water is mainly consumed by the plant (Caron et al., 2016). Research suggests that controlling the growing-season water table at a depth of 0.5–0.65 m below the soil surface optimizes cranberry yield in sandy soil fields while saving water and energy (Caron et al; 2016; Pelletier et al., 2015b; Vanderleest et al., 2017). While a subsurface irrigation system would fulfill the irrigation needs, an overhead sprinkler system remains necessary for frost and heat protection, as well as for providing essential nutrients and pesticides (Elmi et al., 2010; Pelletier et al., 2016). To mitigate overheating, growers are known to briefly activate sprinkler irrigation when a critical temperature threshold is reached (Pelletier et al., 2015a). Furthermore, water use efficiency is optimized with the combined use of sub- and sprinkler irrigation (Sandler et al., 2004).

A study assessed the actual ET of cranberries and compared it with the reference ET. They determined cranberry ETc accounted for 55% of the ETo, concluding that ETo can serve as a reliable indicator of ETc for cranberries when multiplied by the appropriate Kc (Hattendorf and Davenport, 1996). Similarly, Bigah et al (2019) use a crop coefficient of 0.5 to estimate cranberry ETc. Updated standard indicative mid-season Kc values for perennial berry bushes range between 0.4 and 0.9 (Rallo et al. 2021).

2.5.4. Strawberry

The cultivated strawberry (*Fragaria* × *ananassa*) is one of the most valued berries in the world (Kumar and Dey, 2011). It is grown in all provinces of Canada, with Quebec having the greatest

acreage of strawberry production (AAFC, 2021). There are two main types of strawberry cultivars grown in Canada, June-bearing and day-neutral.

Irrigation is an essential water management practice for strawberries in Quebec, since they are a shallow-rooted crop that cannot tolerate drought (AAFC, 2021; Nand and Qi, 2023). Strawberry roots grow in the top 15 cm of soil with 75% of roots are concentrated in the top 8 cm (Craig, 1976). They require a well-drained soil and benefit from a moderate to high organic matter content. They can be grown in sandy soils if irrigation is well managed (AAFC, 2021). Irrigation is applied to maintain soil moisture above 50% AW for continued plant growth (Craig, 1976). Strawberry varieties differ in their sensitivity to water stress (Adak et al., 2017), and their winter hardiness. Over the winter, straw mulch is used to protect plants from low temperatures and alternating freeze thaw cycles (AAFC, 2021; Craig, 1976). Overhead sprinkler irrigation is used in Quebec to protect from frost in the spring (AAFC, 2021). Mulching and irrigation regime have shown to significantly impact strawberry yield, water consumption, root growth, and water use efficiency (Kumar and Dey, 2011). Strawberries are also well suited for drip irrigation and plastic mulching (Morillo et al., 2015; Saridas et al., 2021).

For strawberry cultivation in Quebec, optimal yield and water savings occur at a SMP of –10 kPa under drip irrigation on silty clay loam, sandy loam, or clay loam (Létourneau et al., 2015). Alternatively, employing drip irrigation and scheduling based on a range ($-15\,\text{kPa} \geq \text{SMP} \geq -30\,\text{kPa}$), contingent on predicted ETc, can enhance water use efficiency by 8–44% while achieving optimal yield on clay loam soil (Cormier et al., 2020). Other investigations have also reported increased yield and water productivity with the use of pulse irrigation (Gendron et al., 2018; Létourneau and Caron, 2019).

Field studies have determined maximum Kc values of 0.8 (Amini et al., 2022), 0.8 (Clark et al., 1996), and 0.75 (Hanson and Bendixen, 2004), in Iran, Florida, and California, respectively. The updated standard single and basal crop coefficients are 0.8 and 0.75, respectively (Pereira et al., 2021).

2.6 Crop-water modelling

Crop-water modeling is a valuable tool for famers and decision makers. Recent technological progress has resulted in numerous approaches and tools for assessing crop water needs and stress, frequently incorporating both remote sensing and ground data into crop and soil water models (Cahn and Johnson, 2017; Corbari et al., 2019; Pereira et al., 2020; Tolomio and Casa, 2020). Crop

models have diverse applications in agricultural water management, ranging from on-farm irrigation scheduling to regional assessments and planning. Enhanced detection of crop water stress to improve irrigation scheduling helps optimize water use at the field scale, especially for high-value crops, such as vegetables (Ihuoma and Madramootoo, 2017). Crop models can be embedded in decision support systems for irrigation scheduling to provide real time, site-specific information for farmers and technicians (eg. Gallardo et al., 2020; Zhai et al., 2020), be used to assess the effects of deficit irrigation (Farahani et al., 2009; Montoya et al., 2017; Paredes et al., 2014) or climate change (eg. Kang et al., 2009; Khordadi et al., 2019; Tatsumi, 2017) on crop water requirements and yields. They can also be upscaled using GIS tools to support local and regional decision making (eg. Alaya et al., 2019; Han et al., 2020; Li et al., 2021).

2.6.1. Commonly used Crop Growth Models

Commonly used crop models include DSSAT (Jones et al, 2003; Liu et al., 2011), CropSyst (Singh et al., 2008; Stockle et al., 1994), APSIM (Hammer et al., 2010; McCown et al., 1996), EPIC (Farina et al., 2011; Williams et al., 1989), STICS (Brisson et al., 2003; Jégo et al., 2012), and more recently AquaCrop (Li et al., 2020; Steduto et al., 2009; Vanuytrecht et al., 2014). Crop models can be divided into three main categories: radiation-driven models, carbon-driven models, and water-driven models (Steduto, 2009). These models employ diverse concepts and exhibit distinct structures, scales, and levels of complexity, leading to variations in precision and accuracy across crops and locations (Campbell et al., 2016; Challinor et al., 2014; Tubiello and Ewert, 2002). In adhering to good modeling practices, it is generally recommended to maintain simplicity while incorporating sufficient details to capture the fundamental processes influencing the system's behavior (Adam et al. 2011).

In recent years, the AquaCrop and DSSAT models have been widely use in simulating canopy development, crop evapotranspiration, nitrate leaching, yield production, and water use efficiency across various crops, such as wheat (Iqbal et al., 2014; Jin et al., 2018; Li et al., 2020; Liu et al., 2011), maize (Feng et al., 2022; Malik et al., 2019; Sandhu and Irmak et al., 2019), cotton (Garibay et al., 2019; Tsakmakis et al., 2019), potato (Adekanmbi et al., 2023; Boozar et al., 2022; Casa et al., 2013; Danielescu et al., 2022), and tomato (Ge et al., 2023; Linker et al., 2016; Zhao et al., 2018). These models are applied under diverse conditions such as different planting dates, nitrogen rates, plant densities, and irrigation methods or amounts. DSSAT (Decision Support Systems for Agrotechnology Transfer) combines various models, such as CERES, CROPGRO, SUBSTOR,

and CROPSIM, capable of simulating crop growth, phenology, soil water content, carbon and nitrogen balance, and the effect of diverse factors on crop yield (Jones et al., 2003; Song et al., 2015). AquaCrop is a water-driven model developed by the FAO based on crop yield response to water. It mainly focuses on the available water in the root zone and is particularly suited for water-limited conditions (Raes et al., 2009; Steduto et al., 2009). Compared to other crop models, it requires a relatively low number of input parameters and is well known for its balance of simplicity, robustness, and accuracy (Steduto et al., 2009; Vanuytrecht et al., 2014). AquaCrop can be also applied to a variety of crops (e.g. Battilani et al., 2014; Feng et al, 2022; Geerts et al., 2009; Stricevic et al., 2017), which has led to its widespread use. A recent study directly compared the performance of AquaCrop and DSSAT-SUBSTOR models in simulating potato growth, yield, water productivity, and soil water content, under various fertigation regimes; They found that the simulation accuracy of DSSAT-SUBSTOR potato was lower than that of AquaCrop (Wang et al., 2023).

2.6.2. Spatial upscaling: from field scale to regional scale

Prior research has showcased the efficacy of crop simulation models in accurately estimating crop yields, improving irrigation efficiency, and evaluating the impact of diverse management strategies at field-specific scales (Bhatia et al., 2008; Farahani et al., 2009; Kim et al., 2020; Liu et al., 2011). However, in decision-making processes, stakeholders often require upscaled information encompassing larger spatial extents. In these cases, the reliability of crop model simulations may be compromised by spatial heterogeneity in crop types, soil distribution, climate patterns, and crop management (Guo et al., 2021; Hansen and Jones, 2000). Utilizing crop models at a regional scale requires the consideration of spatial variations in input data (Manevski et al., 2019, Zhao et al., 2015), and the use of Geographic Information System (GIS) to store, manipulate, analyze, and visualize pertinent spatial data (Maguire, 1991; Hartkamp et al., 1999).

Prior research has considered the spatial distribution of input data, including soil type and crop parameters, in regional simulations for irrigation scheduling (Han et al., 2019, Jiang et al., 2019, Yang et al., 2015). For example, Jiang et al. (2019) and Yang et al. (2015) considered spatio-temporal heterogeneities of crop and soil to optimize regional allocations of irrigation water, while Manevski et al. (2019) and Li et al. (2021) considered spatial information on weather, soil, fertiliser, and crop to simulate and up-scale crop yield and nutrient leaching. PTFs were found to be an effective support for the regional application of field-scale models (Manevski et al., 2019).

Guo et al. (2021) developed a framework based on AquaCrop developed to optimize the irrigation schedule of winter wheat under dry, normal, and wet hydrologic scenarios over a large region in China, and to reallocate irrigation water amounts between regions. Their results serve as a useful guide for local producers and irrigation district managers to optimize crop yield, water use and economic benefit for the Fenwei Plain.

It is important to note that upscaling a crop model is associated with increasing spatial variabilities of the inputs, which impacts the model's accuracy (Alaya et al, 2019; Han et al., 2020; Hansen and Jones, 2000). Field to regional scale GIS-based crop simulation typically investigate the effects of soil, cultivar, and management practices on crop yield (Li et al., 2021). Crop rotation is often difficult to include, resulting in a tendency to focus on singular year and crop analyses (Jin et al., 2017; Resop et al., 2012) However, including crop rotation is associated with a more reliable prediction (Li et al., 2021). Therefore, the integration of GIS can expand the scope and applications of crop simulation if the spatial variability of relevant model parameters is taken into account.

2.6.3. Crop modeling for climate change impact

Agriculture must adapt to a changing climate to ensure sustainability and survival. Given the intricacies of both agricultural systems and climate change, crop models frequently play a crucial role in comprehending the influence of climate change on agriculture and the formulation of adaptation strategies. (Asseng et al., 2015). Amidst a changing climate and a growing population, the declining availability of future water resources is a major concern. This stresses the need for more efficient irrigation systems (Elliott et al., 2014; Taylor et al., 2013) and increased crop water productivity (Brauman et al., 2013). Various modeling studies have endeavored to evaluate potential impacts on agricultural water demands and identify potential actions in this context. Process-based models are well-suited to evaluate the effects of climate change due to their ability to simulate the impacts of increased CO_2 concentration and various management practices on crop biomass, yield, and water usage (Ewert et al., 2015; Rötter et al., 2013). However, this remains a challenging task due to substantial uncertainties in future climate and socioeconomic scenarios (Elliott et al., 2014; Haddeland et al., 2014; Wada et al., 2013).

Future meteorological variables are typically generated using global climate models, or general circulation models, (GCMs) for different scenarios (Asseng et al., 2015; Busschaert et al. ,2022). The most current global climate data (CMIP6) are from the latest phase of collaboration under the Coupled Model Intercomparison Project (CMIP), which provides the foundation for the

Intergovernmental Panel on Climate Change's Sixth Assessment Reports (IPCC, 2021). These future climate data are separated into different scenarios based on shared socioeconomic pathways (SSPs). The IPCC's sixth assessment report (2021) relies on this scenario architecture, denoted as SSPx–y, where x represents the SSP, and y indicates the level of radiative forcing in 2100. Five scenarios are defined: SSP1–2.6 (Sustainability; low emissions), SSP2–4.5 (Middle of the Road; medium emissions), SSP3–7.0 (Regional Rivalry; high emissions), SSP4–6.0 (Inequality, high emissions), and SSP5–8.5 (Fossil fuel development, high emissions). Under SSP3–7.0 and SSP5–8.5, global warming is likely to exceed 2∘C by mid-century (IPCC, 2021).

It is crucial to acknowledge that climate change scenarios generated by GCMs have substantial uncertainties stemming from three main sources: the internal processes modeled within the GCMs, the initial conditions, and future greenhouse gas emissions (IPCC, 2021). Downscaling GCM scenarios to local scales for integration into crop simulation models introduces an additional layer of uncertainty (Wilby et al., 2004). The dependability of such downscaling is pivotal for determining crop impact outcomes (Asseng et al., 2015). Climate model outputs are commonly downscaled using two methods: dynamic and statistical downscaling (Madsen et al., 2012). Statistical downscaling has more advantages and ability than dynamic, particularly when cost-effectiveness and rapid evaluation of climatic variables are priorities (Khordadi et al., 2019).

Another method to address uncertainties is the use a range of possible climate change projections, known as a model ensemble (Tao and Zhang, 2013). Early climate change impact studies relied on the outputs of a single GCM (Guo et al., 2010; Jones and Thornton, 2003), but this is no longer an accepted methodology. It is recommended to use multi-model GCM ensembles to generate a range of possible futures and reduce the influence of errors in any one model (Lee et al., 2011; Medellín-Azuara et al., 2008; Weigel et al., 2010).

While acknowledging the persistent challenge of uncertainty in climate change predictions and impact assessments, some consistent findings across various climate change scenarios, can offer valuable insights and practical guidance for decision-makers (IPCC, 2021; Zhang and Cai, 2013). Historical data analysis is particularly beneficial in recognizing past or ongoing changes in regional climates and their repercussions on agriculture, water, and other sectors (Rouge et al., 2013; Bates et al., 2008). Additionally, advancements in refining both GCMs, RCMs, and effective downscaling techniques, have been developed and tested to comprehensively address uncertainties (IPCC, 2021).

2.7 AquaCrop

2.7.1. Model overview and use

AquaCrop is a water-driven model based on the concepts of crop yield response to water (Doorenbos and Kassam, 1979) and water productivity (Steduto et al., 2009). AquaCrop (Raes et al., 2009; Steduto et al., 2009) is known for its balance of simplicity, accuracy, and robustness, using a small number of parameters compared to other crop models, while still maintaining output accuracy. It can be used for a large number of crops and focuses on four main types (fruit and grain crops, root and tuber crops, leafy vegetable crops, and forage crops). As opposed to a scientific-type model, which seeks to improve our understanding of crop physiology and response to environmental changes, AquaCrop is an engineering-type model, which aims to provide sound management advice to farmers or predictions to policy makers (Vanuytrecht et al., 2014). Its main purpose is to help practitioners, such as those working for government and non-governmental associations, farmers associations, consulting engineers, and extension services, and is a useful tool in planning and scenario analysis for economists and policy specialists (Steduto et al., 2009).

Numerous studies have evaluated the performance of AquaCrop for different crops through extensive sensitivity analyses, calibration, and validation, such as for quinoa (Geerts et al., 2009), wheat (Jin et al., 2018; Mkhabela and Bullock, 2012), maize (Mebane et al., 2013; Paredes et al., 2014), cotton (Farahani et al., 2009), and potato (Linker et al., 2016; Montoya et al., 2016; Razzaghi et al., 2017; Wale et al., 2022; Wang et al., 2023). The growing community of AquaCrop users are continually developing new crop, such as cassava (Wellens et al., 2022) as well as forage crops like ryegrass (Stricevic et al., 2017; Terán-Chaves et al., 2022).

Various studies have shown the many applications of the model, such as optimizing irrigation (Paware et al., 2017) and field management strategies (Abrha et al., 2012), and predicting the impacts of climate change on crop yield (Khordadi et el., 2019). Furthermore, recent studies have demonstrated the potential of upscaling crop modeling results using appropriate GIS tools (Alaya et al., 2019; Guo et al., 2021; Jiang et al., 2019).

2.7.2. Model input requirements

The input requirements that define the crop environment are stored in four input files: climate, crop, soil, and management (Raes et al., 2009; Steduto et al., 2009). The climate file includes daily weather, such as minimum and maximum temperature, rainfall, ETo. ETo is calculated by means of the FAO Penman–Monteith equation (Allen et al., 1998). Mean annual CO_2 concentration is

provided from Mauna Loa Observatory data or a specified emissions scenario for climate change analysis. The model delineates conservative crop parameters and non-conservative crop parameters. Conservative crop parameters are specific to each crop and do not change significantly with time, management practices, geographical location, or climate. They are presumed to remain unchanged with different cultivars and are widely applicable without local calibration. Non-conservative parameters, influenced by management and cultivar, are specified by the user. While conservative parameters are available for many calibrated crops, such as maize, potato, quinoa, and tomato (Vanuytrecht et al., 2014), AquaCrop also provides sample values for all required parameters as the starting point for unexplored crops when more specific information is lacking (e.g., Geerts et al., 2009). Soil data required are the saturated hydraulic conductivity (Ksat), VWC at saturation, field capacity, and permanent wilting point. These can be determined experimentally, derived from soil texture using PTFs, or assumed from indicative values provided by AquaCrop. The depth of the groundwater table and water salinity are also specified. Finally, field and irrigation management practices, such as irrigation schedule, irrigation method, mulching, and weeding. (Hsiao et al., 2009; Raes et al., 2009; Steduto et al., 2009; Vanuytrecht et al., 2014)

2.7.3. Soil water balance and calculation scheme in AquaCrop

The AquaCrop model relates its soil-crop-atmosphere components through its soil water balance (Araya et al., 2010). The soil water balance revolves around the root zone functioning as a reservoir, with influxes and outfluxes of water determining water available to the crops. Irrigation, precipitation, and capillary rise of shallow groundwater level are the main inflow sources of soil water are irrigation. The outflow includes soil evaporation, crop transpiration, surface runoff, and deep percolation (Wang et al., 2023). To precisely assess the retention, uptake, and movement of water in the soil profile, AquaCrop segments the soil profile and time into smaller fractions, of 0.1 m depth and one day increments by default. The one-dimensional vertical flow and root water uptake are solved at each node within the soil profile using the finite difference technique, considering independent variables such as time and depth levels, along with the dependent variable, moisture content (Baer, 1972; Raes et al., 2009).

The soil water balance is defined by algorithms for drainage, runoff and infiltration, soil evaporation, crop transpiration, canopy and root zone development, biomass production, and yield formation (Raes et al., 2009). The concepts and calculation procedures of AquaCrop model are discussed in Steduto et al. (2009) and are summarized in **Figure 2**. Processes influenced by water

stress (a to e) and temperature stress (f to g) are shown, and how they relate to green canopy cover (CC), rooting depth (Zr), ETo, normalized biomass water productivity (WP*), harvest index (HI), and growing degree days (GDD). Water stress impacts include impeding canopy expansion (a), hastening canopy senescence (b), potentially decreasing root deepening under severe stress. (c), diminishing stomatal opening and transpiration (d), and influencing harvest index (e). Cold temperature stress results in reduced biomass productivity (f), while hot or cold temperature stress hinders pollination and lowers the harvest index (g) (Vanuytrecht et al., 2014).

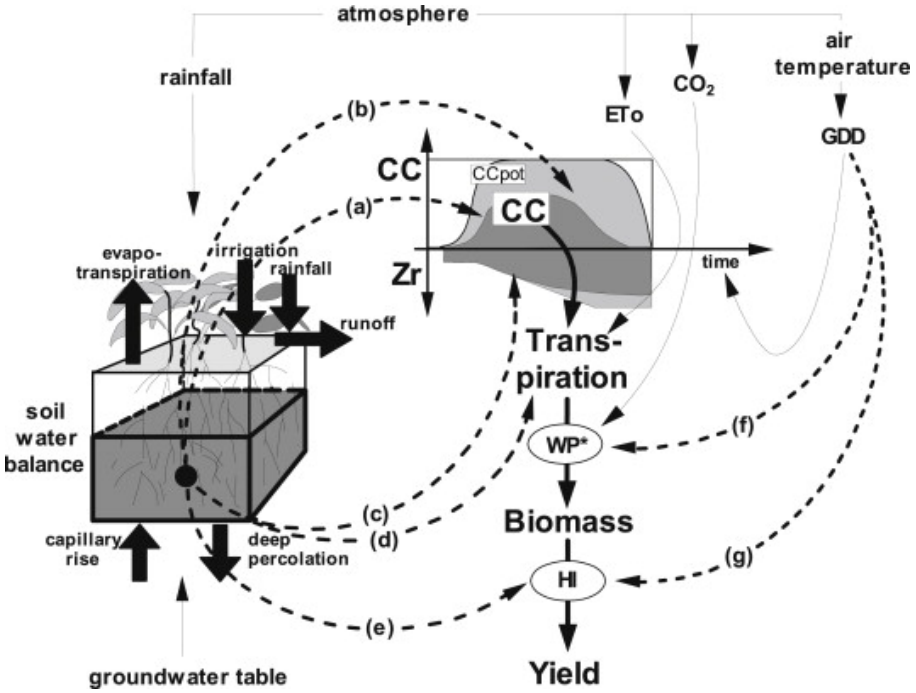

Figure 2. Calculation scheme of AquaCrop indicating processes affected by water and temperature stress. (Source: Vanuytrecht et al., 2014)

2.8 Impacts of climate change on agriculture

Agriculture has been identified as an industry that is highly vulnerable to climate change (Wanniarachchi and Sarukkalige, 2022). Climate change is anticipated to impact both the water availability and crop water requirement significantly, due to changes in rainfall and temperatures at the local and regional levels (Cai et al., 2015; Schewe et al., 2014). As well as affecting long-term trends and shifts in precipitation and temperature, climate change amplifies the frequency, intensity of extreme events, such as floods, droughts, heat waves, and hurricanes, which substantially impact agriculture around the world (IPCC, 2021; Turral et al., 2011). In rainfed dominant agricultural regions, variability in rainfall may force a gradual transition to irrigated

production to maintain crop yields, with precision irrigation playing an important role (Hedley et al., 2014).

2.8.1. Water availability under climate change

Changes in precipitation and temperature at the local and regional levels impact the availability of water for irrigation. (Schewe et al., 2014). Many large-scale irrigation systems rely on surface water resources in lakes, rivers, and reservoirs, which will be impacted by the variable local patterns of precipitation (Bates et al., 2008; IPCC, 2021). Also, glacier retreat due to climate change will severely impact irrigation systems in snow-dominated regions that depend on snow melt during the crop season (Cai et al., 2015). Although groundwater is often seen as a relatively reliable water source, climate change and variability impacts groundwater systems by affecting both groundwater recharge and the withdrawal of groundwater for human water supply (Taylor et al., 2013). Farmers also face the growing challenge of environmental protection and its effect on the supply and allocation water resources (Knox et al., 2010).

2.8.2. Crop response to climate change

Climate change impacts plant production and crop yields through shifts in atmospheric CO_2 concentration, rising temperatures, changes in precipitation and transpiration, increased frequency of extreme weather events, and the proliferation of pests and weeds (Tubiello et al., 2007). Crop yields can increase or decrease due to the combination of these effects, and the net impact will ultimately rely on the interactions between these factors (Asseng et al., 2015). For example, a study on the impacts of climate change on soybean production found that an increase of maximum temperature had a significantly positive effect on yield and biomass, except for yield under severe water stress conditions, in which precipitation had the greatest effect on final yield (Araji et al., 2018). On the other hand, for all models and climate scenarios, Khordadi et al. (2019) simulated reduced future yields for wheat and maize compared to their baseline period.

Elevated atmospheric CO_2 concentrations increases photosynthesis rate, especially in C_3 species, and reduces stomatal conductance, resulting in decreased transpiration rate (Farquhar et al., 1978). Many experimental studies have demonstrated that elevated CO_2 increases biomass production and yield (e.g., Drake et al., 1997; Tubiello et al., 2007), and this impact depends on water and nutrient availability (Kan et al., 2002). Temperature influences most of the underlying crop processes that determine production and yield, and its impact varies greatly between crop

species (Asseng et al., 2015) Higher temperatures can negatively impact production indirectly due to accelerated phenology and therefore less time for biomass accumulation (Menzel et al., 2006; Wang et al., 2013; Xiao et al., 2020). Several studies have proposed longer-maturing hybrids to mitigate the repercussions of accelerated phenology caused by warmer temperatures (Chapman et al., 2012; Khordadi et al., 2019; Olesen et al., 2012). While extreme temperatures can be detrimental, increased temperatures could benefit crops grown in cooler regions (Tian et al., 2012).

Water plays a crucial role in the impact of climate change on crop yield; the combination of water and other factors results in diverse effects, both positive and negative, influenced by crop type, region, and water management practices (Cai et al., 2015). Changing precipitation levels may exert either favorable or adverse effects on agricultural productivity. In semi-arid regions, increased rainfall could enhance growth, whereas reduced rainfall might constrain plant production. Conversely, in high rainfall areas, excessive rainfall may lead to soil waterlogging or nutrient leaching, detrimentally impacting crop development (Araki et al., 2012; Robertson et al., 2009). Furthermore, altered rainfall distribution and extreme events will impact crop growth and yield through effects on soil infiltration, water balance, soil mineralization, and crop water use efficiency (Asseng et al., 2015; Sadras et al., 2012; Wang et al., 2009).

At a global scale, the predicted impacts of climate change on CWRs are inconsistent between studies (Elliott et al., 2014; Fischer et al., 2007; Zhang and Cai, 2013), owing to significant regional heterogeneity (Cai et al., 2015). The shifting timing of growing seasons for specific crops complicates irrigation requirement estimates under climate change (Minguez et al., 2007). Rising temperatures extend growth periods in northern zones by allowing for earlier planting and later harvesting, but reduce them elsewhere (Turral et al., 2011). Longer growth periods are likely to increase crop water needs. In addition, the changing climate may decrease the suitability of certain crops in particular regions. Adaptation measures, such as adjusted calendars, increased crop water use efficiency, and enhanced irrigation technologies, are crucial for managing CWRs (Cai et al., 2015). Thus, it is essential to comprehend the climate change-induced effects at the local and regional levels for informed decision-making (Cai et al., 2015).

2.8.3. Impacts of climate change on Quebec agriculture

In Quebec, between 1948 and 2016, there was a 1.5°C rise in average temperature, accompanied by an increase in the occurrence of heavy rainfall events by 3–4 days (Vincent et al., 2018). Historical summer weather analysis has revealed a significant increase in temperature at

the majority of weather stations in agricultural regions, and a significant decrease in rainfall at 4 out of 25 stations (Assani et al., 2019; Yagouti et al., 2008). Further, an increase in the frequency of droughts in southern Quebec was observed between 2012 and 2021 (Nand and Qi, 2023).

According to Ouranos (2015), summer precipitation in south-western Quebec is projected to show minimal increases in the periods 2041–2070 and 2071–2100. In the projected high emission scenario, average temperatures are expected to rise by approximately 2.5°C between 2041 and 2070 and 4°C between 2071 and 2100, compared the baseline period (1981-2010). Notably, summer temperatures are foreseen to surge by 2.82 and 5.06°C during the corresponding future periods. Thus, a warming Quebec climate is expected to result in a substantial increase in growing degree days (GDD) (Ouranos, 2015). In colder regions, increased GDD has led to longer growing seasons (Jing et al., 2020; Vincent et al., 2018). However, depending on the crop, higher temperatures can accelerate crop stages and shorten the growth cycle (Menzel et al., 2006; Xiao et al., 2020). The fertilization effect of increased CO_2 (especially for C_3 crops) would be limited by the degree of warming. The number of days per year with temperatures surpassing 30 and 32°C is projected to rise by 15 and 6 days in 2041–2070, and 25 and 5 days in 2071–2100, respectively. Anticipated changes include an increase in heatwave events, marked by daily minimum and maximum temperatures exceeding 20°C and 33°C, respectively (Ouranos, 2015), which increase the potential for crop water stress.

The combined effect of warmer temperatures and increased GDD is expected to expand arable land (King et al., 2018), which could create opportunities to expand agricultural production and cultivate new crops (Nand and Qi, 2023). While supplemental irrigation in Quebec has previously shown to increase the yield and economic return (Drouet, 1989; Madramootoo et al., 1995; Tichoux, 1999), agricultural expansion and increased irrigation would exert pressure on water resources. Therefore, effective and sustainable water management practices in Quebec necessitate an assessment of the impact of climate change on irrigation water demand and its subsequent implications for the local environment and water resources.

2.9 Summary

This literature review provided an overview of the interdependent issues between agriculture, the natural environment, water resources, and climate change. The focus was narrowed to the agricultural-peatland complex of the study area in Lanoraie, Quebec, where significant degradation has been observed in the wetlands. Commonly irrigated crops cultivated in the region were

explored, including their general characteristics and management practices. The underlying principles of climate, soil, and water that govern crop water requirements were discussed, as well as experimental approaches for measuring key parameters. Crop water modelling was thoroughly researched and presented as a useful tool for estimating irrigation requirements for regional water resource management. Specifically, AquaCrop was reviewed, revealing its effectiveness in simulating the soil water balance and crop growth cycle for a variety of crops. The vulnerability of agriculture to climate change and the projected variability of Quebec growing season weather highlights the importance of evaluating the irrigation requirements and working towards developing a sustainable water resource management plan for Lanoraie.

3. Methodology

The methodological approach to estimating the irrigation requirements of the Scelaneau study region comprised of field data collection, model calibration, simulation, and statistical analysis. Field data were collected from representative sites and used to calibrate four AquaCrop models. Model performance was evaluated based on soil water content. Next, the calibrated models were run to simulate historical and future net irrigation requirements and test the effects of irrigation treatment and climate. Finally, the gross irrigation requirements were upscaled to the regional level to investigate a potential water supply scenario.

3.1 Study area description

The study area is located between 45.82° and 46.09°N and 73.44° and 73.17°W, enveloping the Lanoraie peatland complex and surrounding agriculture (Figure 3). It spans seven municipalities: Lanoraie, Lavaltrie, Saint-Geneviève-de-Berthier, Saint-Paul, Saint-Sulpice, Saint-Thomas and L'Assomption, and includes five main watersheds: Bras-sud-ouest; Saint-Antoine; Saint-Jean; Saint-Joseph; and Point-du-jour. It borders the Saint-Lawrence river and five rivers flow through the study area. The extent of the study area covers a total of 32 400 ha, including 12 000 ha of cropland and 7 600 ha of wetland. The average temperature and rainfall over the growing season, from May to September are 17.7 °C and 480 mm. The major irrigated crops are potatoes, other vegetables, and small fruit. Water for irrigation is mainly sourced from excavated reservoirs and ponds adjacent to streams, as well as by 12 small dams operated by the municipalities.

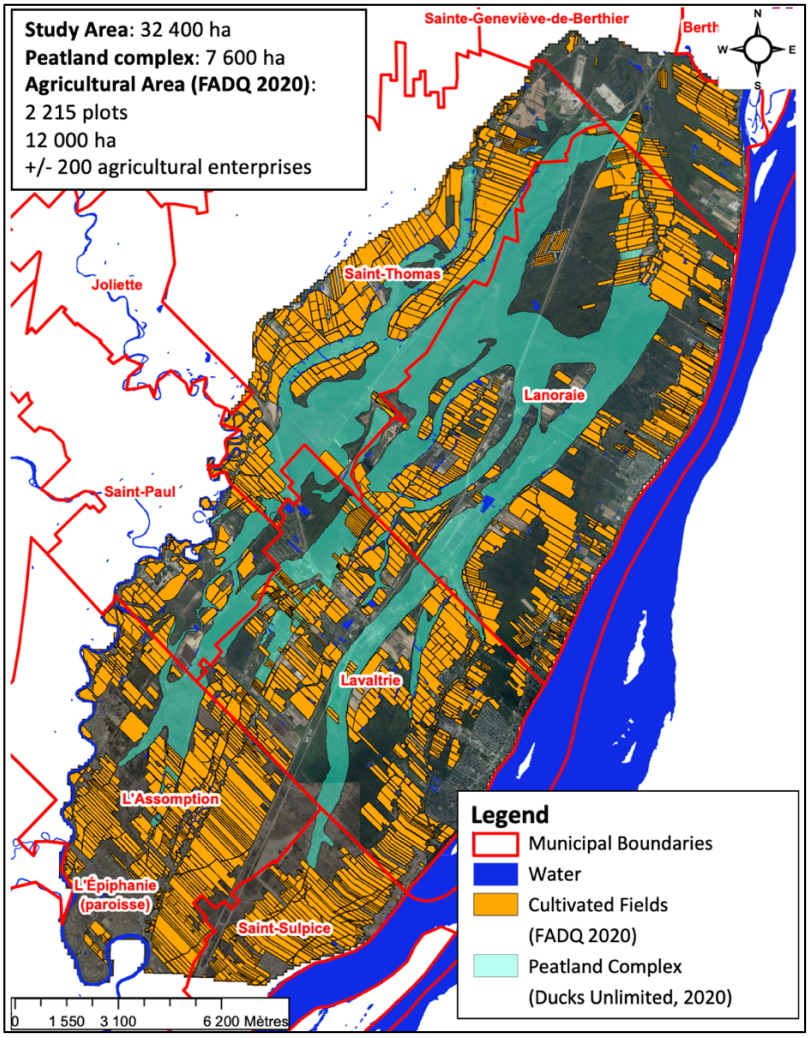

Figure 3. Extent of study area, showing municipal boundaries, waterways, cultivated fields, and Lanoraie peatland complex (Modified from UPA, 2022).

3.2 Field site selection

To estimate regional irrigation requirements for the study area, representative sites were selected at the field scale in the GIS-environment ArcMap (Version 10.8; ESRI, 2023). Upscaling to a regional scale can be done by identifying homogeneous simulation units, in terms of soil, crop, and hydraulic properties. The combinations of soil-crop-water and weather conditions can then be aggregated, and the output of the independent runs can be synthesized over the region (Wesseling and Feddes, 2006).

The geospatial soils data of the study region were provided by IRDA (2022) from the Quebec soils map database. The crop type and related data for the agricultural fields of the region were provided by the UPA de Lanaudière (2022), modified from the Financière Agricole du Québec

(FADQ, 2020) representative of the 2021 crop rotations. The map layers of soil data and crop type were overlayed and processed to identify the most prominent irrigated crops and soil types. Therefore, only crops requiring supplemental irrigation were included in the analysis. In addition, lesser acreage crops were grouped into like categories to condense the scope.

The major irrigated crop is potato, followed by vegetables and gourds, then cranberries, and finally, by other berries and small fruits (Figure 4a). These four categories represent 93% of the irrigated cropland and will form the basis of further analyses. Potatoes account for nearly two thirds of the net irrigated acreage. The cultivated soil type is largely homogeneous, with sandy textured soils covering 76% of irrigated cropland. The highest cultivated acreage is on the soil type Lanoraie fine sand. Table **1** summarizes the primary crops and soil types by acreage.

Field sites were selected to represent the primary irrigated crop groups and soil types in cooperation with local producers. Maps of the primary crop groups, and representative field sites are show in Figure 4 below. The sites were: L1) Potato grown on Lanoraie fine sand; L2) Squash grown on Saint-Thomas fine sand; L3) Strawberry grown on Lanoraie fine sand, and L4) Cranberry grown on Saint-Jude sand (Figure 4b).

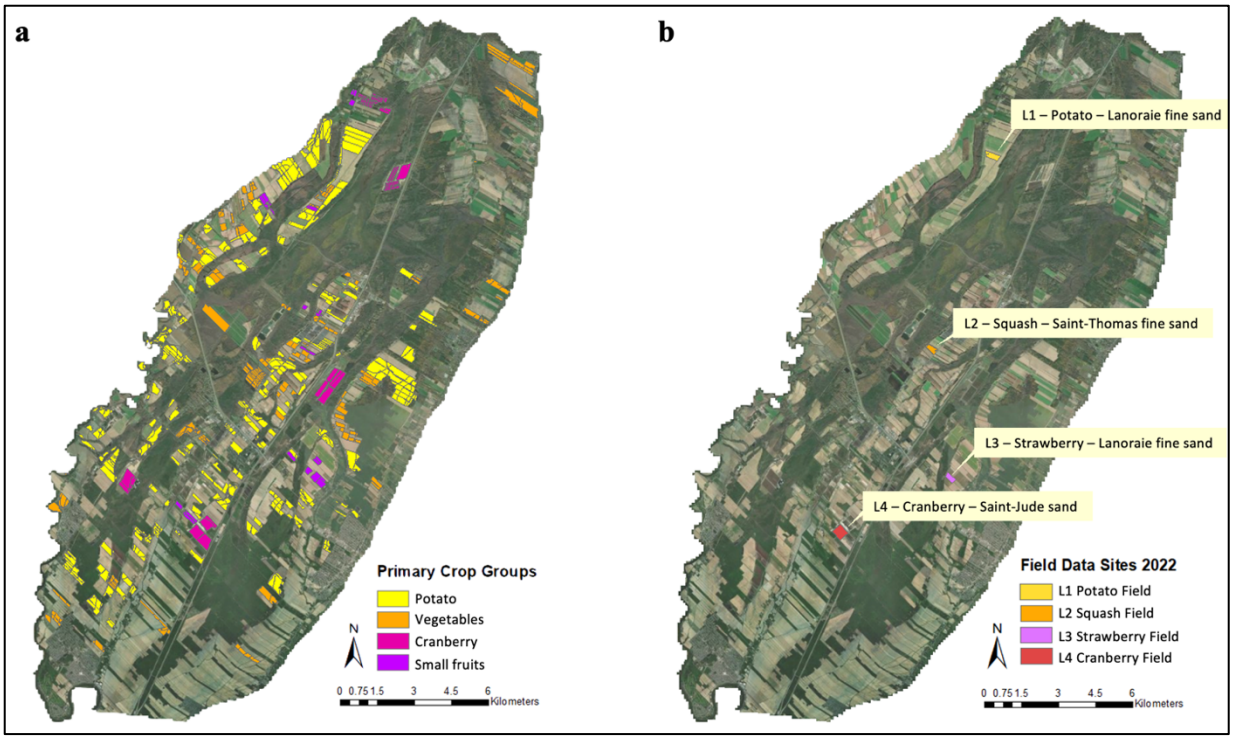

Figure 4. Study area showing a) the primary irrigated crop groups, and b) the selected field data sites.

Table 1. Primary irrigated crops and soil types in the Lanoraie study area.

Crop Category	Soil Type	Area of Irrigated Cropland (ha)	
Potato	Lanoraie fine sand	620	1912
	Saint-Thomas fine sand	318	
	Achigan sand	150	
Vegetables and gourds	Lanoraie fine sand	144	778
	Saint-Thomas fine sand	102	
	Chaloupe sandy loam	100	
Cranberry	Saint-Jude sand	57	256
	Saint-Thomas fine sand	53	
	Dunes	45	
Small fruits and berries	Lanoraie fine sand	52	98
	Dunes	17	
	Saint-Jude sand	12	

Field data were collected over the 2022 growing season to refine the AquaCrop models and are discussed further in sections 3.3 to 3.6 below. At each field site, Decagon capacitance soil moisture sensors (Decagon Devices Inc., Pullman, WA) were installed at two depths and monitored throughout the growing season. Soil samples were collected from each depth at the field sites over the growing season to calibrate the sensors and to conduct soil texture analyses. Weather data were collected from the nearest weather station, in L'Assomption, managed by Environment and Climate Change Canada (ECCC). For the 2022 growing season (May to September), the average temperature was 17.9°C and the total rainfall was 425 mm, above the historical 25-year average. Weather, groundwater level, and water quality were assumed to be consistent over the study area. Additionally, a questionnaire was distributed to each farmer to obtain crop, field, and irrigation management information.

3.3 Crop, field, and irrigation management at field sites

The agriculture of each field site is summarized in Table **2**. Cultivation techniques followed traditional farming practices for the area to maximize crop yield and quality as per the grower's expertise.

Table 2. Crop, soil type, and irrigation system of selected field data sites 2022

Site	Crop	Soil Type	Irrigation System
L1	**Potato**	Lanoraie fine sand	Low-pressure center pivot, drop tube and rotator nozzle
L2	**Squash**	Saint-Thomas fine sand	Solid-set sprinkler
L3	**Strawberry**	Lanoraie fine sand	Solid-set sprinkler
L4	**Cranberry**	Saint-Jude sand	Solid-set sprinkler

At field site L1 (Figure 5a), potato tubers (cultivar Solanum tuberosum FL-2137) were sown on May 11th, 2022, and seedlings emerged June 5th. Observed in Figure 5b, flowering began on July 2nd and lasted 28 days. Plant senescence occurred on August 15th and the harvest was conducted on September 22nd, when tubers reached maturity. Potatoes were grown on a hill furrow design with a row spacing of 0.9 m and plant spacing of 0.3 m. The canopy cover reached a maximum of 90%. Weed management was very good, meaning weeds accounted for only 5% of the canopy cover over the season. Irrigation was applied via a center pivot system with an application pressure of 103 kPa. There were four irrigation events in 2022: July 8th (18 mm), July 14th (18 mm), July 21st (22 mm), and August 1st (25 mm).

Field site L2 can be observed in Figure 6. Winter squash seedlings (*cucurbita maxima*) were transplanted on June 13th, 2022, with a row spacing of 1.2 m and plant spacing of 0.45 m. Flowering began July 13th and lasted approximately 35 days. The field was nearly entirely covered at maximum canopy cover and senescence started August 20th. Squashes were clipped from their vines August 25th and left to cure in the field. Weed management was very good, i.e., 5% relative weed cover. A depth of 25 mm of water was applied to the field by sprinkler irrigation on three occasions during the growing season.

Figure 5. L1 field site of potato grown on Lanoraie fine sand, showing a) geographic location and nearby water intake locations; b) photo capture of flowering crop and center pivot on July 7th, 2022.

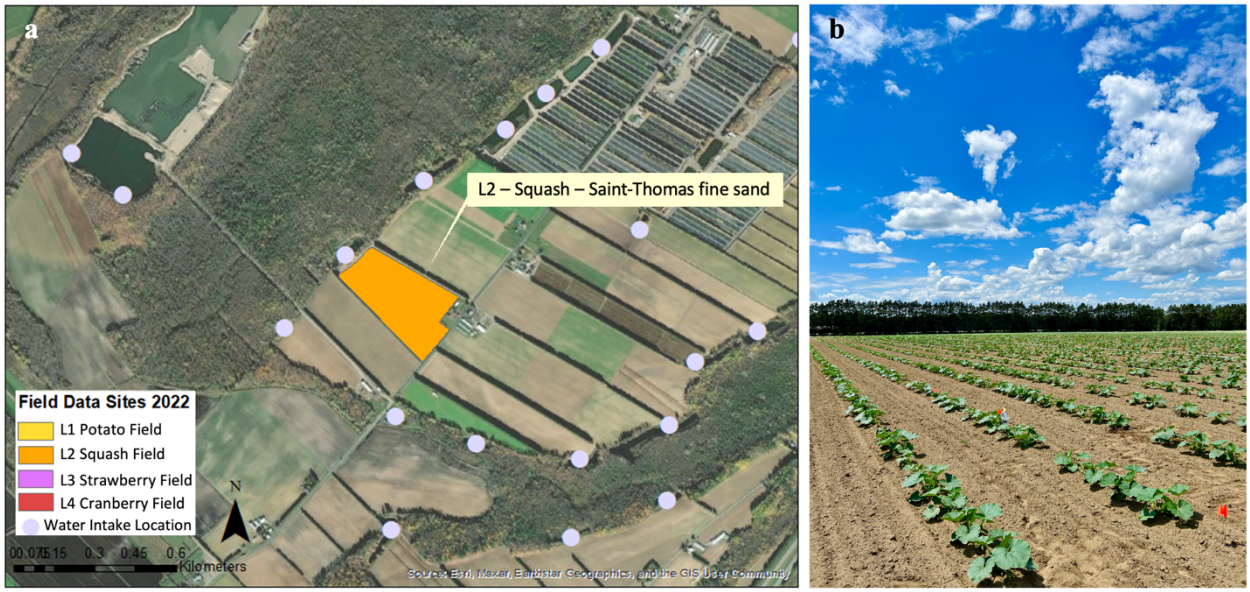

Figure 6. L2 field site of squash grown on Saint-Thomas fine sand, showing a) geographic location and nearby water intake locations; b) photo capture of crop rows and sensor placement on July 7th, 2022.

At the L3 field site (Figure 7), strawberry (*Fragaria ananassa*) seedlings were transplanted 0.35 m apart on April 27th, in rows 1.3 m apart. Flowering began May 10th and lasted until June 5th. Rather than a yield production of fresh berries, the producer was growing strawberry plants for wholesale distribution to other farms. Therefore, irrigation was more frequent to maintain surface soil moisture to promote the rooting of young runners and prevent yield formation. Soil moisture

sensors were installed in rows of a Quebec strawberry cultivar (*Jewel*). Sprinkler irrigation was initiated approximately every two to three days, when there was no rainfall greater than 5 mm. Weed management was perfect (i.e., 0% weed cover) and canopy cover reached a maximum of 75%.

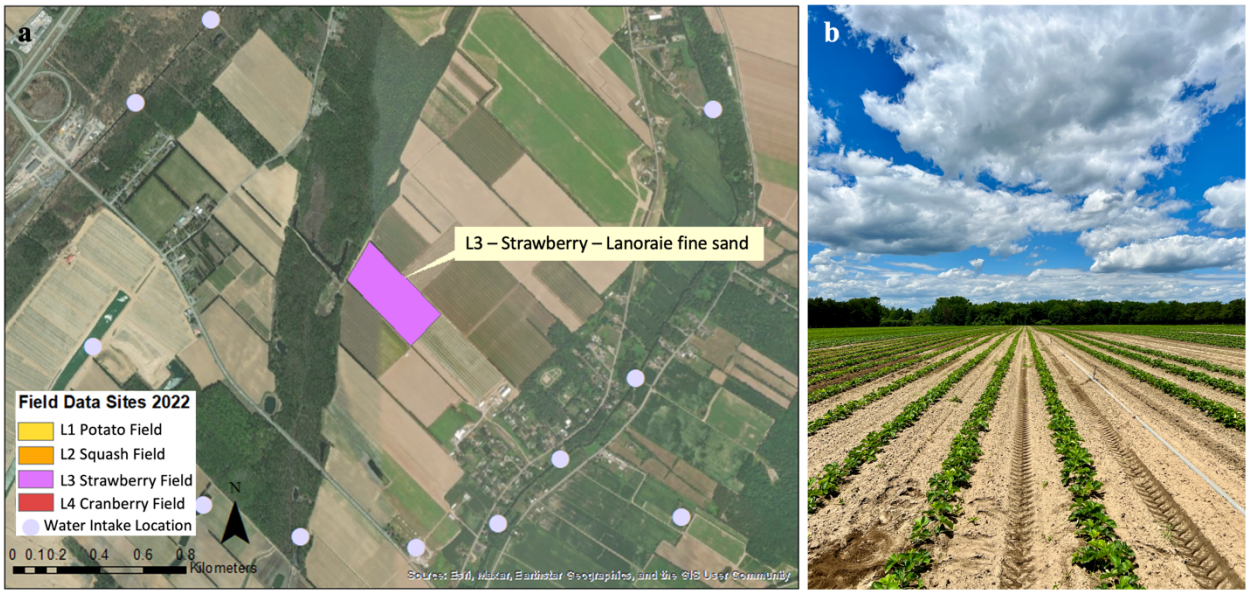

Figure 7. L3 field site of strawberry grown on Lanoraie fine sand, showing a) geographic location and nearby water intake locations; b) photo capture of crop rows and sprinkler system on July 7th, 2022.

The L4 field site is shown in Figure 8. Regrowth in the cranberry bog initiated mid-May and flowering began mid-June. Weed management was very good and the bog was near full crop coverage. Soil tension was actively monitored by the producers with tensiometers in the field. Water was applied by sprinklers for frost protection in early spring and for irrigation and heat protection as necessary in July, August, and September. Approximately 55 mm total was applied for irrigation. Harvest flooding occurred in the fall. Water is supplied from on-farm reservoirs and circulated in a closed-loop system.

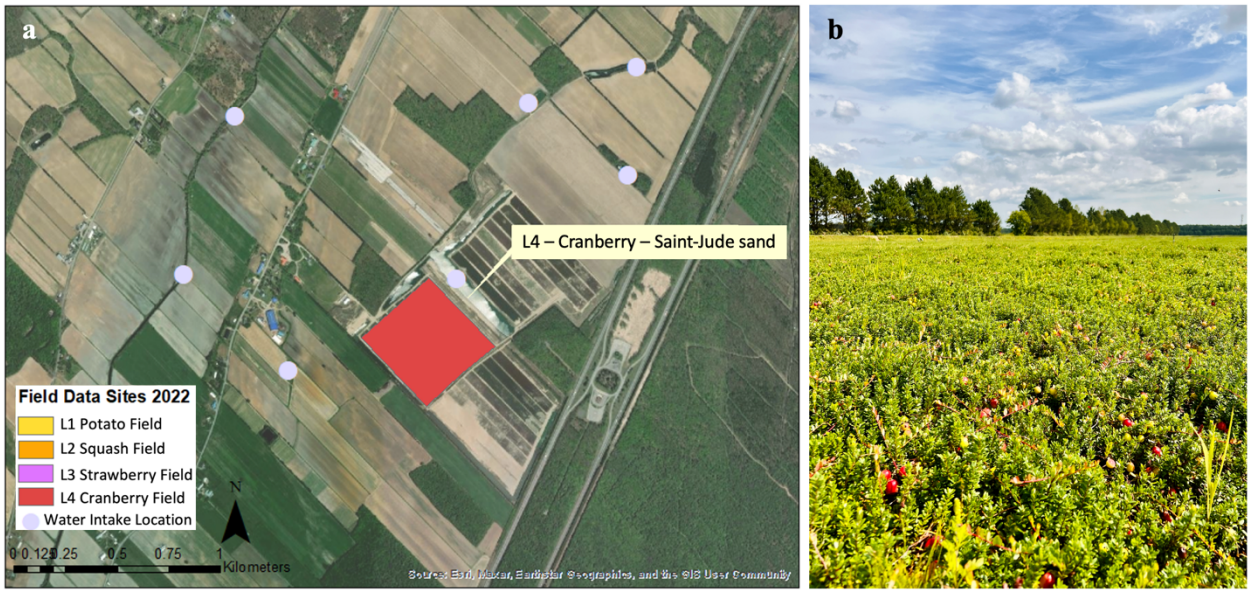

Figure 8. L4 field site of cranberry grown on Saint-Jude sand, showing a) geographic location and nearby water intake locations; b) photo capture of ripening cranberries on August 25th, 2022.

3.4 Meteorological data

The AquaCrop model requires daily values of rainfall, minimum and maximum air temperature, reference crop evapotranspiration, and mean annual carbon dioxide concentration (CO_2). The FAO ETo calculator was used to calculate daily ETo using the daily maximum and minimum temperature, wind speed at 2 m above ground surface, solar radiation, and minimum and maximum relative humidity (RH).

3.4.1. Historical climate data

For the historical analysis, the meteorological data, including precipitation (mm), air temperature (°C), relative humidity (%), and wind speed (m/s), were extracted from the L'Assomption weather station of ECCC on an hourly basis for the years 1997-2022 (ECCC L'Assomption, 2022). Missing data points were filled with measurements from the Montreal St-Hubert weather station, 25 km away (ECCC Montreal St-Hubert, 2022). The hourly data were processed to calculate daily maximum and minimum values for temperature and relative humidity, as well as total daily precipitation and average wind speed. Net solar radiation was obtained from the National Aeronautics and Space Administration Langley Research Center Prediction of Worldwide Energy Resource Project (NASA POWER, 2022). Relative humidity, wind speed and solar radiation were used to calculate ETo, and thereafter determining the ETc of the main crops

for last 25 years. Mean annual atmospheric CO_2 concentrations are provided in AquaCrop from the Mauna Loa Observatory.

3.4.2. Future climate data

To predict the impact of a changing climate, daily downscaled and bias-adjusted variable data were obtained from ClimateData.ca (2022). ClimateData.ca was created through a collaboration between the Pacific Climate Impacts Consortium, Ouranos Inc., the Prairie Climate Centre, ECCC, Centre de Recherche Informatique de Montréal, and Habitat7. The latest phase of the Coupled Model Intercomparison Project (CMIP6) ensemble was selected as it is the most current global climate model data available. The ensemble consists of projections from five climate change models: IPSL-CM6A-LR, CNRM-CM6-1, MIROC6, MIROC-ES2L, and CNRM-ESM2L, under SSP5-8.5 emission scenario. The SSP5-8.5 (high-emissions scenario) was chosen to maintain consistency between the work by the IRDA team for the SCELANEAU project.

Each GCM was statistically downscaled to the study area using BCCAQv2 methodology. BCCAQv2 is a hybrid method combining results from Bias Corrected Constructed Analogs (BCCA; Maurer et al. 2010) and Quantile Delta Mapping (QDM; Cannon et al. 2015). BCCA employs spatial aggregation via a linear combination of historical analogues for daily large-scale fields. QDM uses a modified quantile mapping method that preserves relative changes in GCM quantiles to avoid inflationary effects. CMIP6 datasets have been downscaled to approximately 6 x 10 m (0.0833° latitude x 0.0833° longitude). Mean annual CO_2 concentrations corresponding the SSP5-8.5 scenario were selected in AquaCrop.

Two future periods were defined for the projected simulation results to compare near and far effects on irrigation requirements to the baseline period (1997-2021). The 2050s represents a 30-year average over 2036-2065, and the 2080s represents a 30-year average over 2066-2095. Consistent with the methods recommended by the World Meteorological Organization (Arguez and Vose, 2011), climate normal were first calculated for temperature and precipitation over the baseline and two future periods. A standard climate normal is the average of a climatic period over 30 years (Govere et al., 2022):

$$T_n = \frac{1}{30}\sum_{i=30-x}^{x-1} T_i \qquad \textbf{(6)}$$

Where, T_n is the 30-year climate normal for the parameter T, T_i is the mean of the variable T for the year I, and x is an integer between 1 and 29. The climate normal for the baseline period was compared with the normal for the 2050s and 2080s under the SSP5-8.5 scenario to investigate the projected changes in temperature and precipitation. For estimating future irrigation requirements, each year was run in the model using daily climate data. Simulated net irrigation was subsequently averaged over the 30-year periods to evaluate the effect of climate change.

3.5 Soil texture analysis

Two soil horizons were defined for analysis, consistent with the depths of the soil moisture sensors: 0-15 cm and 15-30 cm. At each of the field sites, soil samples were collected with an auger from three points at random to ensure representative soil characteristics (Bouyoucous, 1936). Prior to collection, the top vegetation layer was carefully removed to minimize organic matter contamination (Gee and Bauder, 1986). The samples were stored in airtight, labeled containers for transport to the laboratory.

The coarse fraction was analyzed by the sieve method according to ASTM standard C136-06. The soil was oven-dried at 110°C for 48 hours. After drying, the samples were gently crushed and any visible roots, stones, or debris were removed (Gee and Or, 2002). Sieves selected according to the CSSC particle size limits were stacked and placed in a mechanical sieve shaker for 15 min. Particles passing the No. 200 sieve (<75μm) are considered the finer-grained portion of the sample.

Particle size analysis of the fine fraction was conducted using the hydrometer method (ASTM D422-63) as described by Kroetsch and Wang (2008). Soil samples were soaked overnight in sodium hexametaphosphate dispersant and mixed with an electric mixer to ensure homogeneity. The suspension was transferred to a graduated cylinder, topped up with distilled water, and manually mixed with a plunger. A hydrometer calibrated to ASTM standards was used to measure the particle density of the soil suspension at specific time intervals (ASTM D422-63). From these measurements, the particle size distribution was calculated using Stoke's law.

The particle size distribution data obtained from the sieve and hydrometer tests were analyzed to determine the percentages of sand, silt, and clay in each soil sample. The textural classification of the soil samples was done according to the CSSC soil textural classification system. Particle size distribution curves were plotted to compare soil grading between field sites. Soil hydraulic properties, such as field capacity, wilting point and saturated hydraulic conductivity, were estimated using the SWCC model's pedo-transfer function developed by Saxton et al. (2006).

3.6 Soil moisture data

Decagon capacitance sensors were installed in duplicate at two depths within the crop's root zone to monitor soil moisture and were connected to EM50 data loggers (METER Group, Pullman, WA, USA). Two sensors measured soil moisture closer to the surface, at a 5 cm depth, while two others measured soil moisture deeper in the root zone at depths varying between 15 cm and 30 cm, depending on the crop. Due to availability of sensors and cooperation from local growers, the capacitance sensors were installed at the field sites L1, L2 and L3, while data from existing tensiometers were shared for the cranberry field at L4. The soil matric potential data collected at L4 underwent conversion to volumetric water content using the van Genuchten-Mualem model. The capacitance sensors at L1, L2, and L3 were installed by auguring a vertical hole to a depth below the root zone of the respective crop, and horizontally inserting the sensors into the soil at the selected depths. The sensor cables were run along the soil surface to the data loggers. Sensor data were retrieved via the EC2H20 Utility 1.8 software (METER Group, Pullman, WA, USA).

Volumetric water content (VWC, $cm^3\ cm^{-3}$) was logged at 5-min intervals throughout the growing season. Field specific calibration of soil moisture sensors is an important step in ensuring the accuracy of the sensor readings (Robinson et al., 2008). Therefore, soil core samples of known volume were collected during eight field visits to the sites throughout the 2022 growing season. The gravimetric samples were collected in duplicate at each sensor depth and converted to volumetric water content using the measured bulk density. Like Wang et al. (2023), measured soil bulk density and gravimetric water content were used to correct the VWC recorded by the sensors.

Consistent with the methods of Danielescu et al. (2022), the corrected VWC was averaged for the replicates at each depth to obtain a representative daily value. Next, daily VWC measurements ($m^3\ m^{-3}$) were multiplied by the thickness of the root zone to achieve an equivalent depth of water column (mm) and allow comparison with simulated soil water content in the root zone.

3.7 AquaCrop model

The AquaCrop models for potato, squash, strawberry, and cranberry were calibrated with the 2022 field data from each site. To facilitate the accurate assessment of irrigation requirements, the soil moisture measurements described in Section 3.6 served as the observed data for the model calibration. Each model was then initialized with parameters corresponding to the field conditions, encompassing climate, crop, soil, and management variables, described in Section 3.7.1 below.

3.7.1. Model parameters

For all crop models, the climate variables for the 2022 growing season were obtained as described in Section 3.4.1. For the calculation of ETo, the geographic coordinates and elevation of each field were specified. ETo was calculated by the FAO-56 Penman-Monteith Equation.

The crop parameters for each model are presented in Table 3 through Table **6**. The conservative crop parameters, those that do not change significantly with time, location, and management, are provided by AquaCrop in the default potato crop file. These values remain be the same for any potato cultivar grown in any region of the world (Hsiao, 2012). For the crops not defined in AquaCrop, values were extracted from literature and calibrated to local conditions if they simulated a response in SWC. These conservative parameters include the crop coefficient for transpiration at full canopy, canopy decline coefficient, biomass water productivity, reference harvest index. Non-conservative parameters, that are management and cultivar specific, are also required. Planting method, plant density, and the dates of planting, emergence, start of senescence and maturity were specified by farmer observations. Planting dates mirrored the actual agricultural practices in the study area, ensuring that the model was aligned with the local agricultural calendar. If not specified by the farmer, parameters such as the dates of maximum canopy cover and the start of yield formation were adopted based on the recommended ranges provided by AquaCrop and subsequently calibrated. The crop response to soil salinity or soil fertility stress was not considered.

Table 3. Potato crop parameters for model calibration

Crop Parameter	Value	Method
Planting method	Sowing	Observed
Plant density	3.3 plants/m^2	Observed
Initial canopy cover, CC_o	Small canopy, 0.17%	Calibrated
Maximum canopy cover, CC_{max}	Almost entirely covered, 92%	Calibrated
Canopy decline coefficient, CDC	Very slow decline, 1.9%/day	Default
Maximum effective rooting depth	0.30 m	Observed
Shape factor for root zone expansion	1.5	Default
Crop transpiration coefficient, $K_{c\ Tr}$	1.10	Default
WP_{ET} normalized for climate and CO_2	0.18 g/m^2	Default
Reference harvest index, HI_o	75%	Default
Date of sowing	May 11th, 2022	Observed
seedling emergence	June 5th, 2022	Observed

start of flowering	July 2nd, 2022	Observed
start of yield formation	July 6th, 2022	Calibrated
end of flowering	July 30th, 2022	Observed
maximum canopy cover	July 15th, 2022	Calibrated
start of canopy senescence	August 15th, 2022	Observed
end of building up HI	September 21st, 2022	Calibrated
maturity	September 22nd, 2022	Observed

Table 4. Squash crop parameters for model calibration

Crop Parameter	Value	Method
Planting method	Transplanting	Observed
Plant density	1.9 plants/m^2	Observed
Initial canopy cover, CC_o	0.13%	Calibrated
Maximum canopy cover, CC_{max}	Almost entirely covered, 95%	Calibrated
Canopy decline coefficient, CDC	Slow decline, 8.4%/day	Calibrated
Maximum effective rooting depth	0.35 m	Calibrated
Shape factor for root zone expansion	1.7	Calibrated
Crop transpiration coefficient, $K_{c\ Tr}$	0.9	Calibrated
WP_{ET} normalized for climate and CO_2	0.15 g/m^2	Literature
Reference harvest index, HI_o	85%	Literature
Date of transplant	June 14th, 2022	Observed
transplant recovery	June 15th, 2022	Observed
start of flowering	July 13th, 2022	Observed
end of flowering	August 18th, 2022	Observed
maximum canopy cover	July 27th, 2022	Calibrated
start of canopy senescence	August 16th, 2022	Observed
length of building up HI	August 12th, 2022	Calibrated
maturity	August 24th, 2022	Observed

Table 5. Strawberry crop parameters for model calibration

Crop Parameter	Value	Method
Planting method	Transplanting	Observed
Initial canopy cover, CC_o	1.10%	Calibrated
Maximum canopy cover, CC_{max}	Fairly covered, 75%	Observed
Plant density	2.2 plants/m2	Observed
Canopy decline coefficient, CDC	Very slow decline, 6.5%/day	Calibrated
Maximum effective rooting depth	0.20 m	Calibrated

Shape factor for root zone expansion	1.3	Calibrated
Crop transpiration coefficient, $K_{c\ Tr}$	0.75	Calibrated
WP_{ET} normalized for climate and CO_2	0.18 g/m2	Literature
Reference harvest index, HI_o	40%	Literature
Date of transplant	April 26th, 2022	Observed
transplant recovery	May 3rd, 2022	Observed
start of flowering	May 10th, 2022	Observed
end of flowering	June 8th, 2022	Observed
maximum canopy cover	September 1st, 2022	Observed*
start of canopy senescence	September 22nd, 2022	Observed*
length of building up HI	June 30th, 2022	Observed*
maturity	October 1st, 2022	Observed

*Due to model restrictions of crop growth stages, dates provided by farmer observations were modified to allow the model to run, simulating flowering and yield formation.

Table 6. Cranberry crop parameters for model calibration

Crop Parameter	Value	Method
Planting method	Regrowth	Observed
Initial canopy cover, CC_o	74.5%	Calibrated
Maximum canopy cover, CC_{max}	Almost entirely covered, 98%	Observed
Plant density	2.8 plants/m^2	Observed
Canopy decline coefficient, CDC	Slow decline, 10.6%/day	Calibrated
Maximum effective rooting depth	0.30 m*	Restricted*
Crop transpiration coefficient, $K_{c\ Tr}$	0.6	Calibrated
WP_{ET} normalized for climate and CO_2	0.17 g/m^2	Literature
Reference harvest index, HI_o	50%	Literature
Date of regrowth	May 14th, 2022	Observed
start of flowering	June 13th, 2022	Observed
end of flowering	July 29th, 2022	Observed
maximum canopy cover	May 28th, 2022	Calibrated
start of canopy senescence	September 9th, 2022	Calibrated
length of building up HI	September 1st, 2022	Calibrated
maturity	September 30th, 2022	Observed

*Root depth for perennial crop models is restricted to a minimum of 0.30 m, therefore default soil water extraction pattern was modified to represent a shorter rooting depth.

The soil profile was defined in two soil horizons based on the particle size analysis. However, due to reduced sample size after sieving, the hydrometer method underestimated silt and clay

particles. Therefore, soil water attributes, such as FC and WP, were derived by applying the bulk density measurements and soil particle distribution from Quebec pedological soil survey data to the SWCC pedo-transfer function and are presented in section 4.2. The soil hydraulic parameters were then evaluated as sensitive parameters. L1, L2, and L3 soils were classified as sandy soil, while L4 was a loamy sand. The model automatically adjusted the Curve Number (CN) to 46 and the Readily Evaporable Water (REW) to 2 mm by default, according to the soil type. The CN was subsequently calibrated while remaining within the range for soil hydrological group A. The initial condition for soil moisture was assumed at FC on May 1st. Capillary rise was negligible since the groundwater table was below 2 m, except in the case of the cranberry bog, where the water table is controlled for irrigation management. In this case, the depth of the groundwater table was defined by target values highlighted in Quebec cranberry studies (Caron et al., 2017; Pelletier et al., 2015b; Vanderleest et al., 2017), and calibrated to the field conditions.

Management parameters associated with irrigation and field practices, such as irrigation events and weed management, were defined as specified by the farmer questionnaire to mimic the irrigation practices employed in the region. This site-specific approach was pivotal in accounting for the conditions and practices of the study area. Each model was calibrated for the 2022 growing season with the above-mentioned data, comparing the simulated output with the field data.

3.7.2. Sensitivity analysis and calibration

An iterative parameter adjustment process was initiated to fine-tune the model. This calibration primarily focused on parameters associated with soil water infiltration, and crop growth. Additionally, a sensitivity analysis (SA) was carried out to identify the parameters that had the most significant influence on model predictions (Cao and Petzold, 2006), providing insights into the critical factors affecting soil moisture dynamics. The SA followed the methodology outlined by Geerts et al. (2009). The parameter inputs were changed one at a time while the others remained constant. The interval of variation of the inputs was chosen as -25 to +25% of the standard value. Model outputs under the changed inputs were compared to the basic output. Variables were assigned a sensitivity level of high, medium, low, if the model's response to the changes was greater than 15%, between 2-15%, or less than 2% respectively (Geerts et al., 2009). The results of the SA helped narrow the calibration efforts. The aim was to minimize the disparity between the model's simulated soil moisture levels and the observed field measurements through a trial-and-error approach.

3.7.3. Statistical metrics for model evaluation

To evaluate the calibrated AquaCrop model's performance, a comprehensive comparison was conducted between its simulated soil moisture values and the observed field data. Due to the individual strengths and weaknesses of statistical indicators, model performance evaluation requires the use of multiple metrics for a comprehensive assessment (Feng et al., 2022; Wilmott, 1982). Consistent with recent AquaCrop model performance studies (e.g. Paredes et al., 2018; Razzaghi et al., 2017; Terán-Chaves et al., 2022; Wang et al., 2023), the goodness-of-fit of each crop model was evaluated using the following statistics: the Pearson correlation coefficient (r), the root mean square error (RMSE), the normalized root mean square error (NRMSE), the Nash-Sutcliffe model efficiency coefficient (EF), and the Willmott index of agreement (d).The r, RMSE, NRMSE, EF, and d are described as follows (Moriasi et al., 2007; Nash and Sutcliffe, 1970; Wilmott, 1982):

$$\textbf{Pearson correlation coefficient, } r = \left[\frac{\sum(O_i-\bar{O})(S_i-\bar{S})}{\sqrt{\sum(O_i-\bar{O})^2\sum(S_i-\bar{S})^2}}\right] \quad (7)$$

$$\textbf{Root Mean Square Error, RMSE} = \sqrt{\frac{\sum(S_i-O_i)^2}{n}} \quad (8)$$

$$\textbf{Normalized Root Mean Square Error, NRMSE} = \frac{1}{\bar{O}}\sqrt{\frac{\sum(S_i-O_i)^2}{n}} * 100\% \quad (9)$$

$$\textbf{Nash-Sutcliffe model efficiency coefficient, EF} = 1 - \frac{\sum S_i-O_i)^2}{\sum(O_i-\bar{O})^2} \quad (10)$$

$$\textbf{Willmott's index of agreement } d = 1 - \frac{\sum(S_i-O_i)^2}{\sum(|S_i-\bar{O}|+|O_i-\bar{O}|)^2} \quad (11)$$

where Oi and Si are the observed and simulated values respectively; $\bar{O}$ and $\bar{S}$ are their means; and n is the number of observations.

The Pearson correlation coefficient ranges from -1 to 1, with values near 1 indicating strong agreement between observed and simulated values. According to FAO (2015) for r, values > 0.90 indicate a very good agreement, while values of 0.70-0.90 and 0.5-0.7 are considered good and acceptable respectively. Values below 0.50 indicate poor agreement. Correlation quantifies dispersion only, so a model consistently overestimating or underestimating observations can still yield a high r value. It is also necessary to analyze the residual error (Si – Oi) (Willmott, 1982).

The RMSE is a widely used statistical indicator for assessing model performance (Jacovides and Kontoyiannis, 1995), measuring the average magnitude of the difference between predictions

and observations. It ranges from 0 to positive infinity, with lower values indicating better model performance. Since the residual errors are calculated as squared values, the RMSE is sensitive to extreme values or outliers (Moriasi et al., 2007). RMSE quantifies the mean difference in the same units as the data, while the NRMSE is expressed as a percentage. It indicates the relative disparity between the simulated and observed data. A simulation can be considered excellent if the NRMSE is less than 10%, good if between 10 and 20%, fair if between 20 and 30%, and poor if greater than 30% (Jamieson et al., 1991).

The Nash-Sutcliffe model efficiency coefficient (EF) determines the relative magnitude of the residual variance compared to the variance of the observations (Nash and Sutcliffe, 1970). It is very commonly used to assess the quality of the modelling approach, and thus has many reported values available in literature (Moriasi et al., 2007). The EF ranges from $-\infty$ to 1. EF approaches 1 when the residual variance is much smaller than the observed data's variance. An EF of 1 indicates a perfect fit, while EF of 0 implies the model is only as accurate as the observed mean, and $EF < 0$ suggests the observed mean is a better estimator than the model (Legates and McCabe, 1999). An EF greater than 0.40 is considered acceptable for SWC in crop modeling studies (Geerts et al., 2009; Paredes et al., 2014; Razzaghi et al., 2017).

The index of agreement (d) represents the ratio of the mean square error to the "potential error", which is the sum of squared absolute distances between predicted and observed values from their respective means. This index rectifies the insensitivity of r and EF to systematic over- or underestimations of the model. It ranges from 0, meaning complete disagreement, to 1, meaning predicted and observed data are identical (Legates and McCabe, 1999; Willmott, 1982).

The simulation results were considered good when the majority of statistical indicators of the model evaluation were classified as good to very good (Terán-Chaves et al., 2022).

It is common practice in hydrological modeling to reserve a separate dataset for model validation, distinct from the data used in the calibration process (Arsenault et al., 2018). However, due to the inaugural phase of the project and limited timeframe, only data from one growing season were collected. Therefore, it was not possible to validate the models. Furthermore, a split-sample approach is not always recommended. A recent study that tested 50 split-sample approaches in hydrological model calibration found that the conventional approach of calibrating hydrological models with older data and validating them with newer data results in inferior model performance.

The results showed that calibrating models with the full available historical data and omitting model validation altogether was the more robust choice (Shen et al., 2022).

These AquaCrop models, calibrated against soil moisture field data, served as the foundation for subsequent irrigation simulations, forming an integral component of the study.

3.8 Simulating irrigation requirements

The AquaCrop model offers an updated approach for estimating crop productivity with respect to water supply and agronomic management based on current concepts of plant physiology and soil-water budgeting (Raes et al., 2009). The model's robustness and ability to depict the impacts of water stress at specific growth stages make it valuable for assessing irrigation strategies and studying factors like climate, soil type, field management techniques, and sowing dates on crop production and water use efficiency. In this study, AquaCrop was employed under different irrigation strategies for each of the four calibrated crop models to estimate the historical irrigation requirements for the last 25 years (1997-2021). Furthermore, the models were used to predict the impact of climate change on the near (2050s) and far (2080s) future irrigation requirements.

3.8.1. Estimating historical irrigation requirements

Each of the calibrated AquaCrop models was used to estimate the net irrigation requirements for the last 25 years (1997-2021) for three different irrigation treatments. The climate data, such as temperature, relative humidity, wind speed, and solar radiation, were obtained as described in section 3.4.1 and input as a climate file. Agronomic management practices, such as planting date and weed control, were kept consistent to the farmer specifications. The crop and soil parameters remained unchanged from their field calibrated values summarized in Table 3-6. The crop file was converted from calendar day format to growing degree days to account for the variability in the duration of the crop cycle due to temperature over the growing season. It was found that calendar day mode made the model inadequately simulate crop growth and water use under non-optimum temperature conditions or for predicted climate change scenarios (Tsakmakis et al., 2019). The planting (or sowing) date was kept constant. For cranberry simulations, the groundwater table file used in model calibration was removed, so that the CWRs would represent the sum of sprinkler and sub-irrigation.

The irrigation file was set to determine the net irrigation requirements. Three irrigation treatments were investigated based on the maximum allowable depletion (MAD) of the available

water content (AW) of the soil. Irrigation was set to trigger when 20%, 35%, or 50% of the total available water in the soil had been depleted. In all cases, water was applied to bring the root zone soil moisture back up to field capacity.

Five dry, five average, and five wet years were identified by comparing the total rainfall over the crop growth period from 1997-2021. The mean simulation results of five years were calculated to represent the historical dry, average, and wet growing season weather conditions.

The simulated output was then compared statistically to evaluate the effects of irrigation treatment and weather on Inet, dry yield and water productivity. The statistical analysis was used to recommend the optimum irrigation strategy in dry, average, and wet growing season conditions.

3.8.2. Assessing the impact of climate change on irrigation requirements

Additionally, the models were used to predict the impact of climate change on the near (2050s) and far (2080s) future irrigation requirements. Each AquaCrop model was run for an ensemble of five GCMs under SSP5-8.5 scenario. The climate files were defined for each GCM and comprised the statistically downscaled climate data described in section 3.4.2. All other parameters remained consistent with the historical simulations. The three irrigation treatments were investigated, corresponding to an MAD of 20%, 35%, and 50% AW.

The simulated net irrigation demand for near and far future climate periods were compared to the baseline period (1997-2021), similarly to Busschaert et al. (2022), to assess changes in the mean irrigation requirements. The simulated results for each model in the ensemble were averaged over 30 years, typical to climate change crop simulation studies (eg. Bird et. al., 2016; Govere et al., 2022). The 2050s represents a 30-year average over 2036-2065, and the 2080s represents a 30-year average over 2066-2095.

The objective was to estimate the mean Inet for near and far future climate periods and relate this to the historical baseline. The effect of irrigation treatment and climate on Inet was investigated with a statistical analysis.

3.8.3. Statistical analysis of significance

The statistical significance of the irrigation treatment and weather or climate were tested using a two-way ANOVA with factorial interaction, executed with the GLM procedure in SAS Studio version 3.81 (SAS Institute Inc., Cary, NC). The significant differences of the F-test were determined at $p = 0.05$. Additionally, the least squared means (LS-means) were computed for each

main effect as well as their interaction, using the LSMEANS statement with a confidence level kept at $p = 0.05$.

3.9 Mapping regional irrigation water requirements

Next, the total irrigation requirements were mapped into water supply sectors to help propose an irrigation supply system. Mean monthly irrigation requirements were derived from the simulation results for the five historical dry years to represent the greatest demand of water. In addition to the simulated irrigation events, water requirements for frost and heat protection were considered for strawberry and cranberry crops, as well as water used for cranberry harvest flooding. The application efficiency was also taken into account for the main irrigation systems used. Gross depths of irrigation requirements were extrapolated over the irrigated cropland of the study area for each month of the growing season.

3.9.1. Frost and heat protection

Strawberry and cranberry growers in the studied region utilize their irrigation systems for frost protection in the spring. Therefore, by analyzing the hourly weather data over the five driest growing seasons, a depth of water was assumed for frost protection events according to respective threshold values for each crop. Strawberry critical thresholds and required rate of water depth were defined by the OMAFRA Factsheet: "Irrigation for frost protection of strawberries" (Shortt et al., 2022). The rate of water applied for strawberry frost protection was determined by the number of hours at a specific air temperature and wind speed. The critical air temperature for starting irrigation was adjusted based on dew point temperature since the lower the dew point, the sooner irrigation should start (Shortt et al., 2022). Developing cranberry buds are equally sensitive to low temperatures and often require irrigation to shield them from spring frost damage (Workmaster and Palta, 2006). Critical temperature at which protection must begin depends on the growth stage and cultivar (DeMoranville, 2000). The temperature thresholds and rates of water application were estimated from the works of Caron et al. (2017), Sandler and DeMoranville (2008), and Workmaster and Palta (2006).

Sprinkler irrigation for evaporative cooling of cranberry crops on very hot days was also considered. Activating sprinkler irrigation for a few minutes when a critical temperature threshold is reached is common cultural practice for cooling cranberry plants and preventing yield losses due to overheating. Research on photosynthetic light and temperature response curves of young

cranberry runners indicates that the peak leaf photosynthesis occurs when the leaf temperature reaches 30°C (Kumudini et al., 2004). Similarly, a recent study on cranberries in Quebec (Pelletier et al., 2016), found that the optimum temperature range for carbon dioxide assimilation was between 25 and 29°C. They determined that the critical temperature at which sprinkler irrigation should be turned on to avoid heat stress and maximize photosynthesis is 33°C, which corresponds to an air temperature of 28°C. When applying 1.5 mm of water via irrigation in the field, leaf temperature was reduced by 5–10°C (Pelletier et al., 2016). Therefore, for each day that the maximum temperature was greater than 28°C, it was assumed that 1.5 mm of water was applied for heat protection of cranberry crops, unless a simulated irrigation event was recorded that day.

3.9.2. Harvest flooding

Water harvesting takes advantage of cranberry fruit buoyancy to save labor costs and maximize berry collection (Sandler and DeMoranville, 2008). The local producer's estimates of water depth applied for harvest flooding was provided by the UPA de Lanaudière (2022). The mean depth from this data was assumed for harvest flooding in the month of October. The water used for flooding is reused by transferring it from field to field at each farm, whereas irrigation is mainly consumed and therefore represents the bulk of water consumed (Caron et al., 2016).

3.9.3. Irrigation system application efficiency

Application efficiency gauges the performance of an irrigation system to deliver a specific amount of water. It is calculated as the fraction of the water depth applied that is stored in the root zone and available for crop use. The water depth applied is also known as gross irrigation, whereas the target water depth intended for crop use is the net irrigation requirement. (Eisenhauer et al., 2021; Water Resources Program, 2023). Therefore, the gross, or applied irrigation depth can be calculated with:

$$\mathrm{I_{gross}} = \frac{\mathrm{AE}}{100\%} \cdot \mathrm{I_{net}} \qquad \textbf{(12)}$$

where: I_{gross} is the applied irrigation depth, AE is the average application efficiency of the irrigation system, and I_{net} is the net irrigation requirement. This calculation assumes uniform distribution over the field areas.

Application efficiency values were assumed by consulting irrigation engineering resources, as well as a main irrigation system supplier in the study area. The potato growers of the study area

primarily irrigate with low pressure center pivot systems, which typically range between 75% and 95% AE (Eisenhauer et al., 2021; Howell, 2004; Irmak et al., 2011; Lamm et al., 2019; Water Resources Program, 2023). An AE of 87% was assumed for potato considering that the center pivot systems are equipped with low-pressure rotator drop nozzles, which offer greater water efficiency (Harnois Irrigation, personal communication, 2021; OFA, 2004). The squash, cranberry, and strawberry producers at the field data sites irrigated with solid-set sprinkler systems. However, observations from the study area and communications with Harnois Irrigation (2021) highlighted a variety of systems used for vegetable and berry crops, ranging from drip irrigation to linear moving sprinkler systems, and the enthusiasm of producers moving towards more efficient systems. Therefore, remaining within the typical range of 70-85% for solid-set sprinkler systems (Eisenhauer et al., 2021; Howell, 2004; Irmak et al., 2011), an AE value of 80% was assumed for vegetable and berry fields to account for system diversity.

3.9.4. GIS analysis

Finally, the water requirements were upscaled from field estimates to the regional scale. To synthesize the irrigation requirements over the study area, the gross irrigation depths were extrapolated over the irrigated cropland in the GIS-environment ArcMap (Version 10.8; ESRI, 2023). The monthly estimates of total irrigation water, in mm, were multiplied by the field area of each of the respective crop groups. The resulting volumes of water per field were aggregated by proximity to identify areas of high demand, for each month of the growing season.

3.10 Water supply scenarios

As a preliminary assessment of potential water supply scenarios, possible pipeline dimensions were proposed for five irrigation sectors in the study area. Irrigation sector boundaries and water sources were determined with the project stakeholders. System flow requirements were designed to peak water use.

3.10.1. Volumetric flow rate

The hydraulic flow rate is the volume of water flowing past a given point in the pipe or channel per unit time, expressed in cubic meters per second. The flow rate is expressed with the following equation (Eisenhauer et el., 2021):

$$Q = v_{avg} A_{cs} \quad \textbf{(13)}$$

where, Q is the volumetric flow rate (m^3/s), v_{avg} is the average flow velocity (m/s), and A_{cs} is the cross-sectional area of the flow (m^2).

The peak monthly volumetric water demand was determined in each of the five sectors. From the simulated irrigation events of the main crops, this peak demand was assumed to be distributed over 15 days of irrigation. Potential flow rates were investigated for 12, 15, and 18 hours of pumping per day for each sector. Therefore, the peak flow rates corresponded to the peak monthly volume of water pumped for 12 hours per day over 15 days.

3.10.2. Pipeline diameter

As water moves through an irrigation system, pressure losses, or friction losses, are affected by factors such as the flow velocity, the inside diameter of the pipe, and the roughness of the pipe. Estimating friction losses is an important part of pipe flow analysis and pipe size selection for specific applications. Many empirical relationships have been developed to describe pressure drop in hydraulic flow due to frictional resistance, such as Manning's equation, the Darcy-Weisbach equation, and the Hazen-Williams formula (Satterfield, 2010; USDA, 2021).

Manning's equation applies to uniform flow in open channels and is commonly used for gravity pipe flow. It provides a relationship between the channel flow or velocity, and the flow area and channel slope (Bryant, 2017; Satterfield, 2010; USDA, 2021):

$$Q = \frac{K}{n} \cdot A_{cs} \cdot {R_h}^{2/3} \cdot S^{1/2} \quad \textbf{(14)}$$

where, Q is the volumetric flow rate (m^3/s); K is a constant that depends on the unit system (K = 1.0 for SI units); n is Manning's roughness coefficient; A_{cs} is the cross-sectional area of the flow (m^2); R_h is the hydraulic radius (m); and S is the hydraulic gradient or slope. When applied to pipelines, the hydraulic radius is defined as the ratio of the pipe's cross-sectional flow area A_{cs} to the wetted perimeter P, and therefore simplifies to $R_h = D/4$. Thus, Equation 8 rearranged to solve for pipeline diameter (D) becomes:

$$D = \left(\frac{4^{5/3}}{\pi} \cdot Q \cdot n \cdot S^{-1/2}\right)^{3/8} \quad \textbf{(15)}$$

The Hazen-Williams equation is the most commonly used formula for turbulent flow in pipes under pressure. The Hazen-Williams equation for circular pipes is (Eseinhauer et al., 2021; Satterfield, 2010; USDA, 2021):

$$Q = K \cdot C_{HW} \cdot A_{cs} \cdot {R_h}^{0.63} \cdot S^{0.51} \quad \textbf{(16)}$$

where, Q is the volumetric flow rate (m^3/s); K is a constant that depends on the unit system (K = 0.849 for SI units); C_{HW} is Hazen-William's roughness coefficient; A_{cs} is the cross-sectional area of the flow (m^2); R_h is the hydraulic radius (m); and S is the slope. With $R_h = D/4$, rearranging to solve for pipeline diameter gives:

$$D = \left(\frac{4^{1.63} \cdot Q}{\pi \cdot K \cdot C_{HW} \cdot S^{0.54}}\right)^{1/2.63} \quad \textbf{(17)}$$

Both Manning's equation and the Hazen-Williams equation were used to calculate pipeline diameter from volumetric flow rate, while considering duration of pumping, pipe material, and slope of the pipe. The pipe materials investigated were polyvinyl chloride (PVC), high-density polyethylene (HDPE), and steel. Slopes varied from 0.2% to 0.8%.

4. Results and Discussion

4.1 Meteorological data

4.1.1. Historical weather and trends

In this study, historical weather data (1997-2021) from the nearest weather station were explored, analyzed, and input into the AquaCrop models for the estimation of historical irrigation requirements. Weather data from 2022 were used in tandem with the field data collected for model calibration. Analyzing historical weather data for the growing season (May 1st to September 30th) revealed a 1-in-25 dry season in 2021, average season in 1998 and wet season in 2015, corresponding to 280 mm, 478 mm, and 602 mm of rainfall, respectively. Figure 9 illustrates substantial year-to-year fluctuations in total growing season rainfall, showing a decreasing trend from 2015 to 2021. Concurrently, there was a general upward trend in mean temperature. The 2021 growing season was the driest and second warmest with a total of 280 mm of rainfall and an average temperature of 18.9°C. This aligns with producers' concerns about increased pressures on irrigation resources and the difficulties they faced during the dry spells of 2021. Interestingly, the growing season ETo shows less variation year to year, ranging between 525 mm and 612 mm, and appears uncorrelated to rainfall. Therefore, rainfall, as well as its distribution throughout the growing season, is expected to have an important influence on the soil water balance. The reference year in which field data were collected was 2022.

Table **7** ranks the historical growing season weather data from least to greatest rainfall, highlighting the dry, average, and wet years in yellow, green, and blue respectively. The 2022 reference year, crucial for model calibration, is highlighted in grey. Considering the preceding 25 years, the 2022 growing season exhibited an above-average total rainfall (524 mm), a typical mean temperature (17.9°C), and standard ET_o (553 mm). Figure 10 depicts daily data for rainfall, ET_o, and maximum and minimum temperature during the 2022 growing season. Despite a 10-day dry spell in early May, rainfall events were distributed across the season. Air temperature reached a maximum of 33.1°C on August 7th and was accompanied by a rainfall event, which resulted in subsequently cooler temperatures. Compared to the historical dry year, an inferior need for irrigation was expected for 2022.

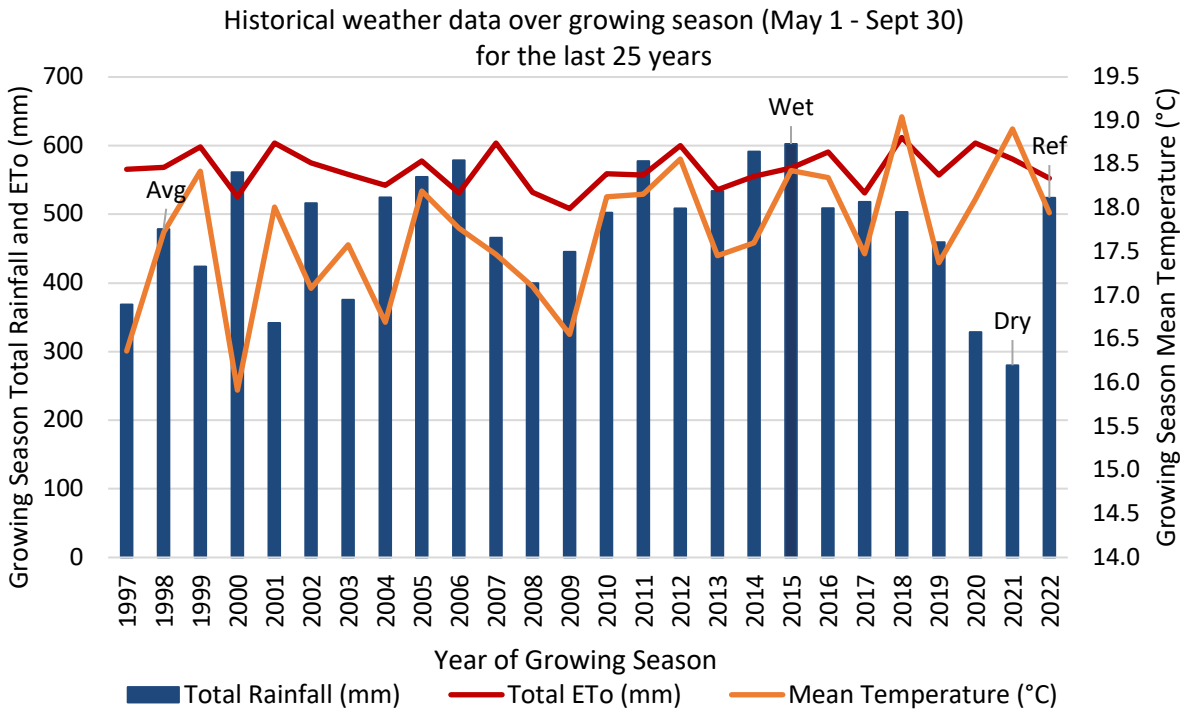

Figure 9. Historical weather data over the growing season from the L'Assomption weather station.

Table 7. Total rainfall, mean temperature, and total reference evapotranspiration, for the May to September growing seasons from L'Assomption weather data (ECCC L'Assomption, 2022).

Year	Total Rainfall (mm)	Mean Temp (°C)	Total ETo (mm)	Year	Total Rainfall (mm)	Mean Temp (°C)	Total ETo (mm)
2021	280	18.9	581	**2012**	509	18.6	600
2020	328	18.1	604	**2016**	509	18.3	591
2001	342	18.0	604	**2002**	516	17.1	575
1997	369	16.4	566	**2017**	518	17.5	531
2003	375	17.6	558	**2022**	524	17.949	552.9
2008	400	17.1	532	**2004**	525	16.7	542
1999	424	18.4	599	**2013**	534	17.5	536
2009	445	16.6	508	**2005**	555	18.2	577
2019	459	17.4	557	**2000**	561	15.9	525
2007	466	17.5	603	**2011**	577	18.2	557
1998	478	17.7	568	**2006**	579	17.8	531
2010	502	18.1	559	**2014**	591	17.6	555
2018	503	19.0	612	**2015**	602	18.4	568

Examining the historical dry years reveals fluctuating precipitation distribution across the months of the growing season. Figure 11 displays the total monthly rainfall depths for the five dry years: 1997, 2001, 2003, 2020, and 2021, as well as the maximum daily rainfall depth for each month. Notably, 2021 exhibited extended dry periods in late May, early June, and late July into August. The longest duration of consecutive days without rainfall occurred over a span of 16 days in August, during which the temperature exceeded 30°C on 8 days. While the cumulative precipitation in June reached 94 mm, a substantial proportion resulted from a single event om June 26th, contributing 55 mm. The air temperature reached a maximum of 34.6°C on June 7th, aligning with the peak daily ET_o of 7.9 mm. Similarly, in 2020, the peak growing season temperature (36.2°C) and ET_o (7.7 mm) occurred in May, accompanied by significant dry periods in May, June, and September. All five years experienced dry spells lasting at least 13 consecutive days, often coinciding with the warmest temperatures. Consequently, the variability and dispersion of rainfall events, along with peak temperatures, emphasize the necessity of supplementary irrigation to support crop growth. CWRs are anticipated to be substantial during months characterized by limited and unevenly distributed rainfall.

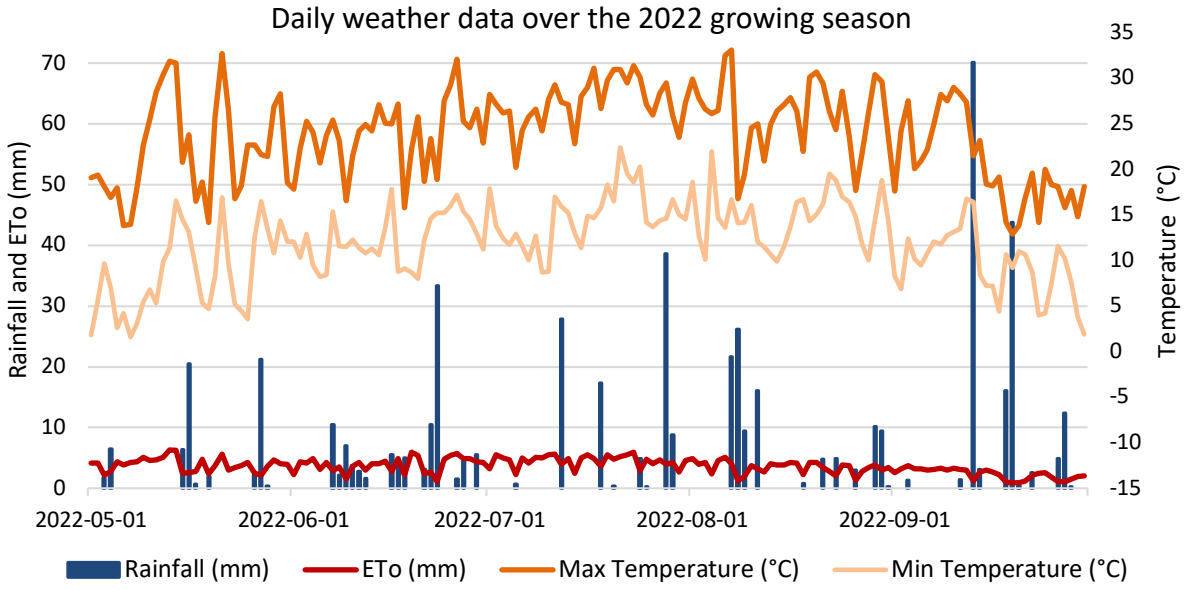

Figure 10. Daily rainfall, potential evapotranspiration, maximum temperature, and minimum temperature for the period of May 1st to September 30th, 2022.

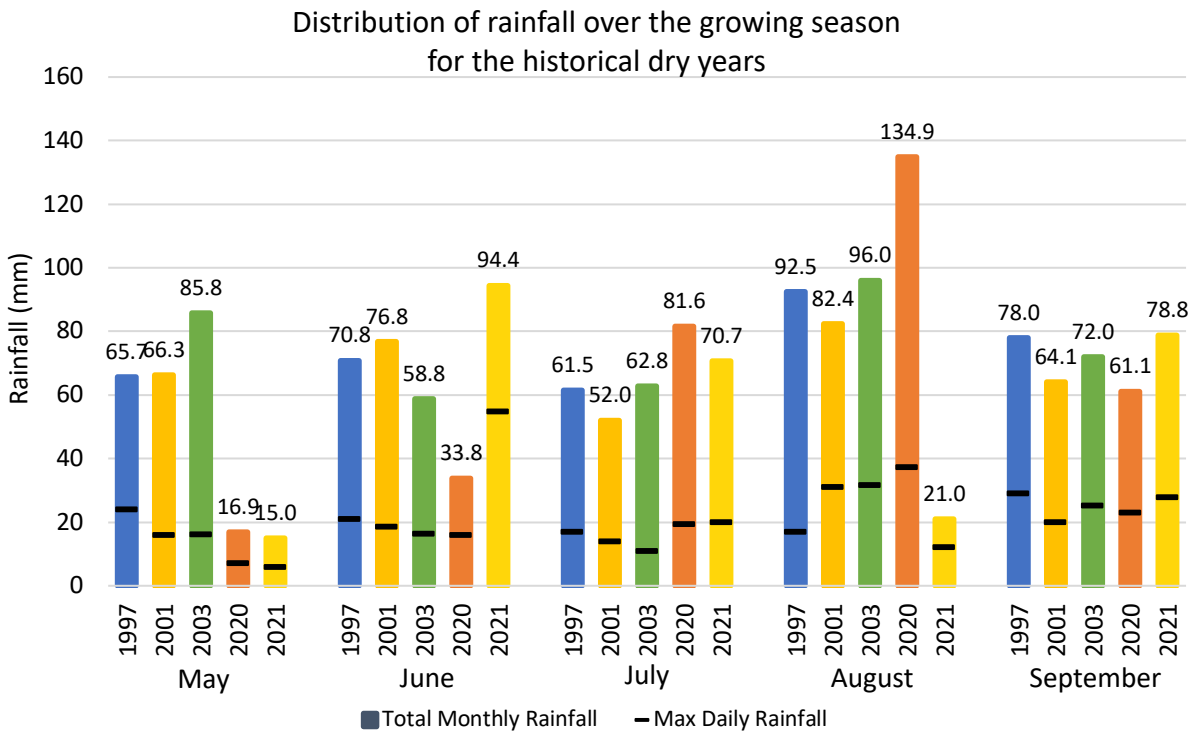

Figure 11. Rainfall distribution of historical dry years, showing total monthly rainfall (vertical bars), and maximum daily rainfall of respective months (horizontal marker).

4.1.2. Projected climate and trends

Climate variables predicted by the CMIP-6 model ensemble were imperative to examine the potential impact of climate change on irrigation demands in the study region. These variables were initially investigated before their integration into the crop-water model. The projected mean temperature and total precipitation over the growing season under SSP5-8.5 are illustrated in Figure 12 *(Climatic data provided by PCIC, Ouranos Inc., PCC, ECCC, CRIM, and Habitat7).* The mean temperature exhibits a discernible upward trajectory, with a simultaneous amplification in the variability among model predictions as the temporal scale extends further into the future. The precipitation during the growing season displays a rising variability from one year to another, alongside fluctuations within the ensemble. These short-term fluctuations and anomalies highlight the importance of averaging data over a 30-year period to provide a statistically stable representation of underlying climate patterns.

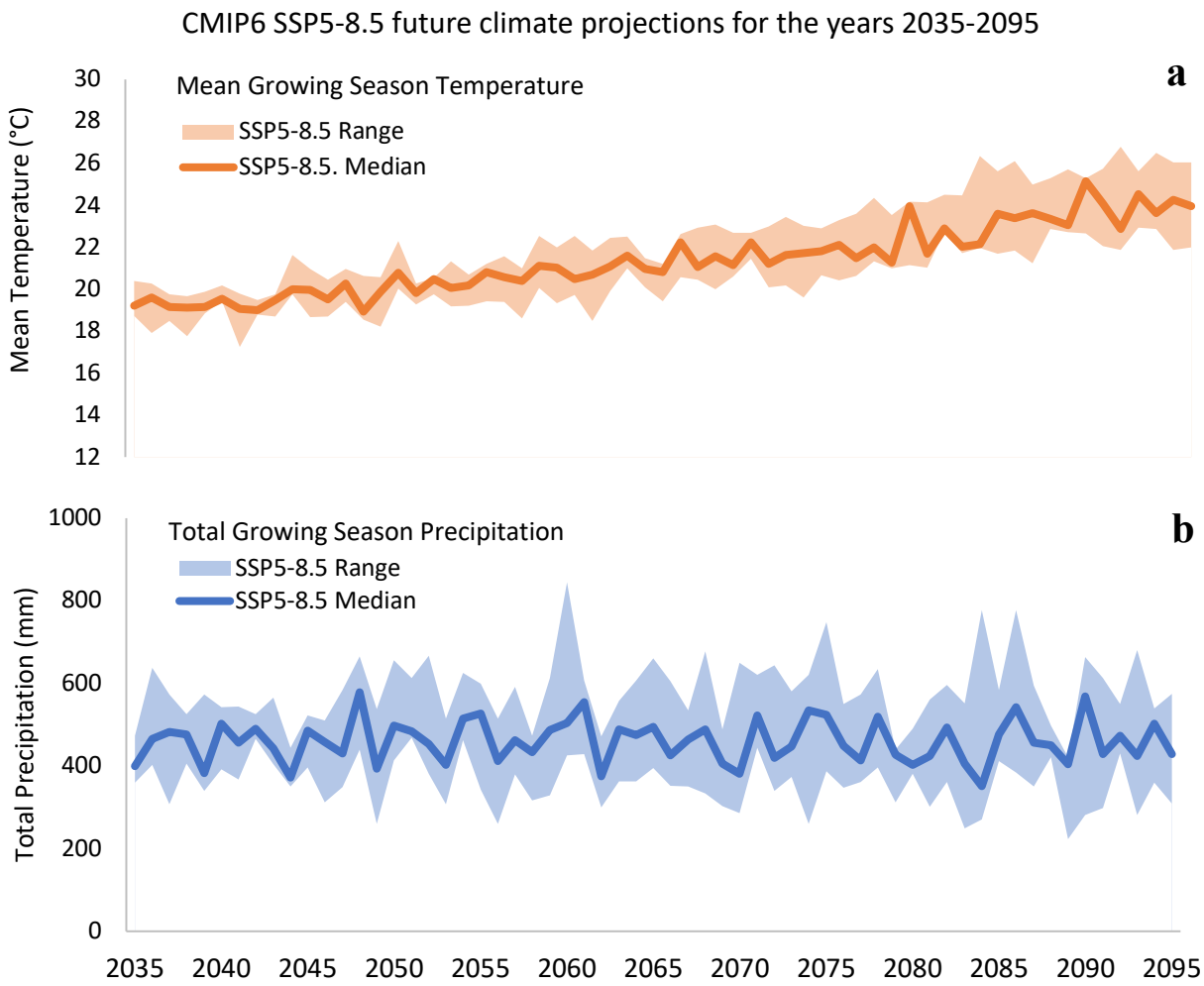

Figure 12. Projected mean temperature and total precipitation over the growing season for 5 GCMs (IPSL-CM6A-LR, CNRM-CM6-1, MIROC6, MIROC-ES2L, and CNRM-ESM2L) under SSP5-8.5 emission scenario.

The future changes in mean temperature and precipitation over the growing season compared to the historical baseline (1997-2021) are presented in Table 8, considering 30-year means. For all models of the ensemble, there is a systematic increase in mean temperature. From the ensemble median, an increase of 2.2°C and 6.7°C is predicted by 2050 and 2080, respectively. The higher increase is logically associated with the farther period given the pessimistic emission scenario. The growing season rainfall is projected to decrease by 6.5 mm by 2050 and by 15.4 mm by 2080 compared to the baseline, considering the ensemble median. However, there are within-ensemble disagreements regarding the direction of change in precipitation. Additionally, this assessment omits the seasonal distribution of rainfall. This stresses the importance of simulating irrigation needs on an annual basis and thereafter evaluating the 30-year mean of net irrigation requirements.

Table 8. Projected change in mean temperature and total precipitation over the growing season for the projected 2050s and 2080s, for each climate model, compared to the historical baseline period. Calculated from 30-year means.

Climate Model	2050s		2080s	
	ΔT_{mean} (°C)	ΔP_{total} (mm)	ΔT_{mean} (°C)	ΔP_{total} (mm)
IPSL-CM6A-LR	2.9	-11.6	6.7	-35.5
CNRM-CM6-1	2.5	-35.5	5.5	-56.7
MIROC6	2.2	-0.9	4.2	10.3
MIROC-ES2L	2.2	-6.5	4.3	-15.4
CNRM-ESM2L	2.2	28.8	4.8	5.1

4.2 Soil physical characteristics

As discussed in Section 3.5, the soil texture of each field site was analyzed in laboratory for two soil horizons. Figure 13 provides a summary of the particle size analyses for soils at the field sites, revealing a predominantly sandy soil classification. The distinctions in particle size distribution between samples from the two soil horizons (0-15 cm and 15-30 cm) at the same field were relatively minor. The strawberry and cranberry fields displayed a balanced distribution of fine, medium, and coarse sand particles, while the squash field featured primarily coarse sand. Intermediate to these, the potato field samples were predominantly composed of coarse and medium sand.

These analyses were intended to characterize soil water properties for the model's soil profile data requirements. However, challenges faced during experimentation, such as a low sample size, raised concerns about potential underestimation of silt and clay content in the experimental particle size analysis. A recent study aimed at improving the hydrometer method found that, compared to the more rigorous pipette method, measurements made using the hydrometer method consistently overestimated the sand fraction (Mwendwa, 2022). Also, due the high sand content, the coarse fraction analysis resulted in insufficient sample mass for the small fraction analysis. Therefore, in addition to field sampled bulk density, soil texture reported by IRDA Quebec pedological data were utilized to obtain the soil physical attributes with the SWCC model's pedo-transfer function developed by Saxton et al. (2006). In an AquaCrop validation study for rainfed maize production in Pennsylvania, Mebane et al. (2013) also employed bulk density and soil survey particle size data to estimate hydraulic parameters. Furthermore, a large-scale field experiment found that crop

model inversion using surface soil moisture measurements is a powerful method for estimating available water content components, namely FC and WP (Krishnan Kutty et al., 2017). Thus, the FC and WP were subsequently calibrated to the field conditions, within a reasonable range for the soil class.

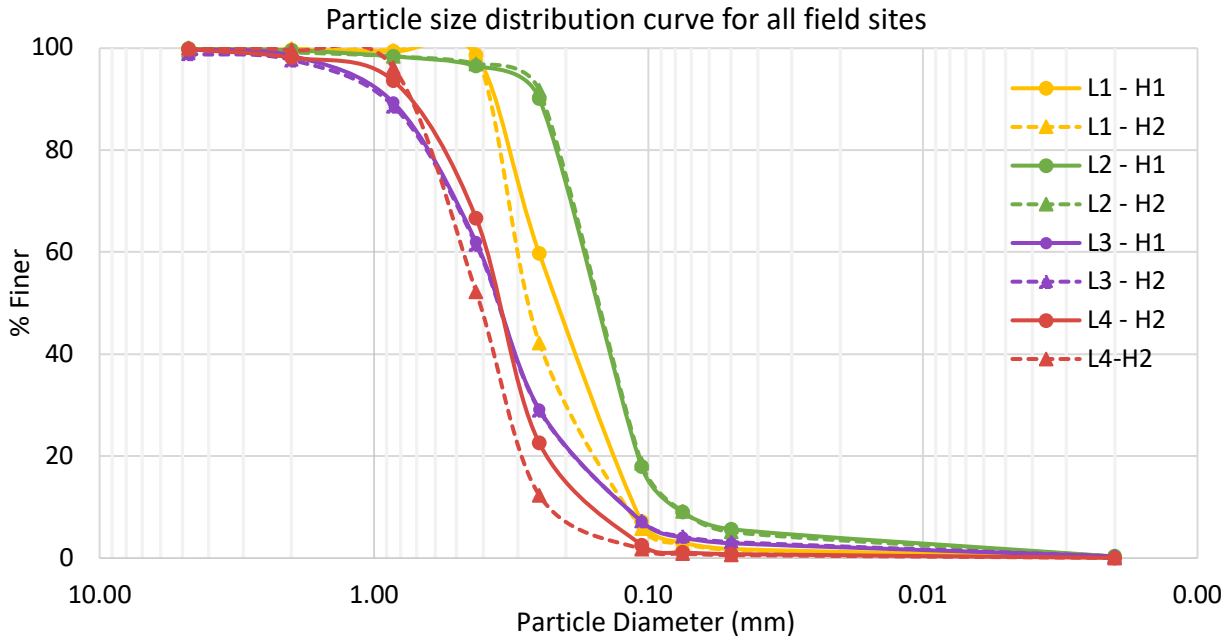

Figure 13. Particle size distribution of potato (L1), squash (L2), strawberry (L3), and cranberry (L4) for surface (H1) and root zone (H2) soil horizons.

The soil physical attributes derived from the SWCC are reported in Table 9. Wilting point varied between 3.5% and 6.5% volumetric water content, in agreement with typical values for sand (2-7%) and loamy sand (4-9%) soil texture classes (Allen et al., 1998; Eisenhauer et al., 2021; Hignett and Evett, 2008). Field capacity ranged between 9.6% and 13.7%, consistent with typical field capacity values for sand (8-16%) and loamy sand (13-20%). Similarly, the available water content of L1 (66 mm/m), L2 (51 mm/m), and L3 (61 mm/m) fell within the typical range of 50-70 mm/m for sand, while the L4 available water content (72 mm/m) was within the range of 70-90 mm/m for loamy sands (Allen et al., 1998; Eisenhauer et al., 2021; Hignett and Evett, 2008). The total available water content for the investigated soil depth is estimated in the last column of Table 9. TAW is used to simulate different irrigation regimes based on maximum allowable depletion.

Table 9. Soil physical characteristics of the 2022 field sites (computed by the SWCC pedo-transfer model by Saxton et al., 2006).

Field Site	Soil Class	FC (vol%)	WP (vol%)	SAT (vol%)	K_{sat} (mm/hr)	AW (mm/m)	Depth (m)	TAW (mm)
L1	Sand	10.1	3.5	53.0	193	66	0.3	20
L2	Sand	9.6	4.5	48.7	157	51	0.33	15
L3	Sand	11.9	5.8	47.6	141	61	0.2	12
L4	Loamy Sand	13.7	6.5	49.5	99.7	72	0.3	19

4.3 Soil moisture dynamics

In this study, soil moisture levels were monitored at four field sites. At L1, L2 and L3, continuous capacitance sensor readings of volumetric water content (VWC) were calibrated with reference gravimetric measurements. Regression analyses were conducted for each capacitance sensor, employing various equations, such as polynomial, logarithmic, and linear models. The results indicate superior correlation performance with the linear regression model, as opposed to logarithmic and polynomial equations, where the latter demonstrated tendencies to over-fit the data. Sample calibration plots are provided in Figures A1 and A2. The highest correlation was observed at the L2 field site, characterized by a regression coefficient of 0.91. This is likely attributed to the wider range of soil water content values measured at the L2 site as opposed to the L1 and L3 sites, where soil moisture readings were relatively proximate at the time of the gravimetric assessments. The extent of the direct VWC measurements was constrained due to field visits predominantly occurring mid-day under dry conditions, limited access to the study area, and the inherent low water holding capacity of sandy soils. Unfortunately, capacitance sensors could not be installed at L4 due to limited access to the site and the sensitivity of the cranberry plants. SMP from tensiometers at L4 were converted to VWC for compatibility with the AquaCrop model.

The soil moisture data for each field site are presented below. Although the soil water response aligned with weather patterns, irrigation application, and crop water uptake, enhanced accuracy and confidence could be achieved through the acquisition of additional soil moisture sensors. This would enable additional replicates and a more comprehensive distribution throughout the site and soil depths to represent field conditions. Furthermore, the conversion from matric potential to

volumetric water content for the cranberry site introduces possible sources of error from the soil characteristics used to estimate the van Genuchten parameters.

4.3.1. L1 field site soil moisture

Figure 14 illustrates the temporal dynamics of soil moisture at the potato field site, presenting continuous sensor readings and gravimetric measurements at two depths. Overall, volumetric water content at a 5 cm depth (depicted in green) shows a more pronounced response to rainfall events compared to the 30 cm depth (depicted in orange). The diminished impact of rainfall on soil moisture at greater depths can be attributed to the superficial root system of the potato crop. The maximum root density is concentrated in the upper 30 cm of soil (Djaman et al., 2022; King et al. 2020; Opena and Porter, 1999; Paredes et al., 2018), which is where the fastest water absorption occurs (Fulton, 1969). In a study on SWC monitoring for irrigated potatoes on sandy soils, Alva (2008) found that water uptake by the plants was primarily at the 0 to 30 cm depth soil, with the major portion of the water uptake being around the 10 cm soil depth. Thus, the observed disparity between the surface and deeper sensor readings reflects the plant water uptake. As a result, only the effects of large rainfall events are observed in VWC readings at 30 cm, during which the water infiltration rate surpassed the plant's water absorption rate.

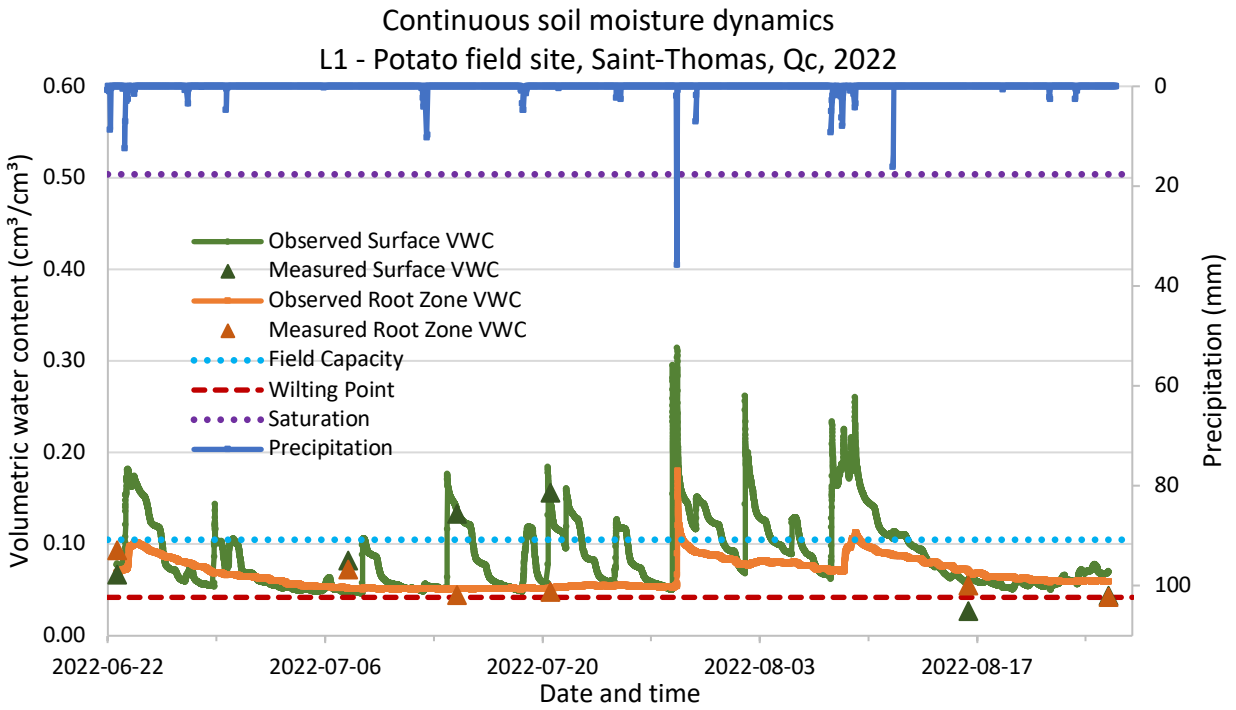

Figure 14. Temporal variation of volumetric water content at 5 cm and 30 cm depths during the 2022 season at the L1 field site. Includes sensor observations, gravimetric measurements, hourly precipitation (ECCC), and critical soil moisture levels.

The average daily VWC is presented in Figure 15, along with daily rainfall and irrigation depths. Over the period of data collection (June 23rd to August 24th, 2022), the VWC at 5 cm and 30 cm was approximately 0.087 (mean) ±0.034 (standard deviation) cm^3/cm3 and 0.067 ±0.015 cm^3/cm^3, respectively. The minimum root zone VWC occurred in July and August. This coincides with the highest rate of absorption during the tuber initiation and bulking. During these critical stages, tubers grow rapidly and consist of 72-86% water (Curwen, 1994; Pavlista, 1995). VWC surpassed FC after notable rainfall and irrigation events. These peaks typically persisted for only short time periods (1-2 days), reflecting the low water holding capacity of the sandy soil. In agreement with field observations, soil moisture was well below the saturation point throughout the season and did not reach below the permanent wilting point. However, the low VWC observed at the start of July and middle of August, correlated to an absence of rainfall or irrigation, suggests that the crop experienced periods of soil water deficit.

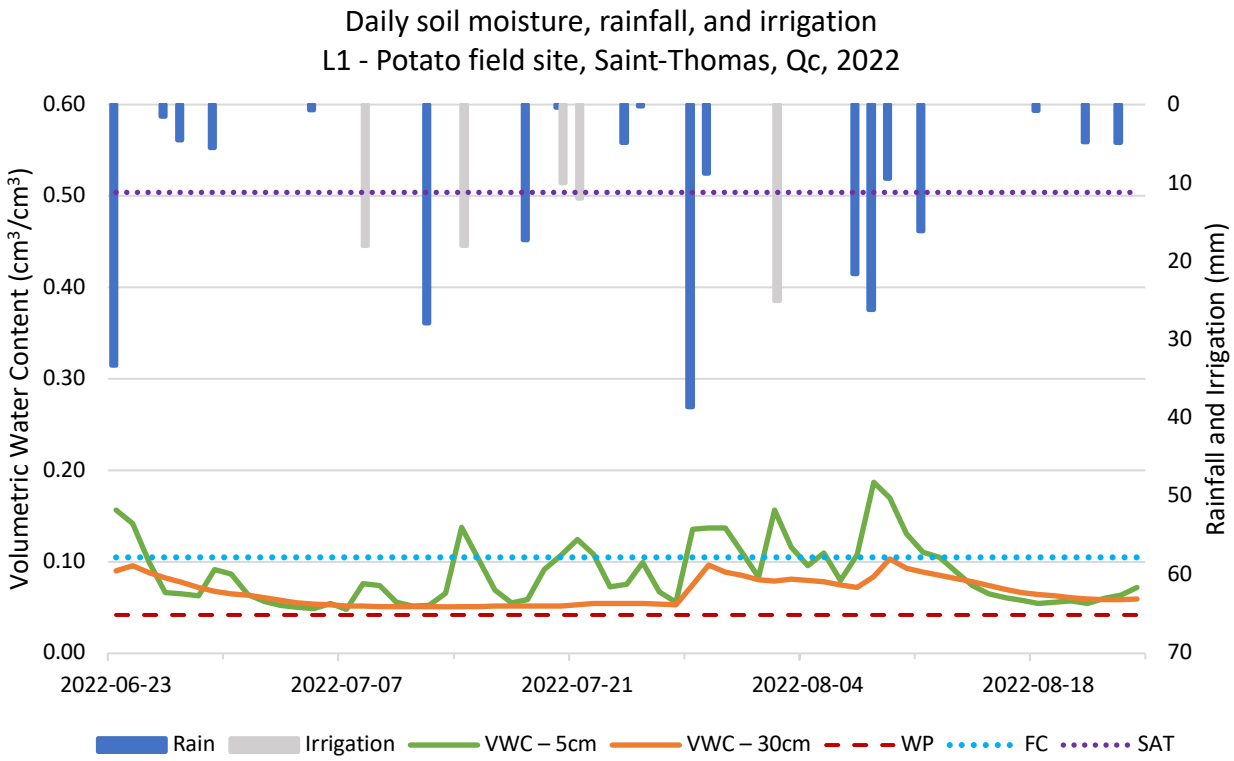

Figure 15. Daily volumetric soil water content at 5 cm and 30 cm depths during the 2022 season at the L1 field site. Includes averaged daily sensor observations, precipitation, irrigation, and key reference points.

The distribution of soil moisture over soil depth observed at L1 was consistent with studies investigating soil moisture dynamics in potato fields (e.g., Kumar et al., 2020; Liao et al., 2016; Yost et al., 2019). For example, Alva (2008) observed sharp jagged VWC trends at shallow soil depths, correlating to rainfall and irrigation, while lower soil depths, such as 30 cm, experienced smoother, and often drier soil moisture conditions. In general, the temporal and depth-related soil moisture dynamics at the L1 site aligned with the observed rainfall patterns, irrigation practices, and the developmental stages of the potato crop.

4.3.2. L2 field site soil moisture

Figure 16 displays the temporal dynamics of soil moisture at the squash field site, presenting continuous sensor readings and gravimetric measurements at two depths. In general, volumetric water content at a 5 cm depth (depicted in green) and 20 cm depth (depicted in orange) follow a similar pattern throughout the growing season. The VWC in the root zone was typically greater than at the soil surface, especially after periods without rainfall. This is likely due to a combination of evaporation at the soil surface and higher absorption rates by plant roots near the surface. Soil

moisture peaks due to rainfall events are followed by a gradual decrease in VWC, pointing to higher water retention capabilities compared to the L1 field site.

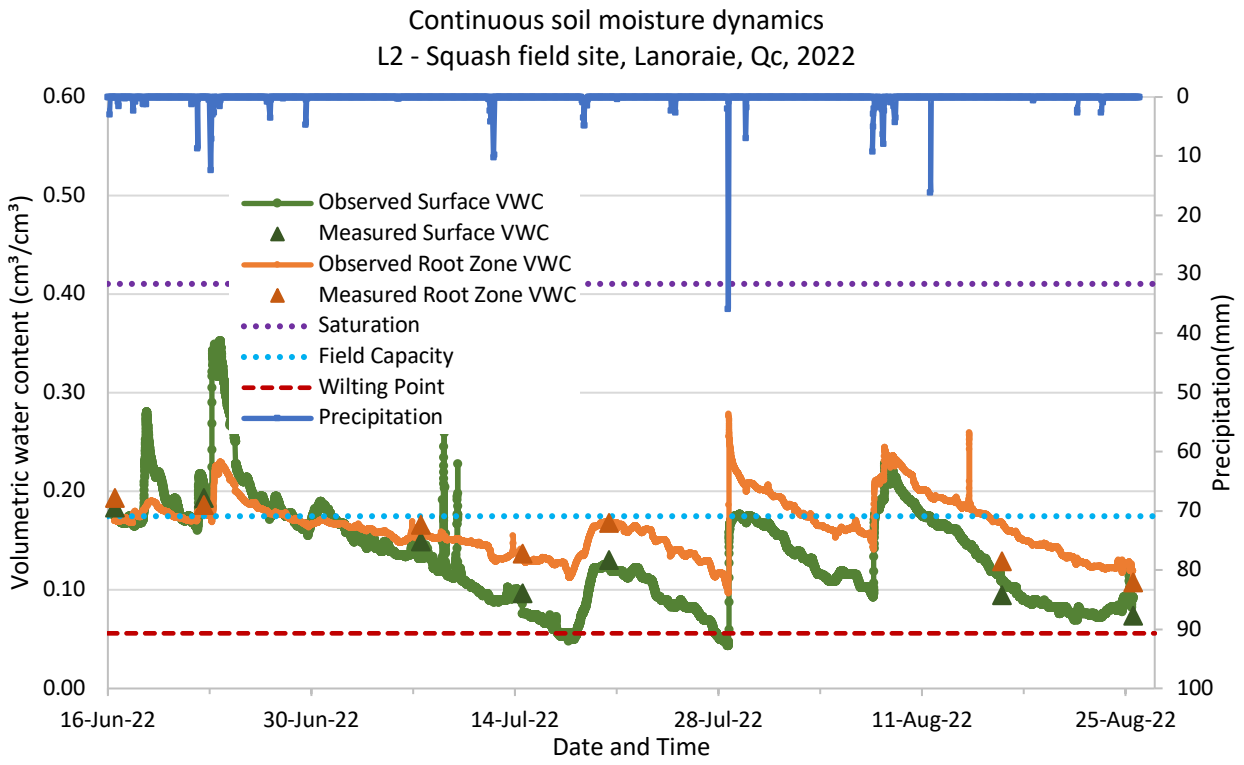

Figure 16. Temporal variation of volumetric water content at 5 cm and 20 cm depths during the 2022 season at the L2 field site. Includes sensor observations, gravimetric measurements, hourly precipitation (ECCC), and critical soil moisture levels.

The average daily VWC at L2 is displayed in Figure 17, including daily rainfall and irrigation applications. Throughout the growing season, from June 17th to August 24th, 2022, the mean VWC at 5 cm was 0.136 ±0.049 cm^3/cm^3, while at 20 cm it was 0.164 ±0.026 cm^3/cm^3. Peaks in VWC correlated with large rainfall events, excluding the 28 mm precipitation on July 12th. The relatively stable soil moisture on that day may indicate different weather conditions between the weather station location and the field site. This could also suggest increased water absorption by the developing roots. Additionally, the impact of the July 8th irrigation event on VWC was likely attenuated by increased water uptake during flowering and fruit formation.

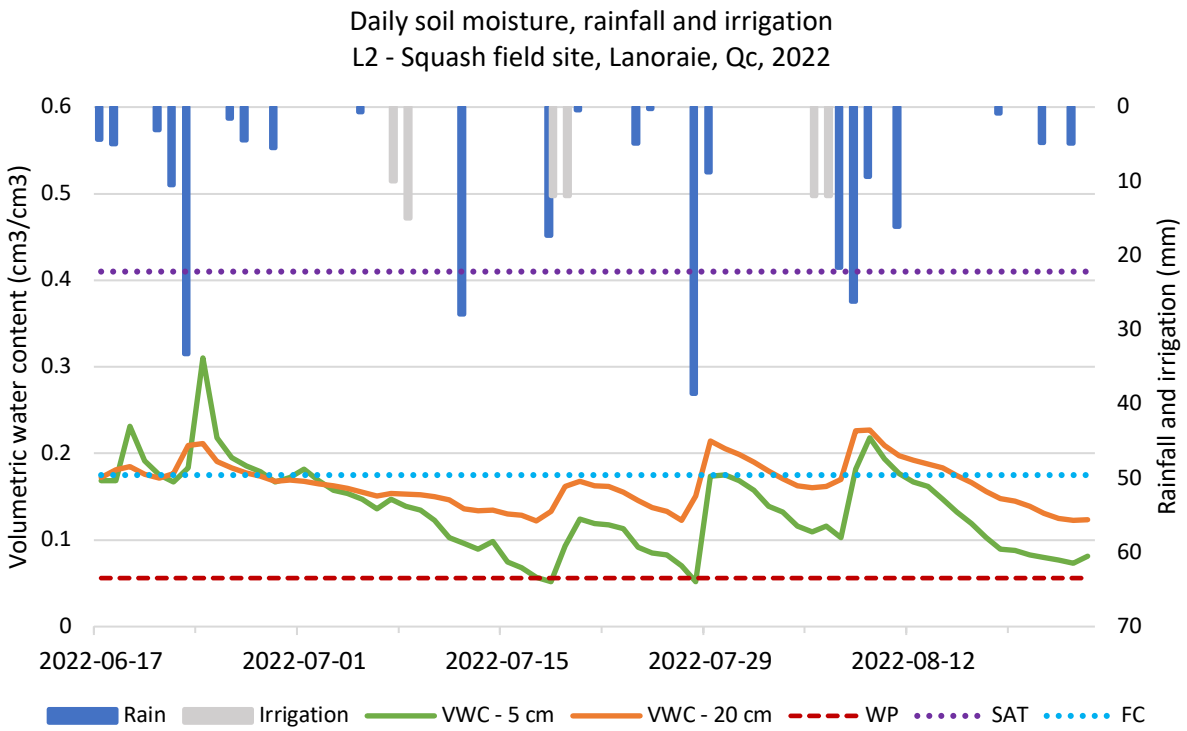

Figure 17. Daily volumetric soil water content at 5 cm and 20 cm depths during the 2022 season at the L2 field site. Includes averaged daily sensor observations, precipitation, irrigation, and key reference points.

4.3.3. L3 field site soil moisture

The continuous sensor readings and gravimetric measurements of volumetric soil water content at the strawberry field site are presented in Figure 18. The impact of rainfall and irrigation application on soil moisture is apparent. Similar to the L1 field site, a more pronounced response in volumetric water content near the surface (5 cm) compared to the root zone (15 cm) is observed. Between June 16th and September 29th, 2022, the mean VWC at a depth of 5 cm, was 0.186 ±0.027 cm^3/cm^3. At 20 cm, the mean VWC was 0.171 ±0.014 cm^3/cm^3. This disparity is attributed to the shallow depth of strawberry root systems, typically concentrated in the upper 15 cm of soil (AAFC, 2021; Morillo et al., 2015). The soil has good drainage, noticeable after rainfall events.

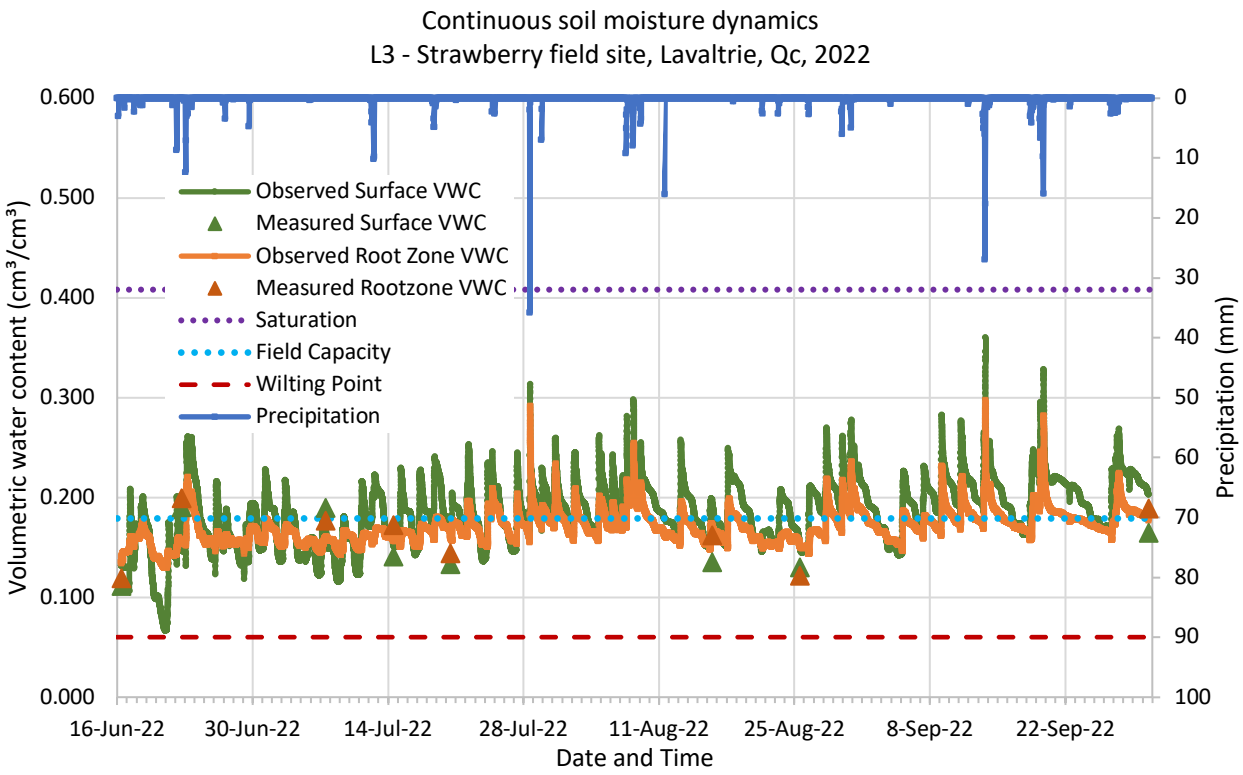

Figure 18. Temporal variation of volumetric water content at 5 cm and 15 cm depths during the 2022 season at the L3 field site. Includes sensor observations, gravimetric measurements, hourly precipitation (ECCC), and critical soil moisture levels.

Daily mean VWC, total precipitation and irrigation applied are presented in Figure 19. The temporal dynamics of soil moisture over the growing season mirror the regimented irrigation schedule provided by the agronomist. Given that this field's strawberry crop was dedicated to producing plants for distribution, meticulous monitoring of soil moisture occurred. To facilitate optimal root growth and inhibit premature flowering and fruit formation, the approach involved the application of small, frequent irrigation depths. Therefore, the irrigation schedule ensured that no soil water deficits occurred.

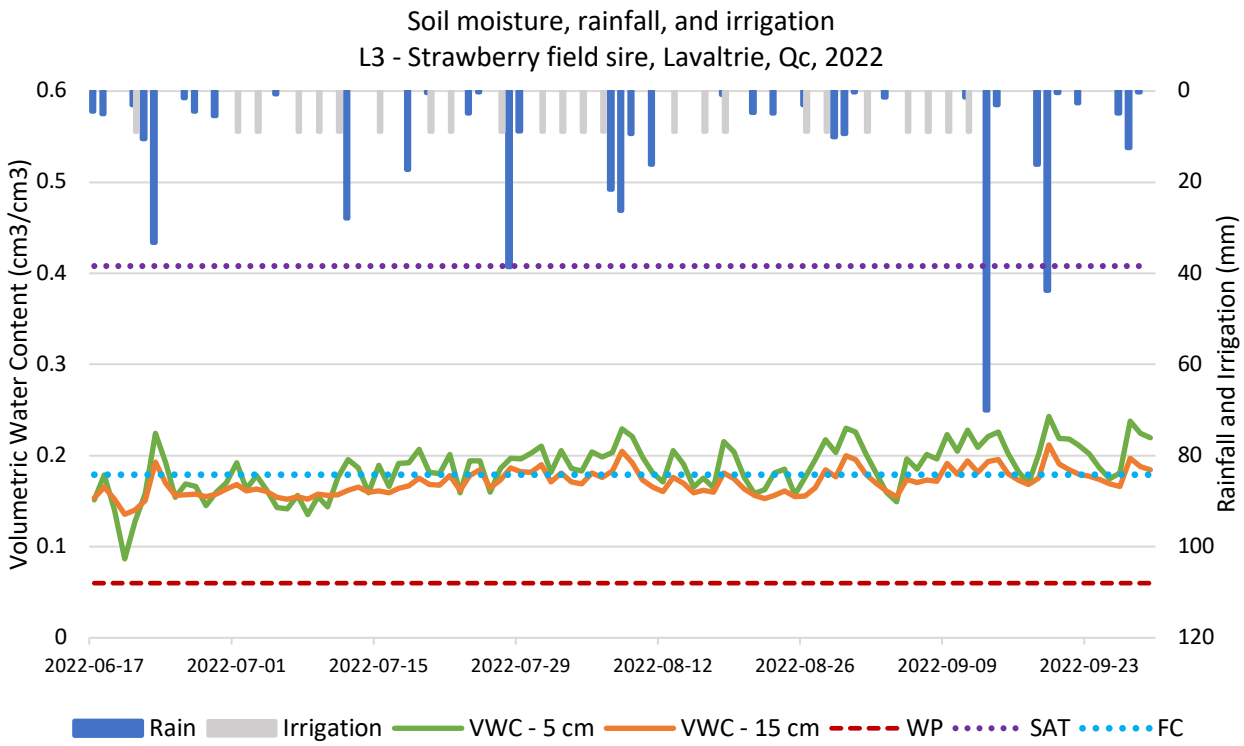

Figure 19. Daily volumetric soil water content at 5 cm and 15 cm depths during the 2022 season at the L3 field site. Includes averaged daily sensor observations, precipitation, irrigation, and key reference points.

4.3.4. L4 field site soil moisture

The continuous tensiometer readings of SMP at a depth of 10 cm are presented in Figure 20. Soil water excess was observed in the spring and as a response to rainfall events. While cranberry crop growth is sensitive to water stress during fruit development from mid-June to early September (Pelletier et al., 2015a, 2015b), July and August are the most critical months, corresponding to flowering and fruit formation (Jeranyama et al., 2017). During these months, the monitored soil water conditions conformed to the recommended range of root zone SMP, between −4 kPa and −8 kPa, as suggested for optimal cranberry production (Caron et al., 2016, 2017; Jabet et al., 2016; Pelletier et al., 2015a). Temporary drier conditions were noted on July 28th and September 4th, potentially in anticipation of forecasted rainfall events. Specifically, 39 mm of precipitation occurred on July 28th, aligning with a substantial rise in SMP. Despite a comparable increase observed on September 4th, no recorded rainfall occurred on that day. This discrepancy could be attributed to variations between conditions at the weather station and those at the field site.

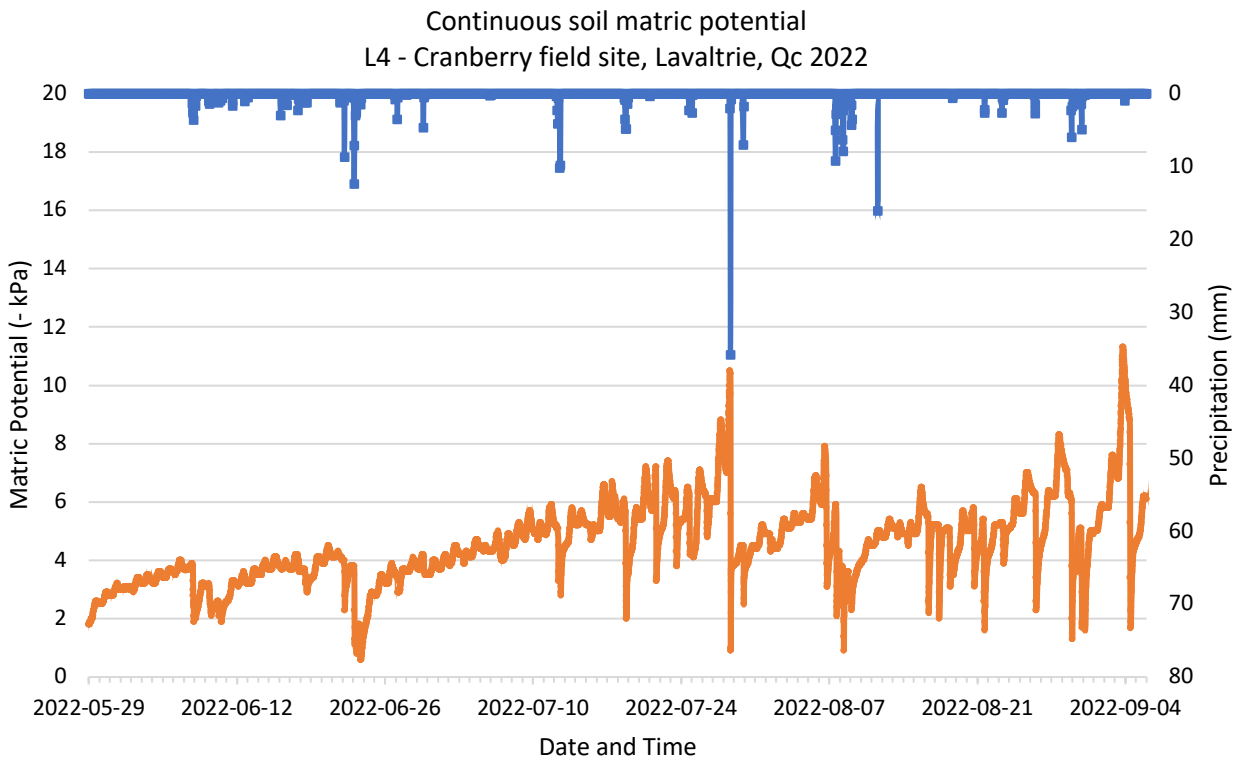

Figure 20. Temporal variation of soil matric potential at 10 cm depth during the 2022 season at the L4 field site. Includes tensiometer observations (Hortau) and hourly precipitation (ECCC).

The soil matric potential data were converted to volumetric water content using the van Genuchten-Mualem model. The essential coefficients governing the relationship between soil matric potential and volumetric water content, known as the van Genuchten parameters, were determined based on the soil texture (ARDA) and measured bulk density. They are outlined in **Table 10**. The resulting daily mean volumetric water content (VWC) at a depth of 10 cm is depicted in Figure 21.

Table 10. Van Genuchten model parameters for sandy loam soil at the L4 field site.

θ_r ($cm^3\ cm^{-3}$)	θ_s ($cm^3\ cm^{-3}$)	$\propto$ (cm^{-1})	n	m
0.049	0.402	0.036	2.14	0.532

Peaks observed in daily VWC correlate to rainfall and irrigation events (Figure 21). Over the period from May 1st to September 30th, 2022, the average VWC was 0.245 cm^3/cm^3 with a standard deviation of 0.052 cm^3/cm^3. The fine and fibrous roots of the cranberry plant typically extend to

depths of 7–15 cm below the soil surface (Sandler and DeMoranville 2008). Thus, the placement of the tensiometer at a depth of 10 cm suggests that it may be situated beneath the soil layer experiencing the most significant water uptake through the roots. Thus, as well as the ample rainfall during the growing season, the elevated moisture in the soil can be attributed to the influence of sub-irrigation practices in the cranberry bog. Optimal cranberry yield and reduced irrigation usage for cranberry production in Quebec were achieved when controlling water table at a depth of 60 cm (Pelletier et al., 2015b). Therefore, assuming ideal water table control at the field site, capillary rise significantly contributes to soil moisture content.

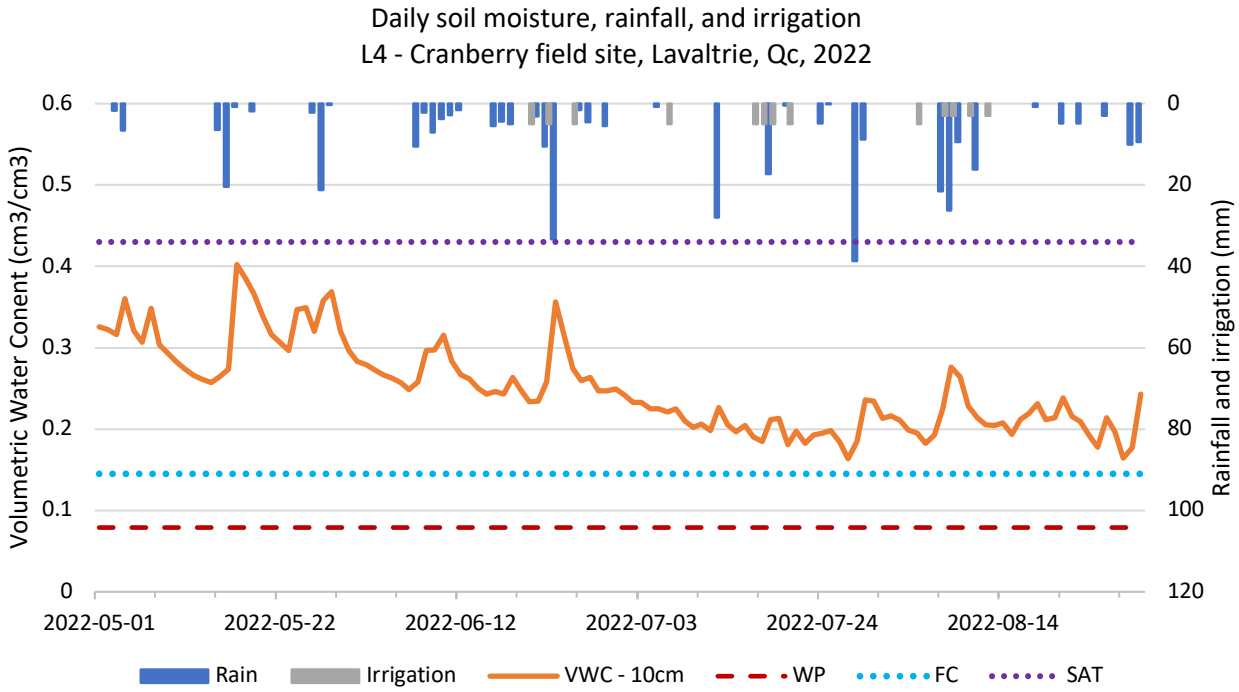

Figure 21. Daily volumetric soil water content at 10 cm depth during the 2022 season at the L4 field site. Includes averaged daily VWC, precipitation, irrigation, and key reference points.

4.4 Calibration of AquaCrop models

To estimate irrigation requirements, the AquaCrop model simulates the soil water balance in daily time steps. In the soil water balance, the root zone can be regarded as a reservoir. By tracking the inflow and outflow of water at the boundary, the fluctuations of soil water content in the root zone can be monitored. In this study, the observed soil water content (SWC) in the root zone was compared to the SWC simulated by AquaCrop for each crop during the 2022 growing season.

Subsequent subsections detail the performance of individual crop models after model calibration. The calibration performance of all four models is summarized in **Table 11** in Section 4.4.5.

4.4.1. Potato grown in Lanoraie fine sand

The sensitivity analysis, following the methodology outlined by Geerts et al. (2009) identified field capacity and wilting point as highly and moderately sensitive parameters, respectively. Conversely, the maximum canopy cover, saturated hydraulic conductivity, and curve number had low sensitivity. This highlights the need for precise field measurements and model calibration of the soil water retention parameters (FC and WP) to enhance the accuracy of simulating soil water content.

Figure 22 presents the comparison between simulated and observed soil water content (SWC) in the effective root zone of the potato crop at the L1 field site. AquaCrop's simulated SWC aligned well with observed trends, responding effectively to precipitation and irrigation inputs. Overall, there was a strong agreement between observed and simulated SWC, indicated by a Pearson correlation (r) of 0.88 and Wilmott index of agreement (d) of 0.91. The model estimated SWC with satisfactory accuracy for the 2022 field conditions, with a Root Mean Square Error (RMSE) of 5.3 mm, Normalized RMSE (NRMSE) of 21.8%, and Nash-Sutcliffe Efficiency (EF) of 0.54. These results are similar to the findings of Montoya et al. (2016), Razzaghi et al. (2017), and Wang et al., (2023), who used AquaCrop to simulate soil water content in potato fields under various irrigation treatments. They found r values between simulated and observed SWC for different irrigation levels varying between 0.67 and 0.86, 0.58 and 0.96, and 0.63 and 0.95, respectively. Furthermore, for 8 calibration fields of quinoa, Geerts et al. (2009) simulated SWC in the 30 cm root zone with an average EF of 0.59. Although this study's RMSE was lower than the range reported range by Wang et al. (6.1-11.5 mm), it is important to note that they simulated SWC across a greater soil depth (0-50cm), and therefore had a lower error when normalized. Minor discrepancies, with slight overestimations and underestimations, were observed at the extreme ranges of SWC (Figure 23). Similar trends were noted by Montoya et al. (2016) when SWC approached or exceeded Field Capacity (FC) or neared Wilting Point (WP). These variations in soil water dynamics could stem from the parametrization of soil water characteristics or from disparities in rainfall amounts at the field site compared to the weather data. Taking into account the results from these other studies, the calibrated potato model performed well at simulating SWC at the L1 field site and could be enhanced with field data from additional sites and growing seasons.

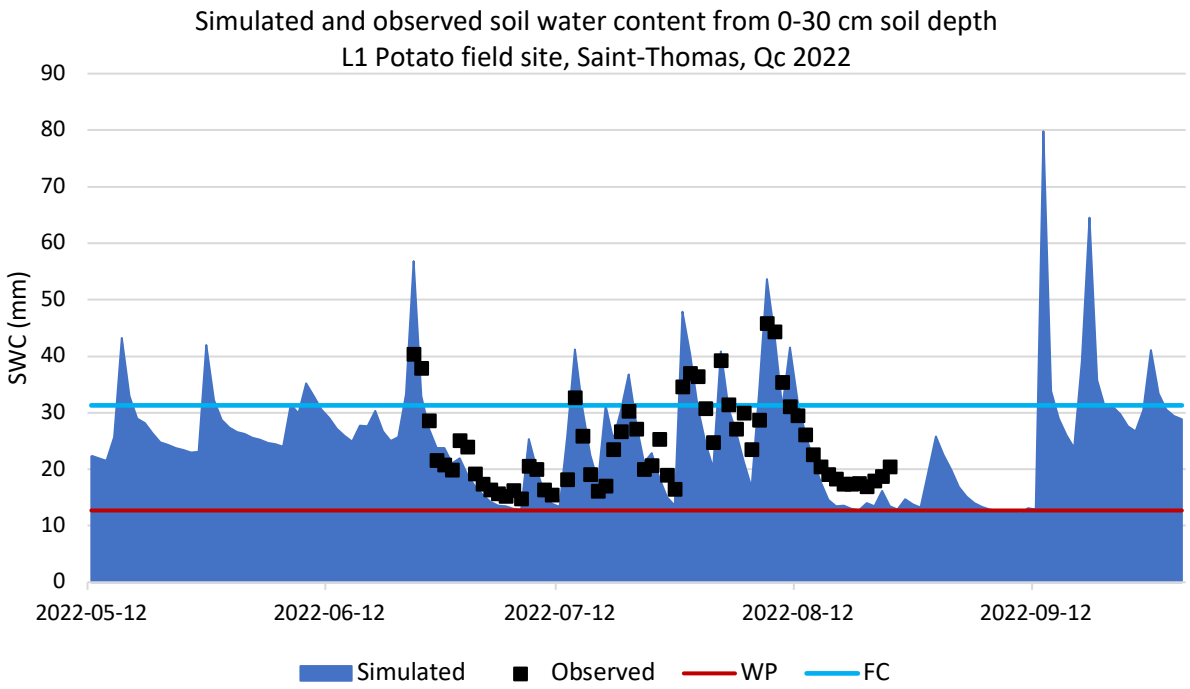

Figure 22. Simulated and observed soil water content (SWC) in the effective potato root zone (0-30 cm) at L1 over the 2022 growing season, including wilting point (WP) and field capacity (FC).

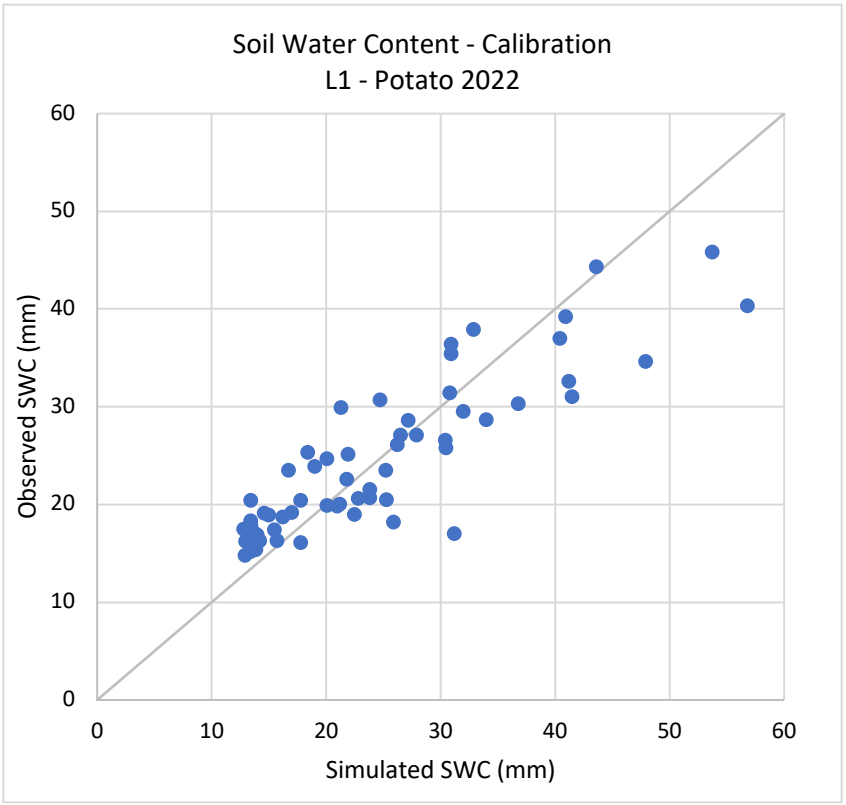

Figure 23. Simulated and observed soil water content from 0-30 cm depth at L1.

4.4.2. Squash grown in Saint-Thomas fine sand

For the squash model, field capacity was also identified as a highly sensitive parameter in simulating SWC, while the crop transpiration coefficient ($K_{c\ Tr}$) showed moderate sensitivity. Due to the absence of a default crop file for squash in AquaCrop, it was initiated with a $K_{c\ Tr}$ calibrated to 0.90. This value is within the reference range of winter squash values of 0.90 to 0.95 (Allen et al., 1998; Pereira et al., 2021) as well as calibrated values of 0.85 to 0.98 for zucchini squash (Darouich et al., 2020). Parameters such as initial and maximum canopy cover, canopy decline coefficient, shape factor for root zone expansion, wilting point, saturated hydraulic conductivity, and curve number exhibited low sensitivity. The sensitivity analysis of the squash model reinforced the dependence of the SWC calculation procedures on soil water retention parameters, such as FC. In addition, reference values of crop coefficients can serve as an essential starting point for calibrating conservative crop parameters that are not previously established in the model's database.

The simulated and observed soil water content (SWC) in the root zone of the squash crop at the L2 field site are presented in Figure 24. In general, the model estimated SWC for the 2022 field conditions with acceptable accuracy, with an r of 0.76, RMSE of 8.7 mm, NRMSE of 19.2%, EF of 0.35, and d of 0.84. AquaCrop's simulated SWC matches the response of the observed SWC to rainfall and irrigation events, except in the case of the precipitation on July 12th, which was previously discussed in section 4.3.2. It is hypothesized that there were differences between the data from L'Assomption weather station and the actual conditions in the field. Furthermore, there is a slight tendency to underestimate SWC, particularly at the start of the crop period (Figure 25). Similar trends were observed by Mebane et al. (2013) who validated the AquaCrop model for maize production in Pennsylvania. They also used field bulk density and sand, silt, and clay proportions from soil survey data to derive soil water characteristics from pedo-transfer function model. Therefore, the model's estimated soil hydraulic characteristics may differ from the actual values in the field, which could be responsible for disagreement of simulated and observed SWC. There could also be error associated with the estimated irrigation depths and schedule provided by the producer. However, for the planning and management of regional irrigation requirements, a bias toward underestimation of SWC is preferred to overestimation to ensure that sufficient water needs are met. Therefore, while the model's performance is acceptable, it is limited to the accuracy of the data acquired for the L2 field site.

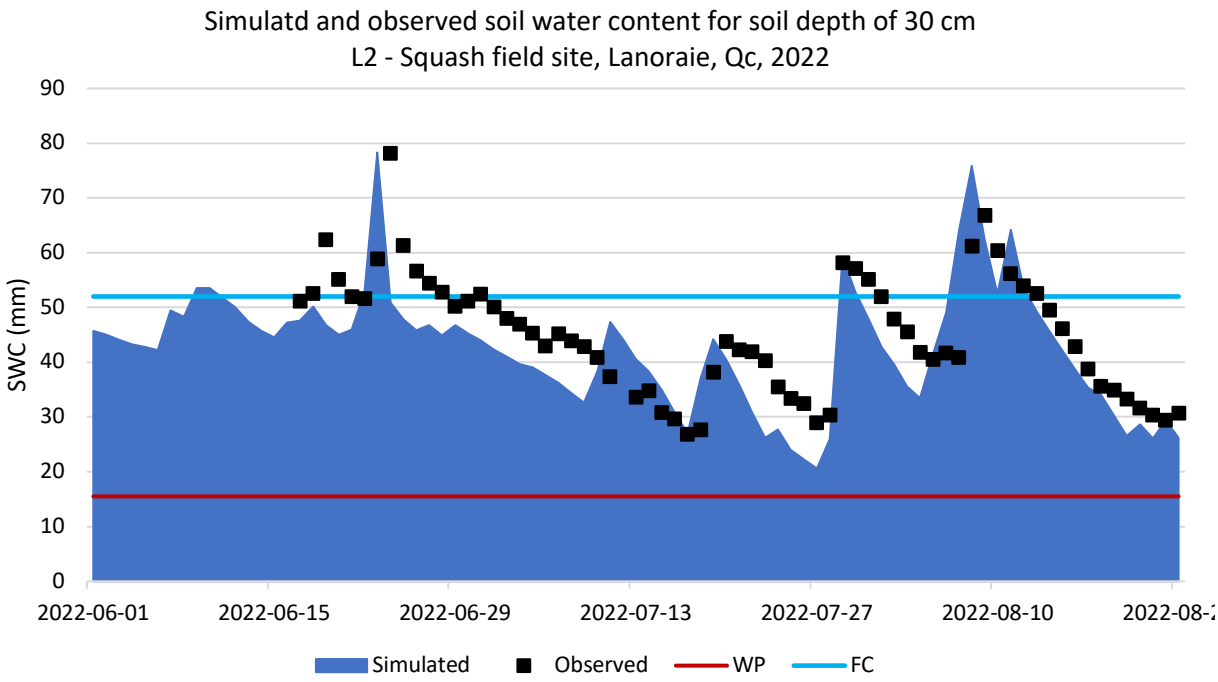

Figure 24. Simulated and observed soil water content (SWC) in the squash root zone (0-30 cm) at L2 over the 2022 growing season, including wilting point (WP) and field capacity (FC).

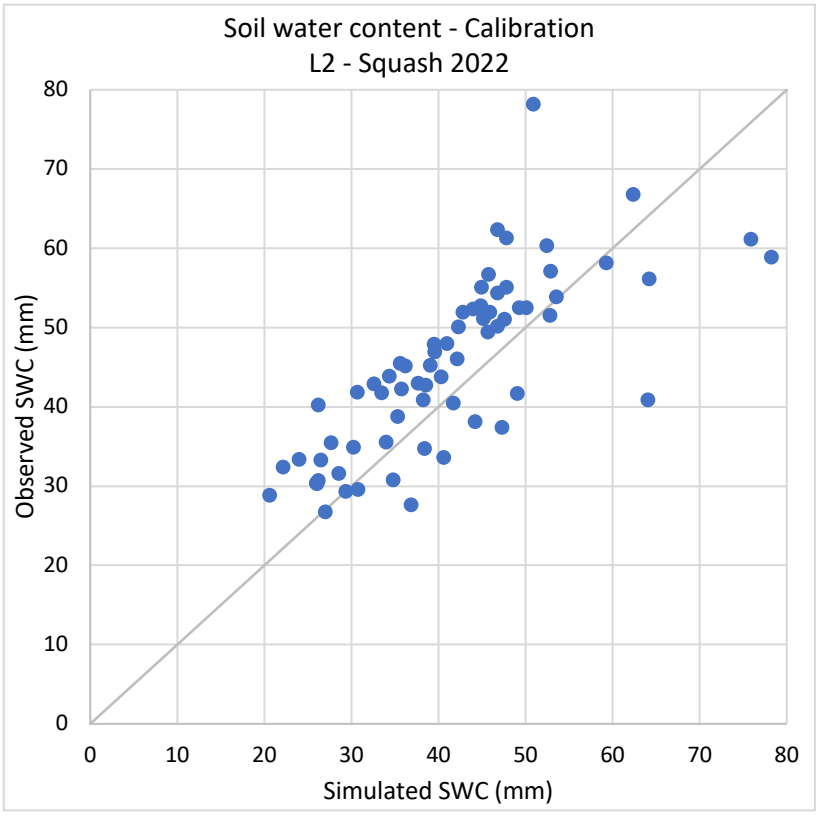

Figure 25. Simulated and observed soil water content from 0-30 cm depth at L2

4.4.3. Strawberry grown in Lanoraie fine sand

Consistent with the squash model, the sensitivity analysis of the strawberry identified the field capacity and the crop transpiration coefficient as highly and moderately sensitive parameters, respectively. To define the conservative crop parameters for strawberry, $K_{c\ Tr}$ was initiated and calibrated to 0.75, which is equal to the updated FAO standard (Pereira et al., 2021). The initial and maximum canopy cover, canopy decline coefficient, shape factor for root zone expansion, wilting point, saturated hydraulic conductivity, and curve number had low sensitivity.

Figure 26 depicts the simulated and observed SWC in the strawberry root zone at the L3 field site over the 2022 growing season. For the strawberry model, the comparison of soil moisture content within the top 20 cm revealed a Pearson correlation (r) of 0.54 and a Willmott index of agreement was 0.65. The RMSE and NRMSE were 6.6 mm and 18.6%, respectively, and the model's EF was -1.76. While the RMSE and NRMSE indicate good model performance, the EF < 0 suggests that the observed mean is a better estimator than the model (Legates and McCabe, 1999). This can be attributed to the small range of soil moisture measurements over the growing season, previously discussed in section 4.3.3. Positive EF values are typically the minimum acceptance criteria for simulating soil water content in crop models (Yang et al., 2014). However, the other statistical parameters indicate that AquaCrop was able to simulate SWC with fair accuracy in this study.

It is crucial to highlight that the farm primarily produces strawberry plants, whereas AquaCrop is configured to simulate a complete crop cycle, including flowering and fruit formation. In this field, the flowering and fruit yield were intentionally suppressed to prioritize extended root and canopy growth. This disparity is evident in AquaCrop's lower water content during periods when the crop would typically demand more water for flowering and fruit formation. Nevertheless, notable agreement is observed around irrigation events, aligning with the farm's practice of tightly controlling irrigation around FC through small and frequent irrigation events. The model tends to overestimate the impact of significant rainfall events. Battilani et al. (2014) and Farahani et al., (2009), experienced similar overestimation of peak SWC values for tomato and cotton crop models, respectively. The disagreements in estimated and observed SWC can be attributed to the non-traditional crop growth cycle and potential differences in soil hydraulics. In summary, the strawberry model performance revealed inefficient in simulating SWC, but had low estimation errors.

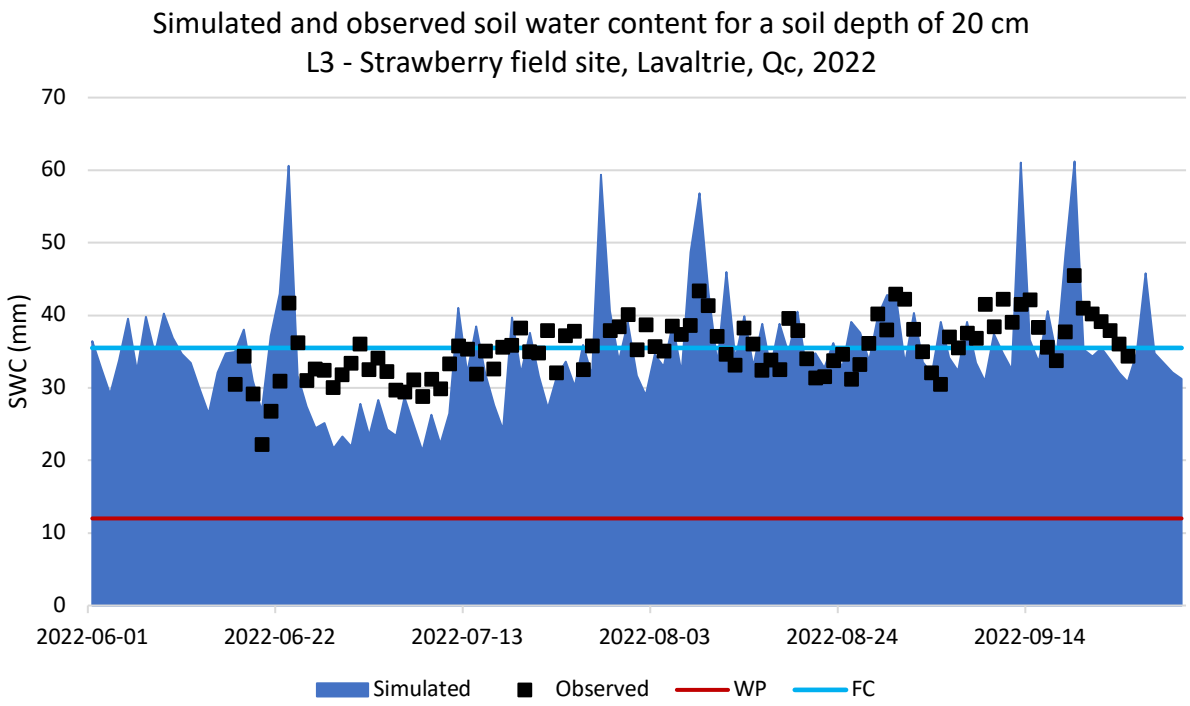

Figure 26. Simulated and observed soil water content (SWC) in the strawberry root zone (0-20 cm) at L3 over the 2022 growing season, including wilting point (WP) and field capacity (FC).

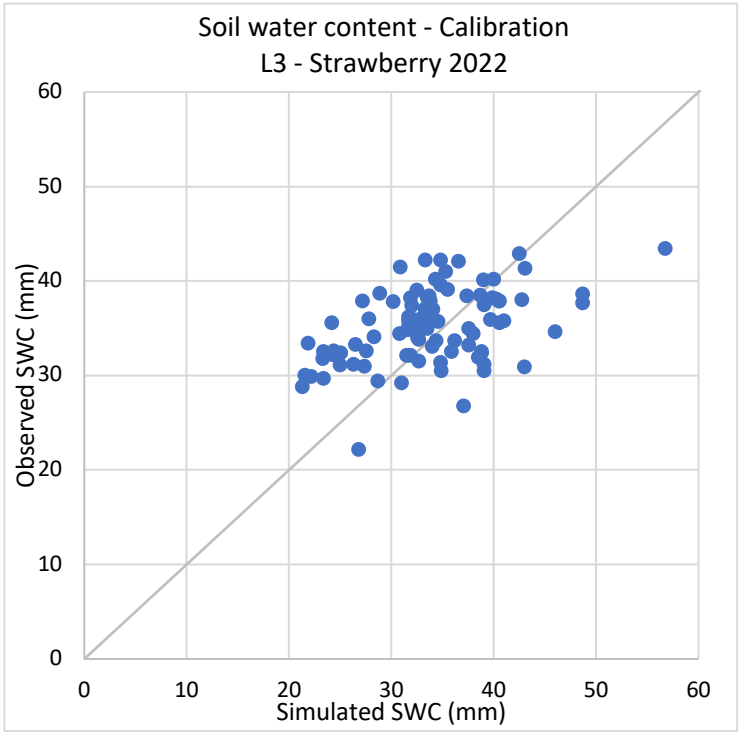

Figure 27. Simulated and observed soil water content from 0-20 cm depth at L3.

4.4.4. Cranberry grown in Saint-Jude sand

For the cranberry model, field capacity was also identified as a highly sensitive parameter in simulating SWC. The groundwater table depth and soil saturation point were moderately sensitive, while the crop transpiration coefficient ($K_{c\ Tr}$) showed low sensitivity. The target depth of the groundwater table of 0.6 m from Quebec cranberry studies (Caron et al., 2017; Pelletier et al., 2015b; Vanderleest et al., 2017), was calibrated to the field conditions. A variable depth was specified in AquaCrop to represent a higher water table (0.5 m) in the spring, an optimal depth (0.6 m) during flowering and fruit formation, and a lower water table (0.8 m) in the fall. In the absence of a default crop file for cranberry in AquaCrop, $K_{c\ Tr}$ was calibrated to 0.60. This value is consistent with the cranberry evapotranspiration study by Hattendorf and Davenport (1996) and between values of 0.5 (Bigah et al., 2019) and 0.83 (Vanderleest and Bland, 2017) found in the literature.

Figure 28 presents the simulated and observed SWC in the root zone of the cranberry crop at the L4 field site. AquaCrop's simulated SWC aligned well with observed trends, responding to precipitation and irrigation inputs. Overall, there was an acceptable agreement between observed and simulated SWC, indicated by a Pearson correlation (r) of 0.68, Wilmott index of agreement (d) of 0.80, and Nash-Sutcliffe Efficiency (EF) of 0.54. The RMSE of 5.3 mm and NRMSE of 11.8% show that the model simulated SWC with good accuracy to the 2022 field conditions. Although these results are closer to the lower ranges of model performance indicators in calibration and validation studies of well documented crop models, such as potato (Montoya et al., 2016; Razzaghi et al., 2017; Wang et al., 2023), they are in line with those of less commonly modeled crops. For example, in the calibration and validation of AquaCrop for perennial ryegrass (Terán-Chaves et al., 2022), statistical indices for SWC simulation were considered reasonable despite variations between treatments (r = 0.83 – 0.86, d = 0.30 – 0.84, RMSE = 6.1 – 20.1 mm, NRMSE = 4.80 – 24.1%, and EF = -23.9 – 0.32). The results of a six-year calibration study of perennial saffron showed that AquaCrop simulated SWC well with an NRMSE of 14% (Mirsafi et al., 2016). Furthermore, the validation runs with AquaCrop for quinoa achieved good results for simulated SWC with comparable average r of 0.80 and average EF of 0.47 (Geerts et al., 2009).

Underestimations of SWC in June, followed by overestimations in July may be attributed to the influence of water table control, as well as the limited data availability of crop parameters governing cranberry crop cycles. While the model performance is considered fair for the purpose

of estimating regional irrigation requirements in the inaugural scope of this study, the scarcity of existing studies in the context of cranberry crop-water modeling highlights a gap in the available data on crucial crop parameters. Further extensive data collection specific to cranberry cultivation could enhance the accuracy and reliability of model calibration.

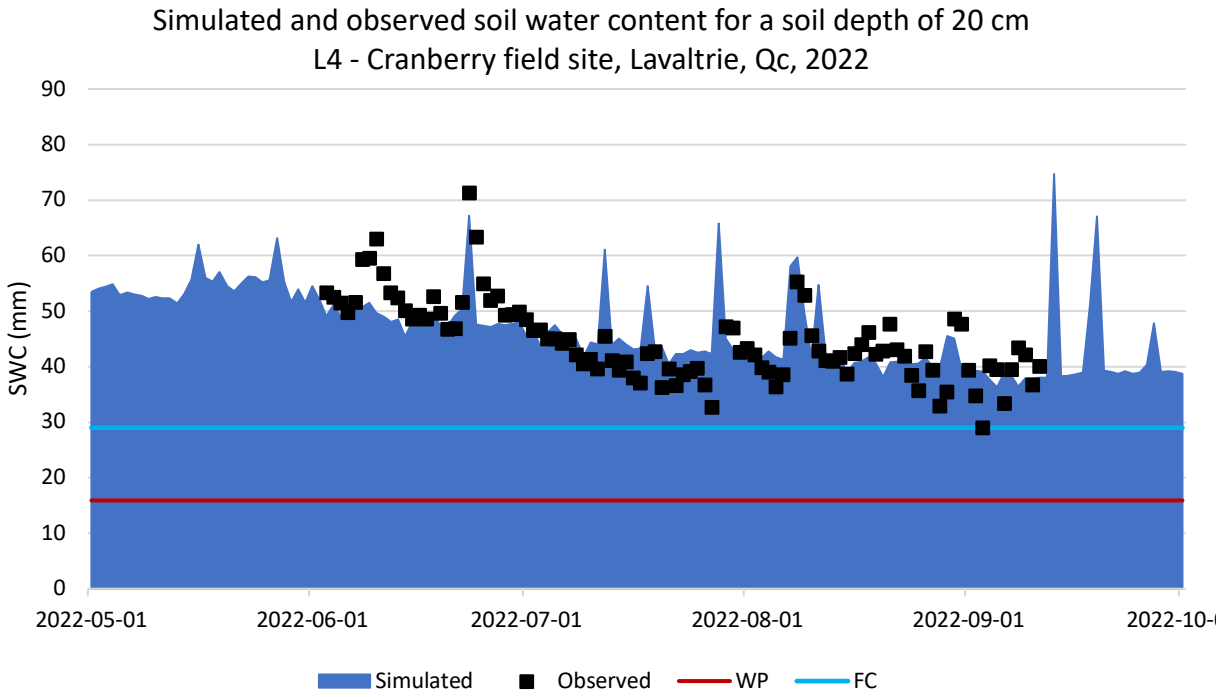

Figure 28. Simulated and observed soil water content (SWC) in the squash root zone (0-20 cm) at L4 over the 2022 growing season, including wilting point (WP) and field capacity (FC).

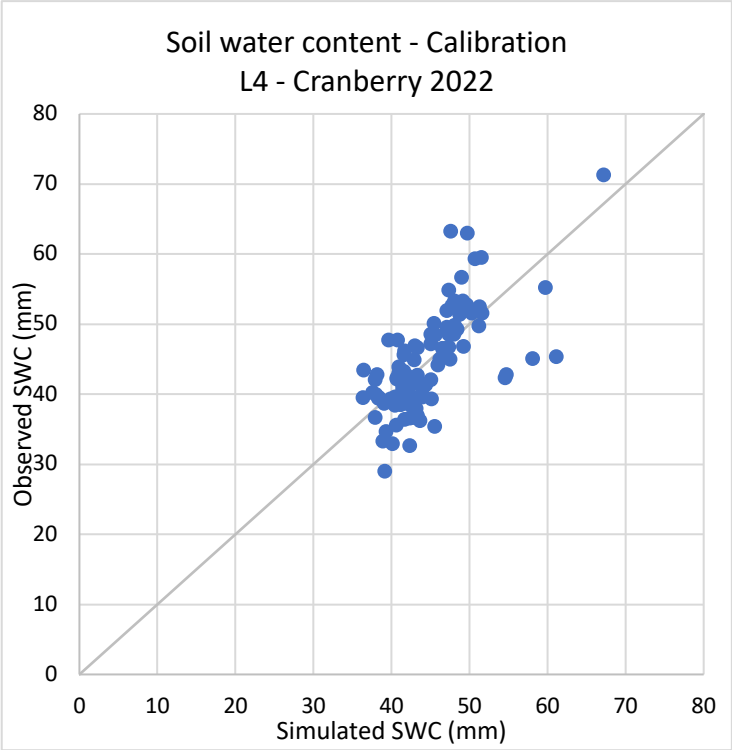

Figure 29. Simulated and observed soil water content from 0-20 cm depth at L4.

4.4.5. Summary of model performance

The evaluation of model performance, as summarized in Table 11 reveals varying degrees of agreement between simulated and observed soil moisture data across the four crop models. Overall, the potato and squash models had the greatest agreement between simulated and observed SWC, comparable to the results of other studies (e.g., Razzaghi et al., 2017; Wang et al., 2023). This aligned with expectations given the predominant representation of vegetables in crop modeling studies (e.g., Montoya et al., 2016; Battilani et al., 2014). Furthermore, these crops represent the highest prevalence of irrigated crops in the region and will therefore have the most significant impact on the total irrigation requirements of the study area.

It is crucial to acknowledge certain limitations in the study. Calibration was exclusively performed for soil moisture content, omitting other relevant output parameters. Furthermore, the absence of model validation, attributed to a single year of available data, introduces a level of uncertainty. The distinctive growth cycle of strawberries at the L3 field site, focusing on plant production rather than fruit production, poses a challenge to accurate modeling and simulation. Additionally, the conversion of cranberry field data from matric potential to volumetric water content introduces a potential source of error in the results. These considerations underscore the

complexity and nuances inherent in crop modeling. The models in this study are a useful tool for estimating regional irrigation requirements. Future research can build on these findings and further refine the models with additional data.

Table 11. Summary of AquaCrop model performance for the simulation of soil water content in the root zone at four field sites in 2022.

Field Site and Crop Model		Statistical Indices				
		r	RMSE (mm)	NRMSE (%)	EF	d
L1	Potato	0.88	5.3	21.8	0.54	0.91
L2	Squash	0.76	8.7	19.2	0.35	0.84
L3	Strawberry	0.54	6.6	18.6	-1.76	0.65
L4	Cranberry	0.68	5.3	11.8	0.46	0.8

4.5 Simulated historical irrigation requirements

The simulated irrigation requirements for each crop model are presented below for historical weather conditions and the future climate change scenario. Crop production and water productivity outputs are included. While the model's crop parameters were not calibrated to field data for yield and water productivity outputs, the default crop parameters from AquaCrop's library provide ways to approximate incomplete information and have shown to accurately simulate production output (Raes et al., 2009). For example, Tsakmakis et al. (2019) found that cotton seed yield was only accurately simulated when the model's default crop file was used.

4.5.1. Simulated historical potato irrigation requirements

The simulated net irrigation requirements (I_{net}), crop yield (Y), and ET water productivity (WP_{ET}) for potato are presented in Table 12 for the historical dry, average, and wet years and three irrigation treatments. The growing season rainfall, ET_o, and mean temperature are provided for reference. Each value represents the mean result of five years, representing the dry, average, and wet historical growing season weather conditions. The irrigation requirement decreases with increasing maximum allowable depletion from 20% to 50% of the available water content, since the lower depletion threshold requires smaller but more frequent irrigation applications. This is due to the shorter depletion time for 20% AW from the FC of the soil, compared to the other treatments. As the irrigation requirement decreases, the total dry yield remains constant, and results in a greater ET water productivity (Figure 30). These results are consistent with recommended

irrigation strategies for potatoes and the general agreement that to maximize yields, AW should not drop below 50-65% in the zone of maximum root activity (Allen et al., 1998; Singh, 1969; Shock et al., 2007; Wright and Stark, 1990). Beyond this threshold, crop water stress is predicted to impact yield production.

Table 12. Historical simulation results for potato. Simulated net irrigation requirement, dry yield, and ET water productivity of potato for different irrigation treatments and historical weather conditions. 5-year means of growing season weather data and simulation results are shown.

Historical Weather 5 years*	**Irrigation Treatment** Back up to FC	**Growing Season (May-Sept)**			**Simulated Results**		
		Rain (mm)	**ETo** (mm)	**Temp** (°C)	**I net** (mm)	**dry Y** (ton/ha)	**WP_{ET}** (kg/m3)
Dry	MAD of 20%AW	339	582	17.8	365	11.0	2.16
	MAD of 35%AW	339	582	17.8	305	10.9	2.30
	MAD of 50%AW	339	582	17.8	265	10.9	2.42
	Rainfed	339	582	17.8	0	4.7	1.89
Average	MAD of 20%AW	500	586	18.4	337	10.6	2.08
	MAD of 35%AW	500	586	18.4	279	10.5	2.23
	MAD of 50%AW	500	586	18.4	249	10.4	2.32
	Rainfed	500	586	18.4	0	5.5	1.90
Wet	MAD of 20%AW	582	547	17.6	287	12.0	2.44
	MAD of 35%AW	582	547	17.6	237	11.8	2.54
	MAD of 50%AW	582	547	17.6	202	12.0	2.68
	Rainfed	582	547	17.6	0	7.5	2.34

Each value represents a mean of five years, representing a historical weather condition.
*Five dry, average, and wet years were selected based on total growing season rainfall (May to September).

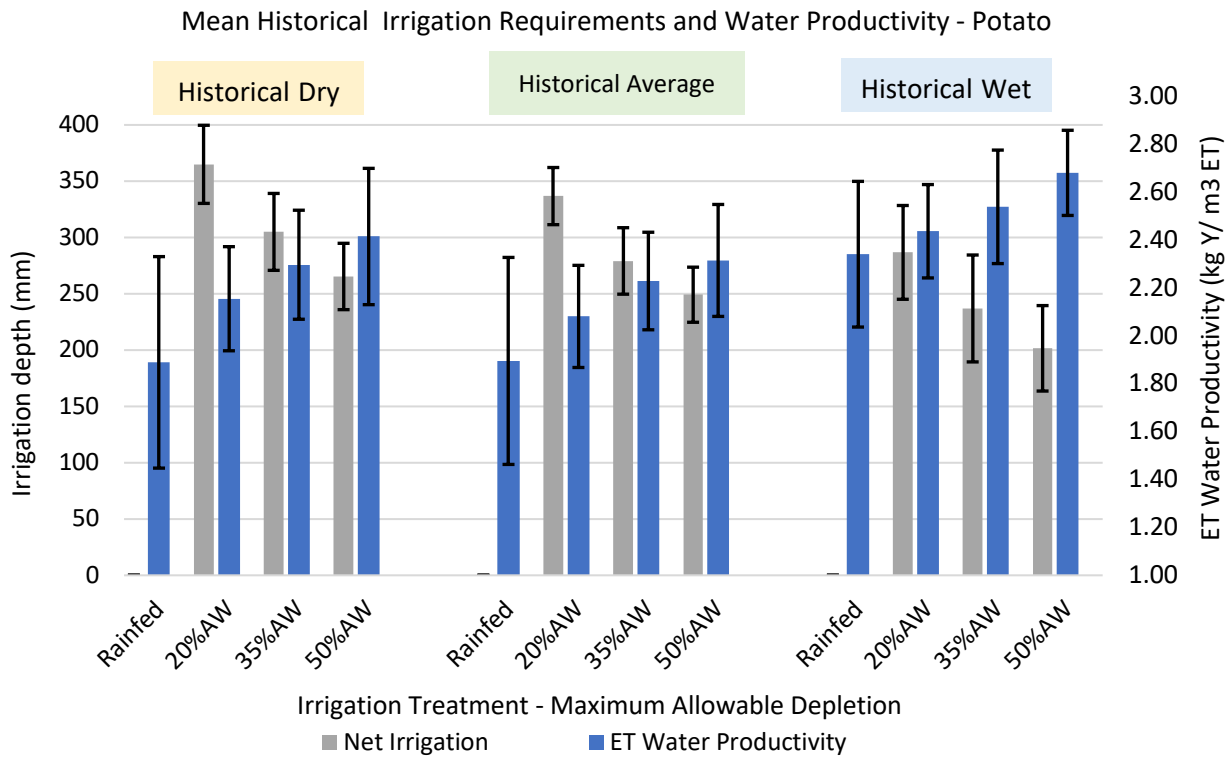

Figure 30. Simulated historical irrigation requirements and ET water productivity for potato under three irrigation treatments and rainfed conditions. Columns represent a 5-yr mean +/- the standard deviation.

The statistical significance of the effects of weather and irrigation treatment obtained from the ANOVA are summarized in Table 13. In this summary, each value represents the mean of all simulation outputs for the respective treatment in the first column. The F-test revealed that, both weather and irrigation treatment had a significant impact on irrigation requirement ($p < .0001$), while the interaction effect did not. In terms of historical weather, as expected, only the wet growing season conditions had significantly lower net irrigation and higher yield than the dry and average years.

Regarding irrigation treatment, all values of I_{net} were significantly different from each other, showing a significant reduction in irrigation requirements with a MAD of 50% of AW. Danielescu et al., (2022) found that the total amount of supplemental irrigation for potato production in PEI also differed significantly between minimal, moderate, and extensive irrigation scenarios, following the same decreasing trend with increased depletion.

On the other hand, irrigation treatment had no significant effect on yield, except in the case of rainfed conditions, confirming the importance of supplemental irrigation for potato production in

Lanoraie. As a result, the 50% depletion had significantly higher water productivity than each of the other irrigation treatments.

In the dry-season scenario, the LS-Means test of the interaction effect revealed that the simulated I_{net} was statistically different under each irrigation treatment, whereas in the average and wet seasons, the MAD35% and MAD50% treatments resulted in similar net irrigation requirements. These results highlight the reduced irrigation water required during historical wet growing seasons, as well as the meaningful impact of a lower water depletion threshold in terms of increasing water productivity. Notably, in dry seasons of highest concern for water availability, the irrigation scheduling of the potato producers has the greatest impact on their net irrigation usage.

Table 13. Statistical analysis of historical potato simulations. Effect of different irrigation treatments and historical weather on net irrigation requirement, dry yield, and ET water productivity of potato crops. Differences between means shown in columns with different letters ($p<0.05$).

Irrigation Treatment	**I net** (mm)	**Dry Y** (ton/ha)	**WP_{ET}** (kg/m3)
MAD of 20%AW	330 a	11.2 a	2.23 a
MAD of 35%AW	274 b	11.1 a	2.36 ab
MAD of 50%AW	239 c	11.1 a	2.47 b
Rainfed	0 d	5.9 b	2.04 ac
Historical Weather			
Dry	234 a	9.4 a	2.19 a
Average	216 a	9.3 a	2.13 a
Wet	181 b	10.8 b	2.50 b
Significance			
Irrigation Treatment	*<.0001	*<.0001	*0.0008
Historical Weather	*<.0001	*0.0018	*0.0002
Interaction	ns	ns	ns

*: significant; ns: non-significant
significant differences between means ($p<0.05$), shown with different letters within columns.

4.5.2. Simulated historical squash irrigation requirements

The historical simulation results for the squash model are presented in Table 14, where each value is the 5-year mean corresponding to the historical weather condition. The simulated I_{net} for squash follows the same trends as the potato simulations, decreasing with augmenting depletion thresholds, as well as from dry to wet growing season conditions. Similarly, as the irrigation

requirement decreases, the yield remains constant, and the ET water productivity increases. Due to the low water holding capacity of the soil, allowing the soil moisture to deplete to the recommended 50% of available water (Maughan et al., 2015), reduces the frequency of irrigation events without permitting the crop to experience drought stress.

Table 14. Historical simulation results for squash. Simulated net irrigation requirement, dry yield, and ET water productivity of squash for different irrigation treatments and historical weather conditions. 5-year means of growing season weather data and simulation results are shown.

Historical Weather 5 years*	Irrigation Treatment Back up to FC	Growing Season			Simulated Results		
		Rain (mm)	ETo (mm)	Temp (°C)	I net (mm)	dry Y (ton/ha)	WP_{ET} (kg/m3)
Dry	MAD of 20%AW	339	582	17.8	222	7.1	2.10
	MAD of 35%AW	339	582	17.8	176	7.1	2.25
	MAD of 50%AW	339	582	17.8	151	7.1	2.36
	Rainfed	339	582	17.8	0	1.7	0.78
Average	MAD of 20%AW	500	586	18.4	208	6.6	2.00
	MAD of 35%AW	500	586	18.4	155	6.5	2.09
	MAD of 50%AW	500	586	18.4	135	6.5	2.18
	Rainfed	500	586	18.4	0	4.9	2.13
Wet	MAD of 20%AW	582	547	17.6	177	7.1	2.18
	MAD of 35%AW	582	547	17.6	136	7.0	2.31
	MAD of 50%AW	582	547	17.6	94	7.0	2.41
	Rainfed	582	547	17.6	0	6.2	2.45

Each value represents a mean of five years, representing a historical weather condition.
*Five dry, average, and wet years were selected based on total growing season rainfall (May to September).

The statistical significance of the effects of weather and irrigation treatment obtained from the ANOVA are summarized in Table 15. Again, each value represents the average value of all simulation outputs for the specified irrigation treatment or weather condition. The evaluated effects followed similar trends for the historical squash simulations as for potato. The growing season weather had a significant effect on I_{net}, yield and WP_{ET}, but only resulted in significantly different results in the wet years (lower I_{net}, higher yield, and higher WP_{ET}).

The significant effect of irrigation treatment resulted in statistically different irrigation requirements with respect to each treatment. Meanwhile, squash yield and WP_{ET} decreased significantly in the case of rainfed conditions only. Overall, the MAD50% irrigation treatment significantly reduces the net irrigation requirement and increase the water productivity.

Table 15. Statistical analysis of historical squash simulations. Effect of different irrigation treatments and historical weather on net irrigation requirement, dry yield, and ET water productivity of squash crops. Differences between means shown in columns with different letters ($p<0.05$).

Irrigation Treatment	I net (mm)	Dry Y (ton/ha)	WP_{ET} (kg/m3)
MAD of 20%AW	202 a	6.9 a	2.09 a
MAD of 35%AW	156 b	6.9 a	2.22 a
MAD of 50%AW	127 c	6.9 a	2.32 a
Rainfed	0 d	4.3 b	1.79 b
Historical Weather			
Dry	137 a	5.7 a	1.87 a
Average	124 a	6.1 a	2.10 a
Wet	102 b	6.8 b	2.34 b
Significance			
Irrigation Treatment	*<.0001	*<.0001	*0.0017
Historical Weather	*0.0002	0.0037	*0.0011
Interaction	ns	*<.0001	*<.0001

*: significant; ns: non-significant
significant differences between means ($p<0.05$), shown with different letters within columns

4.5.3. Simulated historical strawberry irrigation requirements

The simulated net irrigation, total aboveground biomass (B), and water productivity for strawberry are presented in Table 16 for the historical dry, average, and wet years and three irrigation treatments. Each value represents the mean result of five years, representing the dry, average, and wet historical growing season weather conditions. Aboveground biomass is presented as opposed to fruit yield, since the model was calibrated to the plant producing field site. The irrigation requirements are greater in dry years and decrease with increasing maximum allowable depletion from 20% to 50% of the available water content. The aboveground biomass remains constant despite varying depletion thresholds, except when no irrigation is applied. This results in a greater ET water productivity with a 50% maximum allowable depletion.

Table 16. Historical simulation results for strawberry. Simulated net irrigation requirement, ET water productivity, and total aboveground biomass for different irrigation treatments and historical weather conditions. 5-year means of growing season weather data and simulation results are shown.

Historical Weather 5 years*	Irrigation Treatment Back up to FC	Growing Season			Simulated Results		
		Rain (mm)	ETo (mm)	Temp (°C)	I net (mm)	B (ton/ha)	WP_{ET} (kg/m3)
Dry	MAD of 20%AW	339	582	17.8	368	15.0	1.91
	MAD of 35%AW	339	582	17.8	318	15.0	1.96
	MAD of 50%AW	339	582	17.8	289	15.0	2.01
	Rainfed	339	582	17.8	0	1.8	0.34
Average	MAD of 20%AW	500	586	18.4	328	14.0	1.84
	MAD of 35%AW	500	586	18.4	288	14.0	1.88
	MAD of 50%AW	500	586	18.4	241	14.0	1.93
	Rainfed	500	586	18.4	0	5.3	0.71
Wet	MAD of 20%AW	582	547	17.6	288	14.5	2.01
	MAD of 35%AW	582	547	17.6	256	14.5	2.04
	MAD of 50%AW	582	547	17.6	218	14.5	2.09
	Rainfed	582	547	17.6	0	11.7	1.29

Each value represents a mean of five years, representing a historical weather condition.
*Five dry, average, and wet years were selected based on total growing season rainfall (May to September).

The statistical significance between the irrigation regimes and weather conditions obtained from the ANOVA is presented in Table 17. For the historical strawberry simulations, irrigation treatment had a significant effect on net irrigation requirement, with all treatments being significantly different from each other. The I_{net} also differed significantly between dry, average, and wet growing seasons. Irrespective of the irrigation treatment, there was no significant effect on total biomass or WP_{ET}, except under rainfed conditions. The interaction effect was not significant. Especially under dry conditions, the 50% MAD irrigation treatment can help berry producers in the region optimize irrigation water use.

Table 17. Statistical analysis of historical strawberry simulations. Effect of different irrigation treatments and historical weather on net irrigation requirement, total biomass and ET water productivity of strawberry crops. Differences between means shown in columns with different letters ($p<0.05$).

Irrigation Treatment	I net (mm)	Biomass (ton/ha)	WP_{ET} (kg/m3)
MAD of 20%AW	328 a	14.5 a	1.92 a
MAD of 35%AW	287 b	14.5 a	1.96 a
MAD of 50%AW	249 c	14.5 a	2.01 a
Rainfed	0 d	6.3 b	0.78 b
Historical Weather			
Dry	244 a	11.7	1.56
Average	214 b	11.8	1.59
Wet	190 c	13.8	1.86
Significance			
Irrigation Treatment	*<.0001	*<.0001	*<.0001
Historical Weather	*<.0001	ns	ns
Interaction	ns	ns	ns

*: significant; ns: non-significant
significant differences between means ($p<0.05$), shown with different letters within columns

4.5.4. Simulated historical cranberry irrigation requirements

The historical simulation results for the cranberry model are presented in Table 18. The simulated I_{net} decreases with increasing available soil water depletion thresholds. Larger amounts of irrigation are required in dry years to compensate for lack of rainfall. The total aboveground biomass and ET water productivity are consistent between all irrigation treatments and all growing season weather, except in the absence of irrigation. It should be noted that for simulation, the variable groundwater depth calibrated to the field conditions of the cranberry bog was omitted in order to characterize the CWRs met by both sub-irrigation and sprinkler irrigation, since they represent the same resource of water in the study area.

Table 18. Historical simulation results for cranberry. Simulated net irrigation requirement, ET water productivity, and total aboveground biomass for different irrigation treatments and historical weather conditions. 5-year means of growing season weather data and simulation result are shown.

Historical Weather	Irrigation Treatment	Growing Season			Simulated Results		
		Rain (mm)	ETo (mm)	Temp (°C)	I net (mm)	B (ton/ha)	WP_{ET} (kg/m3)
5 years*	Back up to FC						

Dry	MAD of 20%AW	339	582	17.8	203	12.4	2.16
	MAD of 35%AW	339	582	17.8	176	12.3	2.16
	MAD of 50%AW	339	582	17.8	161	12.3	2.16
	Rainfed	339	582	17.8	0	7.6	1.69
Average	MAD of 20%AW	500	586	18.4	183	12.3	2.14
	MAD of 35%AW	500	586	18.4	154	12.2	2.14
	MAD of 50%AW	500	586	18.4	133	12.2	2.15
	Rainfed	500	586	18.4	0	10.0	2.13
Wet	MAD of 20%AW	582	547	17.6	147	12.5	2.33
	MAD of 35%AW	582	547	17.6	131	12.5	2.34
	MAD of 50%AW	582	547	17.6	93	12.5	2.34
	Rainfed	582	547	17.6	0	11.2	2.37

Each value represents a mean of five years, representing a historical weather condition.
*Five dry, average, and wet years were selected based on total growing season rainfall (May to September).

The statistical analysis summarized in. Table 19, reveals that for cranberries, irrigation requirements were significantly different between all irrigation treatments and all growing season conditions. Historical weather also influenced the total crop biomass, which significantly differed in each case. There was no significant effect on WP_{ET}, except under rainfed conditions.

Table 19. Statistical analysis of historical strawberry simulations. Effect of different irrigation treatments and historical weather on net irrigation requirement, total biomass, and ET water productivity of strawberry crops. Differences between means shown in columns with different letters ($p<0.05$).

Irrigation Treatment	**I net** (mm)	**Biomass** (ton/ha)	**WP_{ET}** (kg/m3)
MAD of 20%AW	177 a	12.4 a	2.21 a
MAD of 35%AW	154 b	12.4 a	2.21 a
MAD of 50%AW	129 c	12.4 a	2.22 a
Rainfed	0 d	9.6 b	2.06 b
Historical Weather			
Dry	135 a	11.2 a	2.04 a
Average	117 b	11.7 b	2.14 a
Wet	93 c	12.2 c	2.34 b
Significance			

Irrigation Treatment	*<.0001	*<.0001	*0.0347
Historical Weather	*<.0001	*0.0002	*<.0001
Interaction	ns	*<.0001	*0.0054

*: significant; ns: non-significant
significant differences between means ($p < 0.05$), shown with different letters within columns

In summary, the statistical analysis of historical simulations revealed that both historical weather (wet, average or dry growing season) and irrigation treatment (20%, 35%, or 50% depletion of AW) had a significant effect on the net irrigation requirement. The results highlighted the water saving potential of irrigating at a maximum allowable depletion of 50% available water, especially in dry years where crop-water demand was significantly higher. For all major crops in the study area, the historical AquaCrop simulations found that a 50% MAD significantly reduced net irrigation requirements and increased water productivity, without significantly reducing crop production. Furthermore, irrigation water management should center on the historical dry year requirements, which were significantly greater than for historically wet years.

4.6 Impact of climate change on irrigation requirements

Next, the models were used to predict the impact of climate change on the near (2050s) and far (2080s) future irrigation requirements, compared to the historical baseline (1997-2021). A sample of simulation results for CMIP6 ensemble model under SSP5-8.5 scenario for all years is available in the Figure A3. The 30-year means were calculated for each timeline (baseline, 2050s, and 2080s), model (in the ensemble), crop (potato, squash, strawberry, and cranberry), and irrigation treatment (20%, 30%, and 50%MAD of AW). The median and range of the resulting net irrigation requirements are presented in Figure 31, 32, 33, and 34, for potato, squash, strawberry, and cranberry, respectively.

In Figure 31, the 30-year average simulation results, represented by the median model result with black bars indicating the range, highlight a significant increase in potato irrigation requirements by the projected 2080s period compared to historical baseline, under the selected high emissions scenario. These results support previous findings simulated with the AquaCrop model, evaluated for future irrigation requirements across different climate scenarios. For example, Busschaert et al. (2022) indicated a potential increase in net irrigation requirement of 30% in far future periods (2071–2100) under a high-emission scenario (SSP3–7.0), particularly impacting agriculture in central and southern Europe.

In addition, the results showed an increase in tuber yield production. This aligns with findings in global studies on potato crop modeling in the context of climate change, such as those by Jennings et al. (2020), which suggest increased yields with adaptations. Simulating with AquaCrop, Govere et al. (2022) found a beneficial effect of climate change on wheat yield and water use in Zimbabwe under RCP4.5 and RCP8.5 for projected 2040s and 2080s. They attributed the simulated increase in yields and decrease in crop water use to the CO_2 fertilization effects, which had a dominant effect over the projected higher temperatures. However, a specific modeling study on potato production in Prince Edward Island (Adekanmbi et al., 2023) demonstrated a potential decrease in yield due to climate change without adaptations from current agricultural practices. A recent study on the impact of climate change on fully irrigated, well-fertilized potato crop across the USA under the RCP 8.5 scenario of high emissions indicated that while increasing temperatures will likely reduce potato yields, this will be mostly compensated by elevated atmospheric CO_2 (Zhao et al., 2022). Furthermore, yields may improve in most regions by planting potatoes earlier as adaptation to avoid hot summers. Despite higher temperatures, water use by the potato crop is predicted to decrease as a result of a shorter growing season and greater water use efficiency under elevated atmospheric CO_2 (Zhaeo et al., 2022). Unlike the results of the RADEAU project (Charron et al., 2019), the simulations in this study projected a shortened crop cycle owing to the ability to run the model in GDD format.

Notably, the statistical analysis demonstrates that irrigation treatment plays a significant role in influencing the net irrigation requirement, with a MAD set at 50% of AW showing a considerable reduction. Overall, ANOVA results underscore the substantial impact of both irrigation treatment and climate on net irrigation requirements, indicating an expected increase under the selected climate model scenario, mitigated by the MAD 50%AW treatment. In summary, the simulation results are in line with the anticipated greater water demand due to weather effects, counterbalanced by the potential for increased crop yield attributed to higher CO2 concentration.

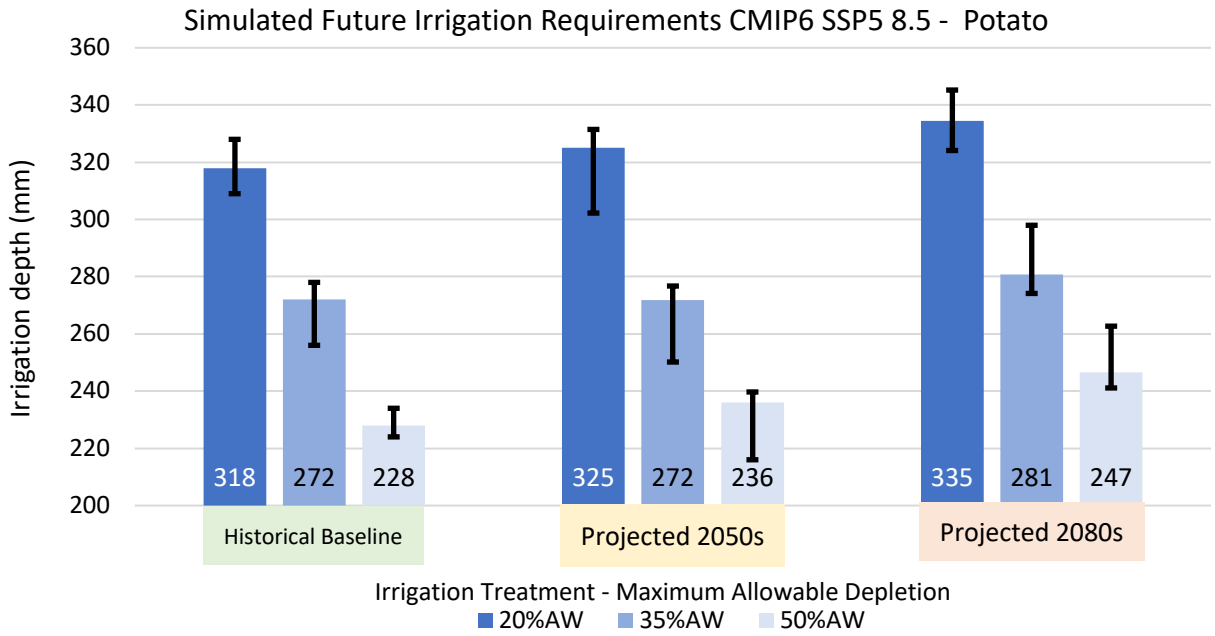

Figure 31. Median and range of projected irrigation requirements under CMIP6 SSP5-8.5 for potato.

For the squash model, the future simulations resulted in stable net irrigation requirements, as well as lower yields in the 2050s and 2080s, under the high emissions scenario. These results may be attributable to the observed reduction in the crop's growth cycle, associated with changes in climatic conditions. While the default values of the conservative AquaCrop parameters (Hsiao, 2012; Raes et al., 2009) for the potato crop file are presumed applicable to a wide range of conditions, the conservative parameters for the squash model, such as upper and lower temperature thresholds for leaf growth, were obtained from the default general vegetable file. Future research and model parametrization could further investigate the effect of climate change on the crop cycle of winter squash. For the purpose of this study, the model is a simplified representation of irrigated vegetable in the Lanoraie study area and presents a possible effect of a high emissions future on vegetable production.

Consistent with the potato simulations, the F-test indicated a significant effect of irrigation treatment on the net irrigation requirements for squash. The maximum depletion level of 50% AW significantly reduces the net irrigation requirements in all climate periods, emphasizing the role of the producer’s selected irrigation regime on irrigation water use.

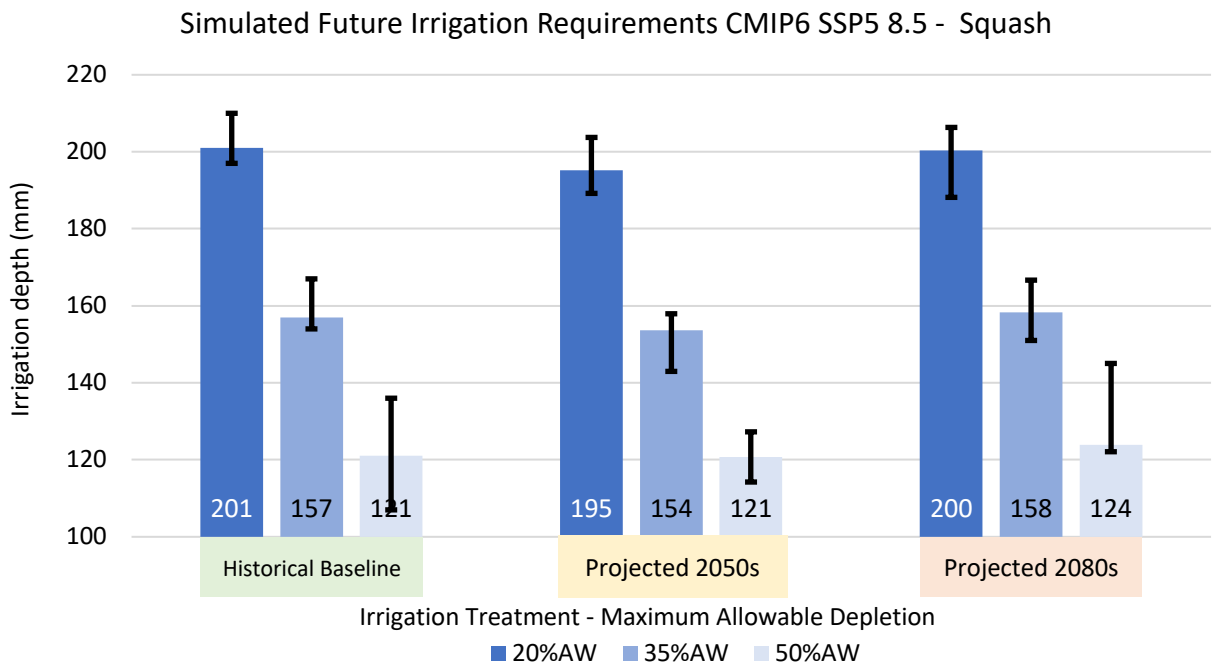

Figure 32. Median and range of projected irrigation requirements under CMIP6 SSP5-8.5 for squash

In the future simulations for strawberry crops, a decline in net irrigation requirements is observed (Figure 33), potentially associated with the shortened simulated crop cycle. Similar trends were observed in cranberry simulations, depicted in Figure 34. Although this aligns with findings from other crop modeling studies, indicating a potential reduction in the crop cycle duration due to climate change, additional data and model calibration are recommended to validate this effect. Furthermore, this presents an opportunity to adapt cultivars to climate change by studying various planting dates and heat tolerances of crops. In simulating climate change impacts on winter wheat and maize in Iran, Khordadi et al. (2019) found that varying the sowing date to optimize yield, as well as selecting cultivars according to varied projected GDD could be effective adaptation strategies to meet agricultural needs in the face of a changing climate. In terms of berry cultivation in temperate regions, Dale (2009) stresses that due to the increased climate variability, cultivars will need withstand fluctuating winter weather and increased heat stress, be able to grow with little chilling, and be able to initiate bud formation under diverse environmental conditions. To address these challenges, breeders should focus on developing everbearing cultivars that are winter-hardy, and adaptable to various environments and cropping systems, necessitating collaboration between breeders and crop physiologists to design effective breeding systems. (Dale, 2009). These collaborative research initiatives are present in Quebec. For example, the *AAC*-

Généreuse strawberry cultivar bred by Dr. Khanizadeh at Agriculture and Agri-Food Canada in Quebec, was commercially tested in Lavaltrie and displayed a high yield and hardiness compared to other mid-season varieties. Also, originally bred for Floridian agriculture, *Florida-Brilliance* was found to be a top-performing mid- late season variety between 2019 and 2021 in The Canadian Berry Trial Network lead by Crawford et al. (2022). Continuing these efforts will be crucial in face of a changing climate.

The ANOVA showed that the substantial impact of irrigation treatment on net irrigation persists in the projected strawberry and cranberry simulations. This emphasizes the impact of irrigation management irrespective of the crop under cultivation.

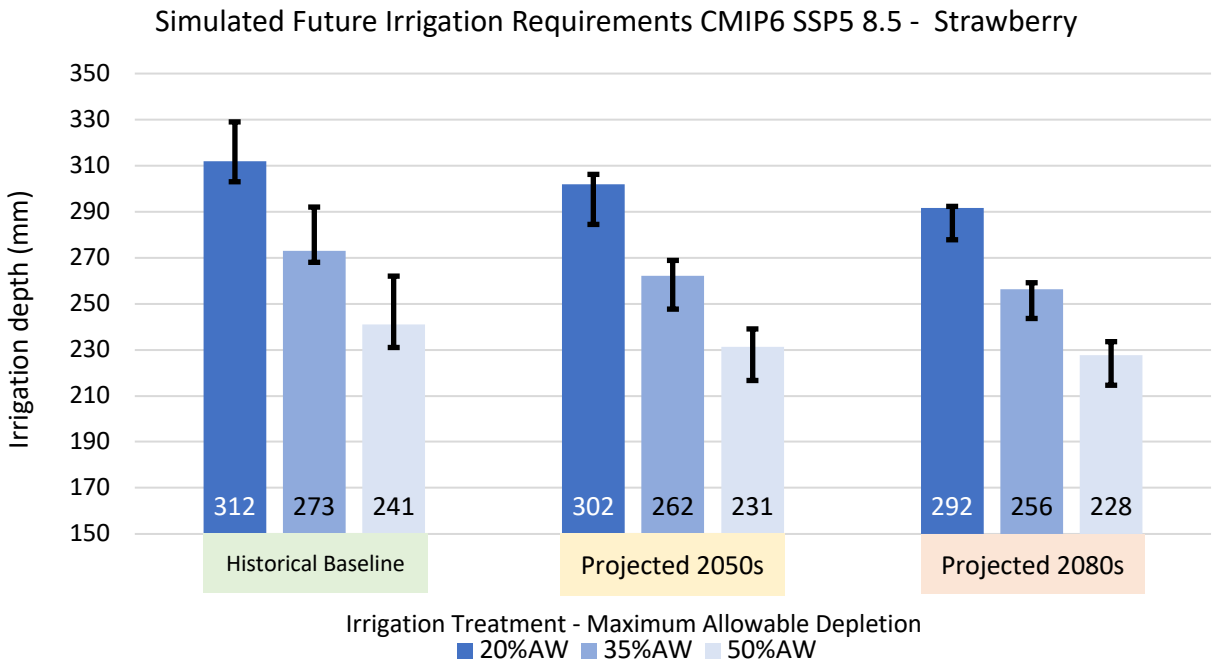

Figure 33. Median and range of projected irrigation requirements under CMIP6 SSP5-8.5 for strawberry

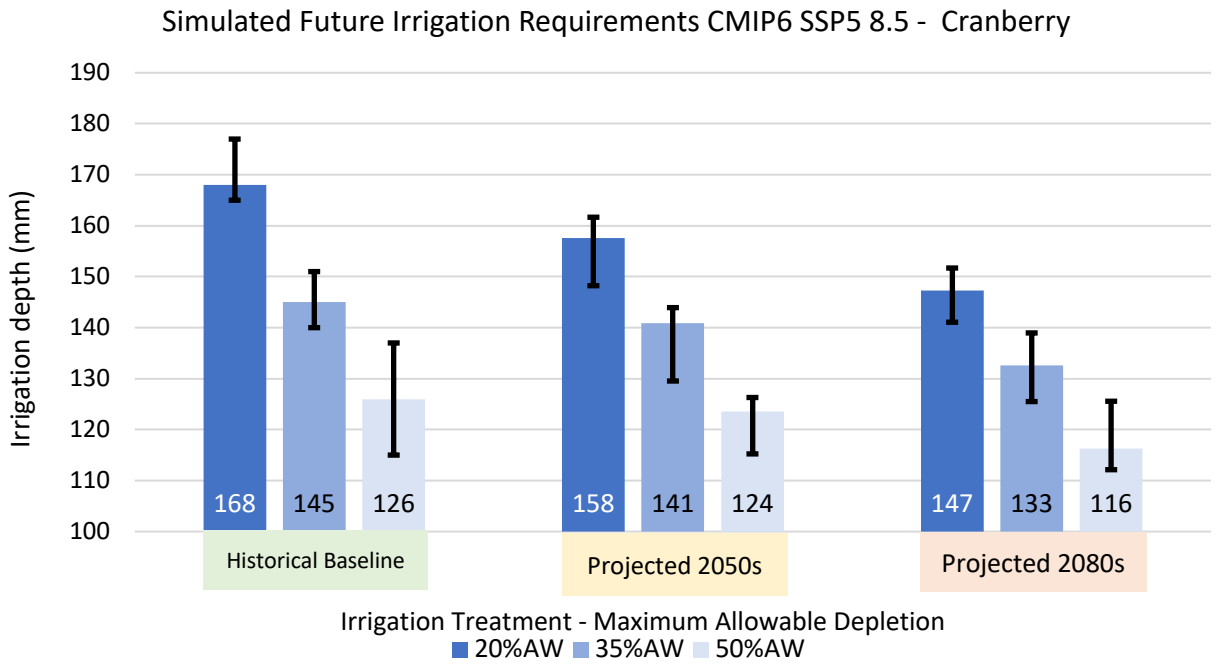

Figure 34. Median and range of projected irrigation requirements under CMIP6 SSP5-8.5 for cranberry

In summary, the climate effect of the CMIP-6 high emissions scenario (SSP5-8.5) was investigated for the major crops in the study area with four AquaCrop models calibrated to local field conditions. The simulations showed that the irrigation requirement for potato will significantly increase by the projected 2080s period compared to the historical period. Projected irrigation requirements for the other crops remained fairly stable with a possible decrease in irrigation requirements predicted for berry crops. However further model calibration is suggested to investigate the effect of climate change on shortened crop growth cycles. Future research could explore the optimization of crop varieties and planting dates to adapt the agricultural region to climate change, as was shown in other studies (e.g. Khordadi et al., 2019; Sharma et al., 2021). For all crops, irrigation treatment significantly impacted the net irrigation requirement. An irrigation treatment of MAD 50% AW can significantly reduce future irrigation requirements.

Further recommendations include incorporating additional socio-economic pathways. Studying the impact of climate change on maize in sub-Saharan Africa, Dale et al., (2017) found robust spatial trends of yield losses across the ensembles used, which corresponded to spatial patterns on aridity increases. They found that the spatial distribution of uncertainty in yield projections is mainly influenced by internal variability, a significant contributor to uncertainty in both within-model and between-model ensembles, emphasizing the importance of adaptive and

robust risk management strategies in the face of climate change uncertainties. Moreover, the AquaCrop model, evaluated for future irrigation requirements across different climate scenarios, indicated a potential increase in net irrigation requirement by 30% in far future periods (2071–2100) under a high-emission scenario (SSP3–7.0), particularly impacting central and southern Europe (Busschaert et al., 2022). However, a high mitigation scenario (SSP1–2.6) suggested a stabilization of Inet increase at around 13 mm per month by the end of the century, accompanied by a smaller rise in interannual variability. These findings highlight substantial disparities in I_{net} projections across various GCMs. Therefore, future studies should explore a more comprehensive range of socio-economic pathways.

4.7 Design of irrigation water supply scenario

4.7.1. Irrigation sector water demand

Finally, the gross irrigation requirements were mapped into water supply sectors to help propose an irrigation supply system. Mean monthly irrigation requirements were derived from the simulation results for the five historical dry years under the recommended 50%MAD irrigation strategy. In addition to the simulated irrigation events, water requirements for frost and heat protection were taken into account for strawberry and cranberry crops, as well as water used for cranberry harvest flooding. The application efficiency was also considered for the main irrigation systems used. Gross depths of irrigation requirements were extrapolated over the irrigated cropland of the study area for each month of the growing season. For the historical dry years, the regional volumes of water required for the major irrigated crops over the growing season were greatest in the months of July and August. This period of highest irrigation water demand coincides with the minimum flows in four streams tributary to the Lanoraie peat complex evaluated by IRDA: the Point-du-Jour; Saint-Jean; Saint-Joseph; and Bras-du-Sud-Ouest (Ricard et al., 2023). In also considering the flow restrictions imposed by the municipalities, it is apparent that these streams do not represent a sustainable source of irrigation water during July and August, especially in dry years. Furthermore, the research conducted by the UQAM team suggests that the excavated irrigation ponds may be intercepting water that would otherwise recharge the wetlands (Chéné and Larocque, 2023). Thus, to meet irrigation water demands without compromising the hydrology of the wetlands, an irrigation pipeline is explored.

As a preliminary assessment of potential water supply scenarios, possible pipeline dimensions are proposed for five irrigation sectors in the study area. Figure 35 outlines the boundaries of the irrigation sectors determined with the project stakeholders and highlights the irrigated cropland that was included in the regional estimate of irrigation requirements. System flow requirements were designed to peak water use. The peak volumetric water demand was determined in each of the five irrigation sectors of the region, occurring in the month of July. From the simulated irrigation events of the main crops, this peak demand was assumed to be distributed over 15 days of irrigation. 12, 15, and 18 hours of pumping per day were investigated. The peak flow rates, if water is pumped for 12 hours per day over 15 days, for each sector are listed in **Table 20**.

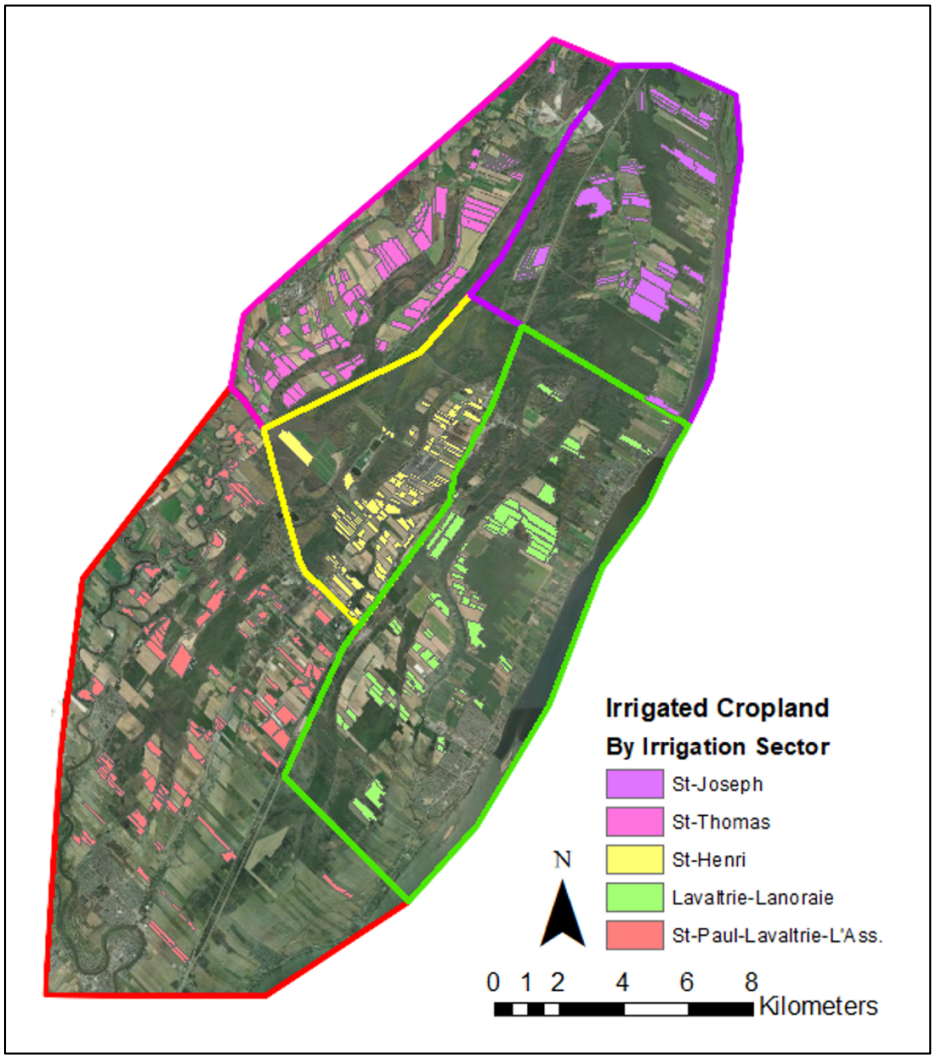

Figure 35. Irrigated cropland considered in regional estimate of irrigation requirements for the proposed irrigation sectors.

Table 20. Peak pipeline flow rate for each irrigation sector in the month of peak volumetric water demand. Assumes 15 days of irrigation with 12 hours of pumping per day.

Irrigation Sector	Irrigated Area (ha)	Peak Demand Vol (m^3)	Peak Flow rate Q (m^3/s)
St-Joseph	565	485927	0.75
St-Thomas	830	832044	1.28
St-Henri	487	454566	0.70
Lavaltrie-Lanoraie	691	664524	1.03
St-Paul-Lavaltrie-L'Ass.	942	903875	1.39

Pipeline diameters were calculated from volumetric flow rate to meet peak demand of each irrigation sector, using Manning's equation and the Hazen-Williams equation, and are presented in Sections 4.7.2 and 4.7.1, respectively.

4.7.2. Manning's derived pipeline diameter

Using volumetric flow rate and Manning's equation, pipeline diameters were calculated for a water supply system, considering duration of pumping, pipe material, and slope of the pipe. The assumptions are summarized in **Table 21**. The pipe materials investigated were polyvinyl chloride (PVC), high-density polyethylene (HDPE), and steel. Slopes varied from 0.2% to 0.8%.

Table 21. List of investigated assumptions for Manning's equation pipeline calculations.

Pumping Durations (hours/day)	Pipe Materials and Roughness Coefficients	Hydraulic Gradients (m/m)
12	PVC (n = 0.009)	0.008
15	HDPE (n = 0.009)	0.006
18	Steel (n = 0.012)	0.004
		0.002

Pipeline diameters for PVC and steel materials can be observed in Figure 36 and Figure 37, under various hydraulic gradients. Assuming 15 hours of pumping on 12 days of irrigation for a PVC pipe with a slope of 0.4%, potential diameters would be 67 cm, 82 cm, 65 cm, 75 cm, and 84 cm for the St-Joseph, St-Thomas, St-Henri, Lavaltrie-Lanoraie, and St-Paul-Lavaltrie-

L'Assomption irrigation sectors. Exact pipeline slope will depend on surveys done in a future study outlining possible pipeline routes.

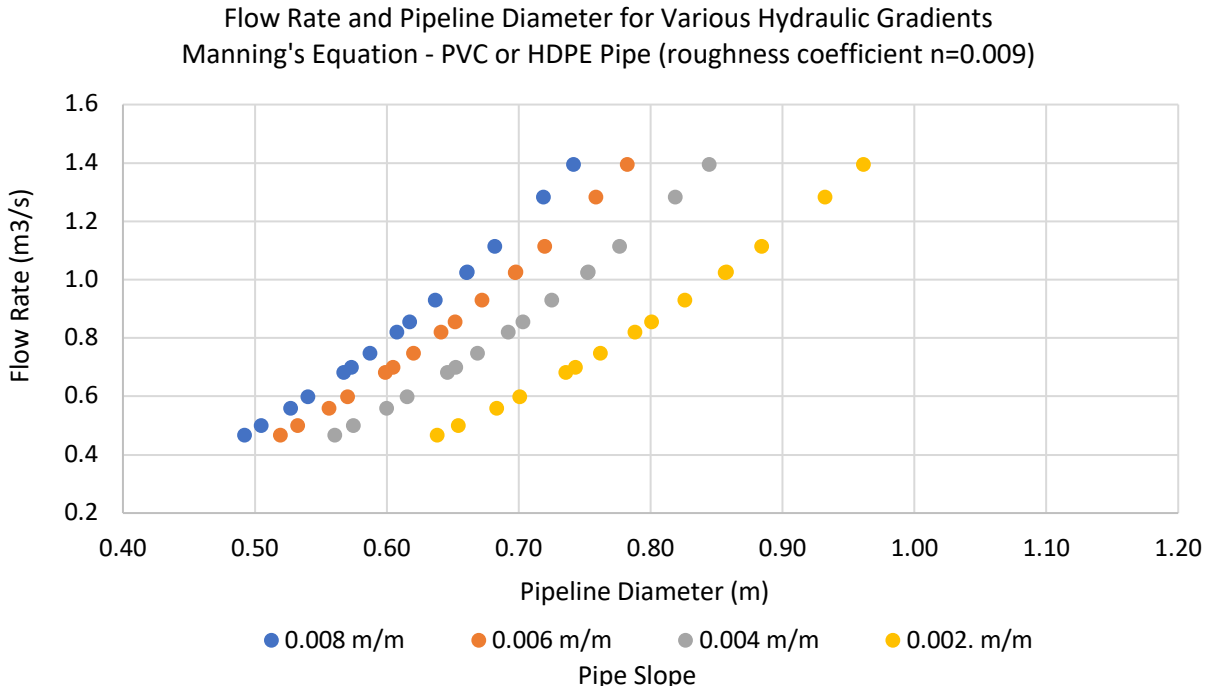

Figure 36. Flow rate and pipeline diameter of PVC (or HDPE) pipeline for various hydraulic gradients under peak demand, derived from Manning's equation.

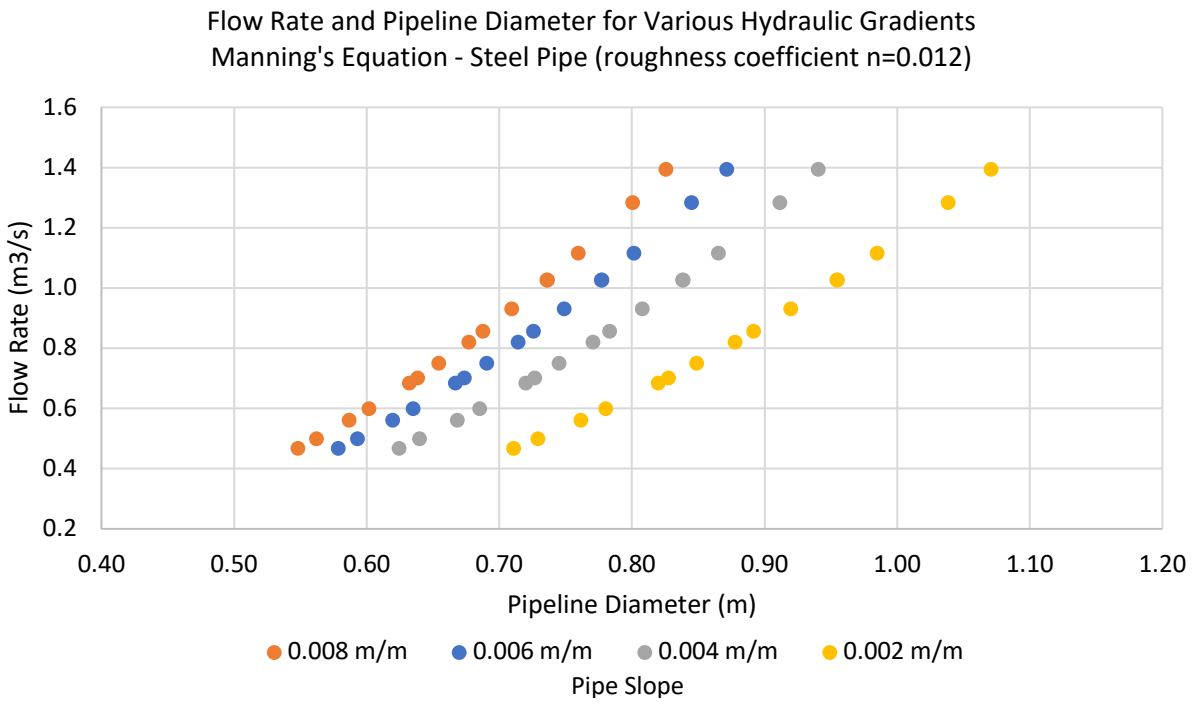

Figure 37. Flow rate and pipeline diameter of steel pipeline for various hydraulic gradients under peak demand, derived from Manning's equation.

4.7.1. Hazen-Williams derived pipeline diameter

Similarly, volumetric flow rate and the Hazen-Williams equation were also used to calculate pipeline diameter from volumetric flow rate, while considering duration of pumping, pipe material, and slope of the pipe. The assumptions considered in the calculations are summarized in.

Table 22. List of investigated assumptions for Hazen-Williams pipeline calculations.

Pumping Durations (hours/day)	Pipe Materials and Roughness Coefficients	Hydraulic Gradients (m/m)
12	PVC (C = 150)	0.008
15	HDPE (C = 140)	0.006
18	Steel (C = 110)	0.004
		0.002

The diameters of pipelines constructed from PVC and steel materials, calculated using the Hazen-Williams equation, are depicted in Figure 38 and Figure 39, considering various hydraulic gradients. Using the same example, for a PVC pipe with a slope of 0.4%, assuming 15 hours of

pumping on 12 days of irrigation, potential diameters are estimated to be 67 cm, 83 cm, 66 cm, 76 cm, and 85 cm for the St-Joseph, St-Thomas, St-Henri, Lavaltrie-Lanoraie, and St-Paul-Lavaltrie-L'Assomption irrigation sectors. Both the Manning's and Hazen-Williams equations yielded pipeline diameters with a negligible difference ranging from 0 to 3%. This empirical analysis provides an initial estimate of the pipeline dimensions needed to meet the irrigation demand for the proposed sectors during peak periods in historically dry years.

A comprehensive design of the conveyance system should consider key factors including elevation, distance, storage facilities, pumping systems, and energy requirements. Future project phases will require evaluating water quality, adhering to environmental and governmental regulations, and conducting a cost-benefit analysis for the irrigation water supply system. Additionally, community engagement will play a crucial role in the project planning process.

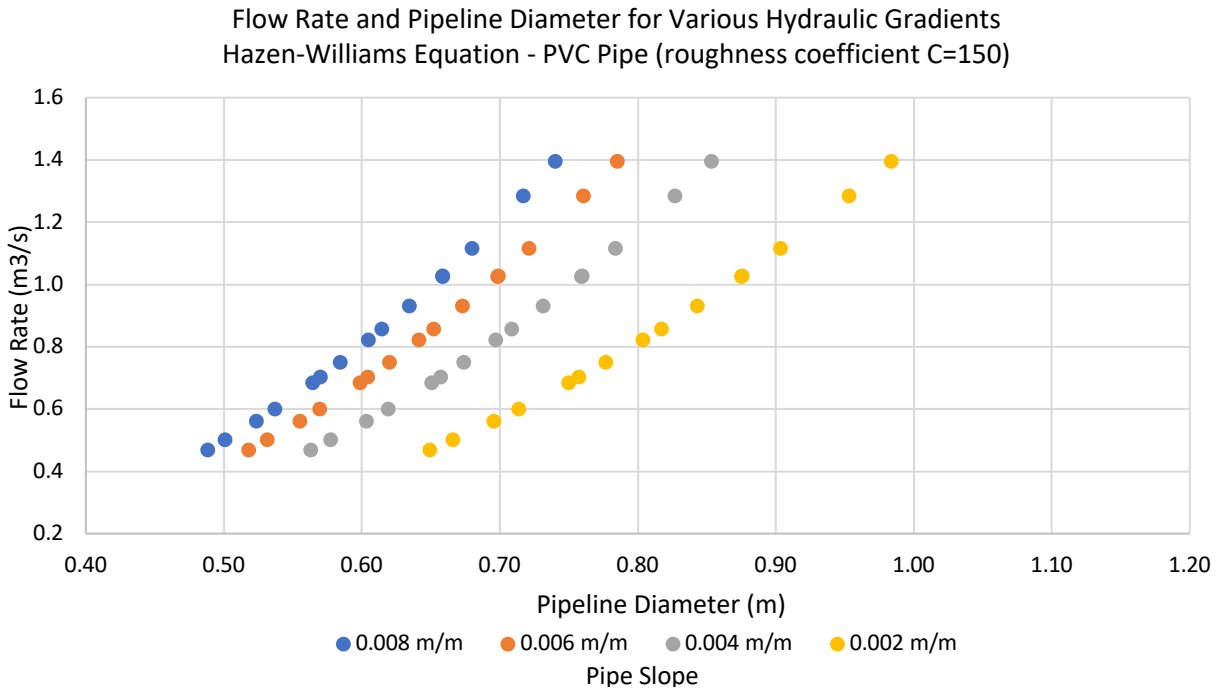

Figure 38. Flow rate and pipeline diameter of PVC pipeline for various hydraulic gradients under peak demand, derived from the Hazen-Williams equation.

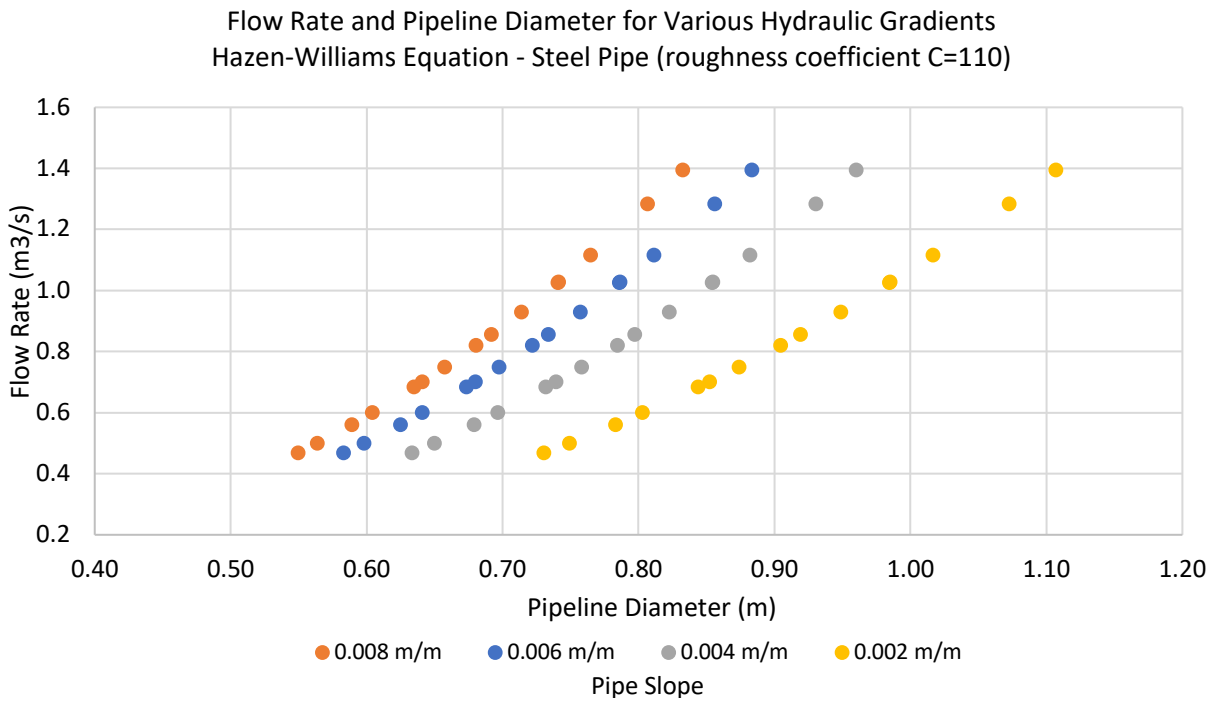

Figure 39. Flow rate and pipeline diameter of steel pipeline for various hydraulic gradients under peak demand, derived from the Hazen-Williams equation.

5. Conclusions and recommendations

5.1 Conclusions

This study aimed to assess the current and future irrigation water requirements for the agriculture-wetland complex of Lanoraie and propose a water supply scenario. Field data gathered from four representative field sites over the 2022 growing season were used to calibrate AquaCrop models to local conditions, refining their accuracy in simulating soil moisture. Subsequently, these refined models were used to estimate the irrigation requirements for historical dry, average, and wet years. Future irrigation needs were estimated by incorporating climatic data from the CMIP-6 model ensemble, downscaled statistically to the study area, under the SSP5-8.5 scenario. Finally, gross irrigation quantities for the major irrigated crops in historical dry scenarios were extrapolated across the study area. This extension facilitated the identification of peak water demands, leading to a preliminary assessment of a water conveyance system designed for five irrigation districts.

Based on the study objectives, the following conclusions are drawn:

a) Overall, AquaCrop simulated soil moisture with satisfactory accuracy (r ranging from 0.54 to 0.88) and served as a useful tool for estimating regional of irrigation requirements. The potato and squash models exhibited the strongest agreement between simulated and observed soil moisture, compared to the cranberry and strawberry models. Lower model efficiency was observed for the simulation of soil water content in the strawberry field. The observed discrepancies may be attributable to atypical growth cycles in the field, stemming from the cultivation of strawberry plants for distribution.
b) Simulating historical irrigation for the predominate crops in the study area highlighted that the irrigation treatment employed by producers significantly influences the net seasonal requirements for each of the major irrigated crops. The prevailing weather condition of the growing season also had a significant impact on the net irrigation. Employing an irrigation management strategy with a MAD set at 50% of AW proved highly effective, significantly reducing the irrigation needs across all major crops. This approach demonstrated particular efficiency in historically dry years, mitigating the considerably increased water demand compared to wet years.
c) Under the SSP5-8.5 high emissions scenario, the future irrigation requirements of each major crop had distinct responses to climate change, yet the significant impact of irrigation

treatment persisted for all crops. For potato, the future climate and irrigation strategy both played a significant role in influencing net irrigation requirements, projecting a significant increase by the 2080s. However, the implementation of the MAD 50%AW treatment helped mitigate this increase. Projections for the other key crops suggested either stable or decreasing seasonal water needs, potentially attributed to shortened crop growth cycles. Across all climate periods, maintaining a maximum depletion level of 50% AW emerged as a recommended practice, consistently reducing net irrigation requirements for all crops. This underscores the pivotal role of producers selected irrigation regime in influencing overall irrigation water use.

d) Mapping the simulated irrigation requirements across the agricultural region of Lanoraie revealed peak water demands in the month of July, coinciding with periods of low stream flow. Considering the drawdown of the peatland complex's water levels, an irrigation pipeline system was explored to convey water to five designated irrigation sectors. Various pipe materials, hydraulic gradients, and pumping durations were investigated. For instance, assuming 15 hours of pumping on 12 days of irrigation for a PVC pipe with a slope of 0.4%, potential diameters of 67 cm, 82 cm, 65 cm, 75 cm, and 84 cm were identified to supply peak flow to the St-Joseph, St-Thomas, St-Henri, Lavaltrie-Lanoraie, and St-Paul-Lavaltrie-L'Assomption irrigation sectors.

5.2 Recommendations for future research

Based on the results of this study, the following recommendations are given for future research and phases of the SCELANEAU project:

a) Future research efforts could benefit from an extended period of data collection to enhance AquaCrop model calibration specific to Lanoraie's local conditions and validate model performance. This entails deploying a greater number of volumetric soil moisture sensors with a strategically distributed network across multiple fields. A thorough soil analysis of the field sites is advised to precisely determine soil water retention parameters, including field capacity, which was highly sensitive parameter in the simulation of soil water content. Additionally, the precise monitoring of crop growth and production variables, such as leaf area index, cumulative biomass, and final yield measurements, is recommended to refine the calibration of crop parameters to strengthen model predictions.

b) A comprehensive field study investigating the plant water stress response of the major irrigated crops to specific irrigation regimes would enhance the substantiation of an irrigation management strategy tailored to the individual needs of each crop.
c) Conducting future model simulations with climate change data modeled under additional shared socio-economic pathways would provide a more expansive and comprehensive understanding of the potential effects of climate change on net irrigation requirements, considering the variability among climate projections. Studying the temperature thresholds and heat stress responses across multiple crop varieties could further explore the impact of climate change on crop cycle length and aid in the selection of cultivars better suited for future climates.
d) Future phases of the project should focus on the detailed engineering design of the proposed irrigation pipeline system. This entails a thorough topographical analysis to determine the most efficient pipeline route, soil and groundwater assessments, material selection, pumping system evaluation, and energy requirement calculations. Water quality and environmental impact assessments will be required to ensure compliance with regulatory standards and to obtain necessary permits, while actively involving local communities for input and to address concerns.
e) A comprehensive cost-benefit analysis, considering both initial construction costs and long-term operational expenses will help determine the feasibility and funding of the proposed irrigation supply system.

6. Bibliography

Abrha, B., Delbecque, N., Raes, D., Tsegay, A., Todorovic, M., Heng, L., Vanutrecht, E., Geerts, S., Garcia-Vila, M., & Deckers, S. (2012). Sowing strategies for barley (Hordeum vulgare L.) based on modelled yield response to water with AquaCrop. *Experimental Agriculture*, *48*(2), 252–271.

Adak, N., Gubbuk, H., & Tetik, N. (2018). Yield, quality and biochemical properties of various strawberry cultivars under water stress. *Journal of the Science of Food and Agriculture*, *98*(1), 304–311. https://doi.org/10.1002/jsfa.8471

Adam, M., Van Bussel, L. G. J., Leffelaar, P. A., Van Keulen, H., & Ewert, F. (2011). Effects of modelling detail on simulated potential crop yields under a wide range of climatic conditions. *Ecological Modelling*, *222*(1), 131–143. https://doi.org/10.1016/j.ecolmodel.2010.09.001

Adekanmbi, T., Wang, X., Basheer, S., Nawaz, R. A., Pang, T., Hu, Y., & Liu, S. (2023). Assessing future climate change impacts on potato yields—A case study for Prince Edward Island, Canada. *Foods*, *12*(6), 1176. https://doi.org/10.3390/foods12061176

Agriculture and Agri-Food Canada. (2021). *Crop Profile for Strawberry in Canada* (A118-10/17-2019E-PDF; Pest Management Program). Agriculture and Agri-Food Canada. https://publications.gc.ca/collections/collection_2021/aac-aafc/A118-10-17-2019-eng.pdf

Agriculture and Agri-Food Canada. (2015). *2015 Land Cover of Canada*. https://open.canada.ca/data/en/dataset/4e615eae-b90c-420b-adee-2ca35896caf6

Agriculture and Agri-Food Canada. (2023). *Canadian Food Inspection Agency—AAC Généreuse*. Government of Canada. https://inspection.canada.ca/english/plaveg/pbrpov/cropreport/str/app00009051e.shtml

Alaya, I., Masmoudi, M. M., Jacob, F., & Ben Mechlia, N. (2019). Up-scaling of crop productivity estimations using the AquaCrop model and GIS-based operations. *Arabian Journal of Geosciences*, *12*(14), 419. https://doi.org/10.1007/s12517-019-4588-5

Allen, R. G., Pereira, L. S., Raes, D., & Smith, M. (1998). *FAO Irrigation and drainage paper 56.* [Methodology Reference]. Food and Agriculture Organization. http://www.fao.org/docrep/x0490e/x0490e00.htm

Allen, R. G., Pruitt, W. O., Wright, J. L., Howell, T. A., Ventura, F., Snyder, R., Itenfisu, D., Steduto, P., Berengena, J., Yrisarry, J. B., Smith, M., Pereira, L. S., Raes, D., Perrier, A., Alves, I., Walter, I., & Elliott, R. (2006). A recommendation on standardized surface resistance for hourly calculation of reference ETo by the FAO56 Penman-Monteith method. *Agricultural Water Management*, *81*(1), 1–22. https://doi.org/10.1016/j.agwat.2005.03.007

Amer, K. H. (2011). Effect of irrigation method and quantity on squash yield and quality. *Agricultural Water Management*, *98*(8), 1197–1206. https://doi.org/10.1016/j.agwat.2011.03.003

Amini, A., Karami, F., Sedri, M. H., & Khaledi, V. (2022). Determination of water requirement and crop coefficient for strawberry using lysimeter experiment in a semi-arid climate. *H2Open Journal*, *5*(4), 642–655. https://doi.org/10.2166/h2oj.2022.030

Anapalli, S. S., Fisher, D. K., Reddy, K. N., Pettigrew, W. T., Sui, R., & Ahuja, L. R. (2016). Vulnerabilities and adapting irrigated and rainfed cotton to climate change in the lower Mississippi Delta region. *Climate*, *4*(4), Article 4. https://doi.org/10.3390/cli4040055

Araji, H. A., Wayayok, A., Massah Bavani, A., Amiri, E., Abdullah, A. F., Daneshian, J., & Teh, C. B. S. (2018). Impacts of climate change on soybean production under different treatments of field experiments

considering the uncertainty of general circulation models. *Agricultural Water Management*, *205*, 63–71. https://doi.org/10.1016/j.agwat.2018.04.023

Araki, H., Hamada, A., Hossain, Md. A., & Takahashi, T. (2012). Waterlogging at jointing and/or after anthesis in wheat induces early leaf senescence and impairs grain filling. *Field Crops Research*, *137*, 27–36. https://doi.org/10.1016/j.fcr.2012.09.006

Arguez, A., & Vose, R. S. (2011). The Definition of the Standard WMO Climate Normal: The Key to Deriving Alternative Climate Normals. *Bulletin of the American Meteorological Society*, *92*(6), 699–704.

Assani, A. A., Maloney-Dumont, V., Pothier-Champagne, A., Kinnard, C., & Quéssy, J.-F. (2019). Comparison of the temporal variability of summer temperature and rainfall as it relates to climate indices in southern Quebec (Canada). *Theoretical and Applied Climatology*, *137*(3), 2425–2435. https://doi.org/10.1007/s00704-018-2750-8

Assani, A., Zeroual, A., Kinnard, C., & Roy, A. (2022). Spatial–temporal variability of seasonal daily minimum flows in southern Quebec: Synthesis on the impacts of climate, agriculture and wetlands. *Hydrology Research*, *53*(12), 1494–1509. https://doi.org/10.2166/nh.2022.070

Asseng, S., Zhu, Y., Wang, E., & Zhang, W. (2015). Chapter 20—Crop modeling for climate change impact and adaptation. In V. O. Sadras & D. F. Calderini (Eds.), *Crop Physiology (Second Edition)* (pp. 505–546). Academic Press. https://doi.org/10.1016/B978-0-12-417104-6.00020-0

Association des Producteurs de Canneberges du Québec. (2021). *Conventional and Organic Cranberry production in Quebec* [dataset]. file:///Users/backup/Downloads/Cranberry-production-in-Quebec--conventional--organic--1992-2021.pdf

ASTM. (2006). *C136-06: Standard test method for sieve analysis of fine and coarse aggregates*. ASTM International. https://doi.org/10.1520/C0136-06

ASTM. (2007). *D422-63: Standard test method for sieve analysis of fine and coarse aggregates*. ASTM International. https://doi.org/10.1520/D0422-63R07

ASTM. (2019). *D2216-19: Standard Test Methods for Laboratory Determination of Water (Moisture) Content of Soil and Rock by Mass*. ASTM International. https://doi.org/10.1520/D2216-19

Baer, J. (1972). Dynamics of fluids in porous media. *America Elsevier Pubilishing Company*.

Bates, B., Kundzewicz, Z., Wu, S., & Palutikof, J. (2008). *Climate Change and Water. Technical Paper of the Intergovernmental Panel on Climate Change.* IPCC. https://www.ipcc.ch/publication/climate-change-and-water-2/

Battilani, A., Letterio, T., & Chiari, G. (2014). *AquaCrop model calibration and validation for processing tomato crop in a sub-humid climate*. 167–174.

Battisti, R., Sentelhas, P. C., & Boote, K. J. (2018). Sensitivity and requirement of improvements of four soybean crop simulation models for climate change studies in Southern Brazil. *International Journal of Biometeorology*, *62*(5), 823–832. https://doi.org/10.1007/s00484-017-1483-1

Bhatia, V. S., Singh, P., Wani, S. P., Chauhan, G. S., Rao, A. V. R. K., Mishra, A. K., & Srinivas, K. (2008). Analysis of potential yields and yield gaps of rainfed soybean in India using CROPGRO-Soybean model. *Agricultural and Forest Meteorology*, *148*(8), 1252–1265. https://doi.org/10.1016/j.agrformet.2008.03.004

Bigah, Y., Rousseau, A. N., & Gumiere, S. J. (2019). Development of a steady-state model to predict daily water table depth and root zone soil matric potential of a cranberry field with a subirrigation system. *Agricultural Water Management*, *213*, 1016–1027. https://doi.org/10.1016/j.agwat.2018.12.024

Bird, D. N., Benabdallah, S., Gouda, N., Hummel, F., Koeberl, J., La Jeunesse, I., Meyer, S., Prettenthaler, F., Soddu, A., & Woess-Gallasch, S. (2016). Modelling climate change impacts on and adaptation strategies for agriculture in Sardinia and Tunisia using AquaCrop and value-at-risk. *Science of The Total Environment*, *543*, 1019–1027. https://doi.org/10.1016/j.scitotenv.2015.07.035

Bittelli, M., & Flury, M. (2009). Errors in Water Retention Curves Determined with Pressure Plates. *Soil Science Society of America Journal*, *73*(5), 1453–1460. https://doi.org/10.2136/sssaj2008.0082

Boisvert, J., Dwyer, L., & Lemay, M. (1992). Estimation of Water Use By Four Potato (Solarium tuberosurn L.) Cultivars for Irrigation Scheduling. *Canadian Agricultural Engineering*, *34*(4), 319.

Boozar, N., Egdernezhad, A., & Boroomand Nasab, S. (2022). Sensitivity analysis of potato growth parameters using aquacrop model under different irrigation managements (Case Study: Shahrekord). *Water Management in Agriculture*. https://wmaj.iaid.ir/article_159856.html

Bourgault, M. A., Larocque, M., & Roy, M. (2013). Simulation of aquifer-peatland-river interactions under climate change. *Hydrology Research*, *45*(3), 425–440. https://doi.org/10.2166/nh.2013.228

Bragazza, L., Buttler, A., Habermacher, J., Brancaleoni, L., Gerdol, R., Fritze, H., Hanajík, P., Laiho, R., & Johnson, D. (2012). High nitrogen deposition alters the decomposition of bog plant litter and reduces carbon accumulation. *Global Change Biology*, *18*(3), 1163–1172.

Brander, L., Brouwer, R., & Wagtendonk, A. (2013). Economic valuation of regulating services provided by wetlands in agricultural landscapes: A meta-analysis. *Ecological Engineering*, *56*, 89–96. https://doi.org/10.1016/j.ecoleng.2012.12.104

Brauman, K. A., Siebert, S., & Foley, J. A. (2013). Improvements in crop water productivity increase water sustainability and food security—A global analysis. *Environmental Research Letters*, *8*(2), 024030. https://doi.org/10.1088/1748-9326/8/2/024030

Brisson, N., Gary, C., Justes, E., Roche, R., Mary, B., Ripoche, D., Zimmer, D., Sierra, J., Bertuzzi, P., & Burger, P. (2003). An overview of the crop model STICS. *European Journal of Agronomy*, *18*(3–4), 309–332.

Brooks, R. H., & Corey, A. T. (1966). Properties of porous media affecting fluid flow. *Journal of the Irrigation and Drainage Division*, *92*(2), 61–88.

Bryant, W. (2017). *Review of pipe flow: Darcy-Weisbach, Manning, Hazen-Williams equations, Moody diagram—Free Download PDF*. https://silo.tips/download/lecture-1-review-of-pipe-flow-darcy-weisbach-manning-hazen-williams-equations-mo

Bubier, J. L., Moore, T. R., & Bledzki, L. A. (2007). Effects of nutrient addition on vegetation and carbon cycling in an ombrotrophic bog. *Global Change Biology*, *13*(6), 1168–1186.

Busschaert, L., de Roos, S., Thiery, W., Raes, D., & De Lannoy, G. J. M. (2022). Net irrigation requirement under different climate scenarios using AquaCrop over Europe. *Hydrology and Earth System Sciences*, *26*(14), 3731–3752. https://doi.org/10.5194/hess-26-3731-2022

Cahn, M. D., & Johnson, L. F. (2017). New approaches to irrigation scheduling of vegetables. *Horticulturae*, *3*(2), Article 2. https://doi.org/10.3390/horticulturae3020028

Cai, J., Liu, Y., Lei, T., & Pereira, L. S. (2007). Estimating reference evapotranspiration with the FAO Penman–Monteith equation using daily weather forecast messages. *Agricultural and Forest Meteorology*, *145*(1), 22–35. https://doi.org/10.1016/j.agrformet.2007.04.012

Cai, X., Zhang, X., Noël, P. H., & Shafiee-Jood, M. (2015). Impacts of climate change on agricultural water management: A review. *WIREs Water*, *2*(5), 439–455. https://doi.org/10.1002/wat2.1089

Campbell, B. M., Vermeulen, S. J., Aggarwal, P. K., Corner-Dolloff, C., Girvetz, E., Loboguerrero, A. M., Ramirez-Villegas, J., Rosenstock, T., Sebastian, L., Thornton, P. K., & Wollenberg, E. (2016). Reducing risks to food security from climate change. *Global Food Security*, *11*, 34–43. https://doi.org/10.1016/j.gfs.2016.06.002

Campbell, G. S., & Mulla, D. J. (1990). Measurement of soil water content and potential. *Agronomy*, *30*, 127–142.

Cannon, A. J., Sobie, S. R., & Murdock, T. Q. (2015). Bias correction of gcm precipitation by quantile mapping: how well do methods preserve changes in quantiles and extremes? *Journal of Climate*, *28*(17), 6938–6959. https://doi.org/10.1175/JCLI-D-14-00754.1

Caron, J., Bonin, S., Pepin, S., Kummer, L., Vanderleest, C., & Bland, W. L. (2016). Determination of irrigation set points for cranberries from soil- and plant-based measurements. *Canadian Journal of Soil Science*, *96*(1), 37–50. https://doi.org/10.1139/cjss-2015-0037

Caron, J., Pelletier, V., Kennedy, C. D., Gallichand, J., Gumiere, S., Bonin, S., Bland, W. L., & Pepin, S. (2017). Guidelines of irrigation and drainage management strategies to enhance cranberry production and optimize water use in North America. *Canadian Journal of Soil Science*, *97*(1), 82–91. https://doi.org/10.1139/cjss-2016-0086

Casa, A. de la, Ovando, G., Bressanini, L., & Martínez, J. (2013). *Aquacrop Model Calibration in Potato and Its Use to Estimate Yield Variability under Field Conditions*. *2013*. https://doi.org/10.4236/acs.2013.33041

Challinor, A., Martre, P., Asseng, S., Thornton, P., & Ewert, F. (2014). Making the most of climate impacts ensembles. *Nature Climate Change*, *4*(2), Article 2. https://doi.org/10.1038/nclimate2117

Chapman, S. C., Chakraborty, S., Dreccer, M. F., & Howden, S. M. (2012). Plant adaptation to climate changeopportunities and priorities in breeding. *Crop and Pasture Science*, *63*(3), 251–268. Scopus. https://doi.org/10.1071/CP11303

Chen, D., & Chen, H. W. (2013). Using the Köppen classification to quantify climate variation and change: An example for 1901–2010. *Environmental Development*, *6*, 69–79. https://doi.org/10.1016/j.envdev.2013.03.007

Chimner, R. A., Cooper, D. J., Wurster, F. C., & Rochefort, L. (2017). An overview of peatland restoration in North America: Where are we after 25 years? *Restoration Ecology*, *25*(2), 283–292. https://doi.org/10.1111/rec.12434

Clapp, R. B., & Hornberger, G. M. (1978). Empirical equations for some soil hydraulic properties. *Water Resources Research*, *14*(4), 601–604.

Clark, G. A., Albregts, E. E., Stanley, C. D., Smajstrla, A. G., & Zazueta, F. S. (1996). Water requirements and crop coefficients of drip-irrigated strawberry plants. *Transactions of the American Society of Agricultural Engineers*, *39*(3), 905–913. Scopus.

ClimateData.ca. (2023). [dataset].

Cobos, D. R., & Chambers, C. (2010). *Calibrating ECH2O Soil Moisture Sensors*. Decagon Devices.

Corbari, C., Salerno, R., Ceppi, A., Telesca, V., & Mancini, M. (2019). Smart irrigation forecast using satellite LANDSAT data and meteo-hydrological modeling. *Agricultural Water Management*, *212*, 283–294. https://doi.org/10.1016/j.agwat.2018.09.005

Cosby, B. J., Hornberger, G. M., Clapp, R. B., & Ginn, T. R. (1984). A statistical exploration of the relationships of soil moisture characteristics to the physical properties of soils. *Water Resources Research*, *20*(6), 682–690. https://doi.org/10.1029/WR020i006p00682

Craig, D. L. (1976). *Strawberry culture in Eastern Canada*. Agriculture Canada. https://doi.org/10.5962/bhl.title.59427

Crawford, jennifer, Amyotte, B., Gerbrandt, E., Lafontaine, P., & Znadstra, J. (2022). *The Canadian Berry Trial Network Update to Industry Report* (Canadian Agri-Science Cluster for Horticulture 3, p. 5).

Currey, P. M. (2009). *Interactions between atmospheric nitrogen deposition and carbon dynamics in peatlands*.

Dahl, T. E. (1990). *Wetlands: Losses in the United States 1780's to 1980's* (p. 21). U.S. Department of the Interior, Fish and Wildlife Service. https://www.fws.gov/wetlands/documents/wetlands-losses-in-the-united-states-1780s-to-1980s.pdf

Daigle, J.-Y., & Gautreau-Daigle, H. (2001). *Canadian peat harvesting and the environment* (Second edition). North American Wetlands Conservation Council Committee.

Dale, A. (2008). *How climate change could influence breeding and modern production systems in berry crops*. 161–168.

Dale, A., Fant, C., Strzepek, K., Lickley, M., & Solomon, S. (2017). Climate model uncertainty in impact assessments for agriculture: A multi-ensemble case study on maize in sub-Saharan Africa. *Earth's Future*, *5*(3), 337–353. https://doi.org/10.1002/2017EF000539

Danielescu, S., MacQuarrie, K. T. B., Zebarth, B., Nyiraneza, J., Grimmett, M., & Levesque, M. (2022). Crop water deficit and supplemental irrigation requirements for potato production in a temperate humid region (Prince Edward Island, Canada). *Water*, *14*(17), Article 17. https://doi.org/10.3390/w14172748

Darouich, H., Karfoul, R., Eid, H., Ramos, T. B., Baddour, N., Moustafa, A., & Assaad, M. I. (2020). Modeling Zucchini squash irrigation requirements in the Syrian Akkar region using the FAO56 dual-Kc approach. *Agricultural Water Management*, *229*, 105927. https://doi.org/10.1016/j.agwat.2019.105927

Davidson, N. C. (2014). How much wetland has the world lost? Long-term and recent trends in global wetland area. *Marine and Freshwater Research*, *65*(10), 934–941. https://doi.org/10.1071/MF14173

de Groot, R., Brander, L., van der Ploeg, S., Costanza, R., Bernard, F., Braat, L., Christie, M., Crossman, N., Ghermandi, A., Hein, L., Hussain, S., Kumar, P., McVittie, A., Portela, R., Rodriguez, L. C., ten Brink, P., & van Beukering, P. (2012). Global estimates of the value of ecosystems and their services in monetary units. *Ecosystem Services*, *1*(1), 50–61. https://doi.org/10.1016/j.ecoser.2012.07.005

DeMoranville, C., & Sandler, H. A. (2000). Frost Management. *Cranberry Station Best Management Practices Guide - 2000 Edition*. https://scholarworks.umass.edu/cgi/viewcontent.cgi?article=1008&context=cranberrybmp

Déziel, M.-H., Chartrand, C., Beaudoin, A., Robitaille, J., Oulatounde, J., Cargas, R., & Lavoie, C. (2019). *Portrait-diagnostic sectoriel de l'industrie de la pomme de terre au Québec*. Ministère de l'Agriculture, des Pêcheries et de l'Alimentation du Québec.

Déziel, M.-H., Chauvette, S., Dangbédji, J., Robitaille, J., Kesri, K., & Lapointe, L. (2017). *Portrait-diagnostic sectoriel des légumes frais au Québec*. Ministère de l'Agriculture, des Pêcheries et de l'Alimentation du Québec.

Djaman, K., Koudahe, K., Lombard, K., & O'Neill, M. (2018). Sum of hourly vs. Daily Penman-Monteith grass-reference evapotranspiration under semiarid and arid climate. *Irrig. Drain Syst. Eng*, *7*.

Djaman, K., Koudahe, K., Saibou, A., Darapuneni, M., Higgins, C., & Irmak, S. (2022). Soil water dynamics, effective rooting zone, and evapotranspiration of sprinkler irrigated potato in a sandy loam soil. *Agronomy*, *12*(4), Article 4. https://doi.org/10.3390/agronomy12040864

Doorenbos, J., & Kassam, A. (1979). Yield response to water. *Irrigation and Drainage Paper*, *33*, 257–280.

Doorenbos, J., & Pruitt, W. O. (1977). Crop water requirements. *FAO Irrigation and Drainage Paper*, *24*, 1–144.

Drake, B. G., Gonzàlez-Meler, M. A., & Long, S. P. (1997). more efficient plants: a consequence of rising atmospheric CO2? *Annual Review of Plant Physiology and Plant Molecular Biology*, *48*(1), 609–639. https://doi.org/10.1146/annurev.arplant.48.1.609

Driessen, P. M., & Konijn, N. T. (1992). *Land-use systems analysis*. WAU and Interdisciplinary Research (INRES). https://research.wur.nl/en/publications/land-use-systems-analysis

Droogers, P., & Allen, R. G. (2002). Estimating Reference Evapotranspiration Under Inaccurate Data Conditions. *Irrigation and Drainage Systems*, *16*(1), 33–45. https://doi.org/10.1023/A:1015508322413

Drouet, M. P. (1989). *An economic analysis for subsurface irrigation of maize in Quebec*.

Dubé, P., & Rochette, P. (1985). *Les déficits hydriques*. *2*, 27–114.

Eck, P. (1976). Cranberry growth and production in relation to water table depth. *Journal of the American Society for Horticultural Science*, *101*(5), 544–546.

Eisenhauer, D. E., Martin, D. L., Heeren, D. M., & Hoffmann, G. J. (2021). *Irrigation Systems Management*. American Society of Agricultural and Biological Engineers. https://www.asabe.org/Portals/0/aPubs/Books/ISM/IrrigationSystemsManagement.pdf

Elliott, J., Deryng, D., Müller, C., Frieler, K., Konzmann, M., Gerten, D., Glotter, M., Flörke, M., Wada, Y., Best, N., Eisner, S., Fekete, B. M., Folberth, C., Foster, I., Gosling, S. N., Haddeland, I., Khabarov, N., Ludwig, F., Masaki, Y., … Wisser, D. (2014). Constraints and potentials of future irrigation water availability on agricultural production under climate change. *Proceedings of the National Academy of Sciences*, *111*(9), 3239–3244. https://doi.org/10.1073/pnas.1222474110

Ells, J. E., McSay, A. E., Kruse, E. G., & Larson, G. (1994). Root distribution and proliferation of field-grown acorn squash as influenced by plastic mulch and water. *HortTechnology*, *4*(3), 248–252. https://doi.org/10.21273/HORTTECH.4.3.248

Elmi, A., Madramootoo, C., Handyside, P., & Dodds, G. (2010). Water requirements and subirrigation technology design criteria for cranberry production in Quebec, Canada. *CANADIAN BIOSYSTEMS ENGINEERING*, *52*. https://library.csbe-scgab.ca/docs/journal/52/C0906.pdf

Environment and Climate Change Canada. (2022a). *Historical Data* [dataset]. Environment and Climate Change Canada. https://climate.weather.gc.ca/historical_data/search_historic_data_e.html

Environment and Climate Change Canada. (2022b). *Historical Data* [dataset]. Environment and Climate Change Canada. https://climate.weather.gc.ca/historical_data/search_historic_data_e.html

Environmental Systems Research Institute, Inc. (2022). *ArcGIS Desktop* (10.8) [Computer software]. Environmental Research Systems Institute.

Ewert, F., Rötter, R. P., Bindi, M., Webber, H., Trnka, M., Kersebaum, K. C., Olesen, J. E., Van Ittersum, M. K., Janssen, S., & Rivington, M. (2015). Crop modelling for integrated assessment of risk to food production from climate change. *Environmental Modelling & Software*, *72*, 287–303.

Farahani, H. J., Izzi, G., & Oweis, T. Y. (2009). Parameterization and Evaluation of the AquaCrop Model for Full and Deficit Irrigated Cotton. *Agronomy Journal*, *101*(3), 469–476. https://doi.org/10.2134/agronj2008.0182s

Farina, R., Seddaiu, G., Orsini, R., Steglich, E., Roggero, P. P., & Francaviglia, R. (2011). Soil carbon dynamics and crop productivity as influenced by climate change in a rainfed cereal system under contrasting tillage using EPIC. *Soil and Tillage Research*, *112*(1), 36–46. https://doi.org/10.1016/j.still.2010.11.002

Farquhar, G. D., Dubbe, D. R., & Raschke, K. (1978). Gain of the feedback loop involving carbon dioxide and stomata: Theory and measurement. *Plant Physiology*, *62*(3), 406–412.

Favreau, M., Pellerin, S., & Poulin, M. (2019). Tree Encroachment Induces Biotic Differentiation in Sphagnum-Dominated Bogs. *Wetlands*, *39*(4), 841–852. https://doi.org/10.1007/s13157-018-1122-6

Feng, D., Li, G., Wang, D., Wulazibieke, M., Cai, M., Kang, J., Yuan, Z., & Xu, H. (2022). Evaluation of AquaCrop model performance under mulched drip irrigation for maize in Northeast China. *Agricultural Water Management*, *261*, 107372. https://doi.org/10.1016/j.agwat.2021.107372

Feng, Y., Cui, N., Gong, D., Zhang, Q., & Zhao, L. (2017). Evaluation of random forests and generalized regression neural networks for daily reference evapotranspiration modelling. *Agricultural Water Management*, *193*, 163–173. https://doi.org/10.1016/j.agwat.2017.08.003

Ferriol, M., & Picó, B. (2008). Pumpkin and Winter Squash. In J. Prohens & F. Nuez (Eds.), *Vegetables I: Asteraceae, Brassicaceae, Chenopodicaceae, and Cucurbitaceae* (pp. 317–349). Springer. https://doi.org/10.1007/978-0-387-30443-4_10

Finlayson, M., Cruz, R. D., Davidson, N., Alder, J., Cork, S., Groot, R. S. de, Lévêque, C., Milton, G. R., Peterson, G., Pritchard, D., Ratner, B. D., Reid, W. V., Revenga, C., Rivera, M., Schutyser, F., Siebentritt, M., Stuip, M., Tharme, R., Butchard, S., … Taylor, D. (2005). *Millennium Ecosystem Assessment: Ecosystems and human well-being: wetlands and water synthesis* (p.). World Resources Institute. https://library.wur.nl/WebQuery/wurpubs/344031

Fischer, G., Tubiello, F. N., van Velthuizen, H., & Wiberg, D. A. (2007). Climate change impacts on irrigation water requirements: Effects of mitigation, 1990–2080. *Technological Forecasting and Social Change*, *74*(7), 1083–1107. https://doi.org/10.1016/j.techfore.2006.05.021

Fityus, S., Wells, T., & Wenxiong, H. (2011). Water content measurement in expansive soils using the neutron probe. *Geotechnical Testing Journal*, *34*(3), 1–10.

Food and Agriculture Organization. (2008). *International Year of the Potato 2008—New Light on a Hidden Treasure*.

Food and Agriculture Organization. (2015). Statistical Indicatiors. In *AquaCrop New Features and Updates Version 5.0* (pp. 82–85). FAO. https://www.pmf.unizg.hr/_download/repository/AQUA_CROP_upute_model.pdf

Food and Agriculture Organization. (2021). Valuing Water, Chapter 5: Food and Agriculture. In The United Nations world water development report 2021: Valuing water (pp. 67–78). UNESCO. https://unesdoc.unesco.org/ark:/48223/pf0000375737

Food and Agriculture Organization. (2022). *AQUASTAT - FAO's Global Information System on Water and Agriculture* [dataset]. https://data.apps.fao.org/aquastat

Gallardo, M., Elia, A., & Thompson, R. B. (2020). Decision support systems and models for aiding irrigation and nutrient management of vegetable crops. *Agricultural Water Management*, *240*, 106209. https://doi.org/10.1016/j.agwat.2020.106209

Gallichand, J., Broughton, R., Boisvert, J., & Rochette, P. (1991). Simulation of irrigation requirements for major crops in South Western Quebec. *Canadian Agricultural Engineering*, *33*(1), 1–9.

Gao, Z., He, J., Dong, K., & Li, X. (2017). Trends in reference evapotranspiration and their causative factors in the West Liao River basin, China. *Agricultural and Forest Meteorology*, *232*, 106–117. https://doi.org/10.1016/j.agrformet.2016.08.006

Gardner, W. H. (1986). Water Content. In *Methods of Soil Analysis* (pp. 493–544). John Wiley & Sons, Ltd. https://doi.org/10.2136/sssabookser5.1.2ed.c21

Garibay, V. M., Kothari, K., Ale, S., Gitz, D. C., Morgan, G. D., & Munster, C. L. (2019). Determining water-use-efficient irrigation strategies for cotton using the DSSAT CSM CROPGRO-cotton model evaluated with in-season data. *Agricultural Water Management*, *223*, 105695. https://doi.org/10.1016/j.agwat.2019.105695

Ge, J., Yu, Z., Gong, X., Ping, Y., Luo, J., & Li, Y. (2023). Evaluation of Irrigation Modes for Greenhouse Drip Irrigation Tomatoes Based on AquaCrop and DSSAT Models. *Plants*, *12*(22), Article 22. https://doi.org/10.3390/plants12223863

Gee, G. W., & Bauder, J. W. (1986). Particle-size Analysis. In *Methods of Soil Analysis* (pp. 383–411). John Wiley & Sons, Ltd. https://doi.org/10.2136/sssabookser5.1.2ed.c15

Gee, G. W., & Or, D. (2002). 2.4 Particle-Size Analysis. In *Methods of Soil Analysis* (pp. 255–293). John Wiley & Sons, Ltd. https://doi.org/10.2136/sssabookser5.4.c12

Geerts, S., Raes, D., Garcia, M., Miranda, R., Cusicanqui, J. A., Taboada, C., Mendoza, J., Huanca, R., Mamani, A., Condori, O., Mamani, J., Morales, B., Osco, V., & Steduto, P. (2009). Simulating Yield Response of Quinoa to Water Availability with AquaCrop. *Agronomy Journal*, *101*(3), 499–508. https://doi.org/10.2134/agronj2008.0137s

Gendron, L., Létourneau, G., Cormier, J., Depardieu, C., Boily, C., Levallois, R., & Caron, J. (2018). Using Pulsed Water Applications and Automation Technology to Improve Irrigation Practices in Strawberry Production. *HortTechnology*, *28*(5), 642–650. https://doi.org/10.21273/HORTTECH04001-18

Ghanbarian-alavijeh, B., Liaghat, A., Huang, G.-H., & Van genuchten, M. Th. (2010). Estimation of the van Genuchten Soil Water Retention Properties from Soil Textural Data. *Pedosphere*, *20*(4), 456–465. https://doi.org/10.1016/S1002-0160(10)60035-5

Ghanbarian-Alavijeh, B., & Liaghat, A. M. (2009). Evaluation of soil texture data for estimating soil water retention curve. *Canadian Journal of Soil Science*, *89*(4), 461–471. https://doi.org/10.4141/cjss08066

Govere, S., Nyamangara, J., & Nyakatawa, E. Z. (2022). Beneficial effect of climate change on wheat yield and water footprints in the Middle-Manyame sub-catchment, Zimbabwe. *Journal of Water and Climate Change*, *13*(8), 2895–2910. https://doi.org/10.2166/wcc.2022.038

Gunnarsson, U., Malmer, N., & Rydin, H. (2002). Dynamics or constancy in Sphagnum dominated mire ecosystems? A 40-year study. *Ecography*, *25*(6), 685–704. https://doi.org/10.1034/j.1600-0587.2002.250605.x

Guo, D., Olesen, J. E., Manevski, K., & Ma, X. (2021). Optimizing irrigation schedule in a large agricultural region under different hydrologic scenarios. *Agricultural Water Management*, *245*, 106575. https://doi.org/10.1016/j.agwat.2020.106575

Guo, R., Lin, Z., Mo, X., & Yang, C. (2010). Responses of crop yield and water use efficiency to climate change in the North China Plain. *Agricultural Water Management*, *97*(8), 1185–1194. https://doi.org/10.1016/j.agwat.2009.07.006

Haddeland, I., Heinke, J., Biemans, H., Eisner, S., Flörke, M., Hanasaki, N., Konzmann, M., Ludwig, F., Masaki, Y., & Schewe, J. (2014). Global water resources affected by human interventions and climate change. *Proceedings of the National Academy of Sciences*, *111*(9), 3251–3256.

Hammer, G. L., van Oosterom, E., McLean, G., Chapman, S. C., Broad, I., Harland, P., & Muchow, R. C. (2010). Adapting APSIM to model the physiology and genetics of complex adaptive traits in field crops. *Journal of Experimental Botany*, *61*(8), 2185–2202. https://doi.org/10.1093/jxb/erq095

Han, C., Zhang, B., Chen, H., Liu, Y., & Wei, Z. (2020). Novel approach of upscaling the FAO AquaCrop model into regional scale by using distributed crop parameters derived from remote sensing data. *Agricultural Water Management*, *240*, 106288. https://doi.org/10.1016/j.agwat.2020.106288

Han, C., Zhang, B., Chen, H., Wei, Z., & Liu, Y. (2019). Spatially distributed crop model based on remote sensing. *Agricultural Water Management*, *218*, 165–173. https://doi.org/10.1016/j.agwat.2019.03.035

Hansen, J. W., & Jones, J. W. (2000). Scaling-up crop models for climate variability applications. *Agricultural Systems*, *65*(1), 43–72. https://doi.org/10.1016/S0308-521X(00)00025-1

Hanson, B., & Bendixen, W. (2004). Drip irrigation evaluated in Santa Maria Valley strawberries. *California Agriculture*, *58*(1), 48–53.

Hanson, R. L. (1991). Evapotranspiration and droughts. *US Geological Survey Water-Supply Paper*, *2375*, 99–104.

Harnois Irrigation. (2021). *Irrigation Systems in Lanoraie* [Personal communication].

Hartkamp, A. D., White, J. W., & Hoogenboom, G. (1999). Interfacing geographic information systems with agronomic modeling: A review. *Agronomy Journal*, *91*(5), 761–772.

Hattendorf, M. J., & Davenport, J. R. (1996). Cranberry Evapotranspiration. *HortScience*, *31*(3), 334–337. https://doi.org/10.21273/HORTSCI.31.3.334

He, J., Dupras, J., & G. Poder, T. (2017). The value of wetlands in Quebec: A comparison between contingent valuation and choice experiment. *Journal of Environmental Economics and Policy*, *6*(1), 51–78.

Hedley, C. B., Knox, J. W., Raine, S. R., & Smith, R. (2014). Water: Advanced Irrigation Technologies. In N. K. Van Alfen (Ed.), *Encyclopedia of Agriculture and Food Systems* (pp. 378–406). Academic Press. https://doi.org/10.1016/B978-0-444-52512-3.00087-5

Hefting, M. M., van den Heuvel, R. N., & Verhoeven, J. T. A. (2013). Wetlands in agricultural landscapes for nitrogen attenuation and biodiversity enhancement: Opportunities and limitations. *Ecological Engineering*, *56*, 5–13. Scopus. https://doi.org/10.1016/j.ecoleng.2012.05.001

Hemes, K. S., Chamberlain, S. D., Eichelmann, E., Anthony, T., Valach, A., Kasak, K., Szutu, D., Verfaillie, J., Silver, W. L., & Baldocchi, D. D. (2019). Assessing the carbon and climate benefit of restoring degraded agricultural peat soils to managed wetlands. *Agricultural and Forest Meteorology*, *268*, 202–214. https://doi.org/10.1016/j.agrformet.2019.01.017

Hess, M., Bill, M., Jason, S., & John, S. (1997). Oregon state University Western Oregon squash irrigation guide, vol. 541. *Department of Bioresource Engineering, Corvallis, OR*, 737–6304.

Hignett, C., & Evett, S. R. (2008). Direct and surrogate measures of soil water content. In *Field Estimation of Soil Water Content: A Practical Guide to Methods, Instrumentation, and Sensor Technology.* (pp. 1–22). International Atomic Energy Agency. https://www.ars.usda.gov/research/publications/publication/?seqNo115=208573

Hillel, D. (1990). Role of irrigation in agricultural systems. *Agronomy*, *30*, 5–30.

Hillel, D. (2003). 6. - Water Content and Potential. In D. Hillel (Ed.), *Introduction to Environmental Soil Physics* (pp. 93–125). Academic Press. https://doi.org/10.1016/B978-012348655-4/50007-1

Howell, T. (2003). *Sprinkler package water loss comparisons*. Proceedings for 2004 Central Plains irrigation conference, Kearney Nebraska, February 17-18.

Hsiao, T. C., Heng, L., Steduto, P., Rojas-Lara, B., Raes, D., & Fereres, E. (2009). AquaCrop—The FAO Crop Model to Simulate Yield Response to Water: III. Parameterization and Testing for Maize. *Agronomy Journal*, *101*(3), 448–459. https://doi.org/10.2134/agronj2008.0218s

Huffman, R. L., Fangmeier, D. D., Elliot, W. J., Workman, S. R., & Schwab, G. (2013). *Soil and water conservation engineering*. American Society of Agricultural and Biological Engineers St. Joseph, MI.

Hurkuck, M., Brümmer, C., Mohr, K., Spott, O., Well, R., Flessa, H., & Kutsch, W. L. (2015). Effects of grass species and grass growth on atmospheric nitrogen deposition to a bog ecosystem surrounded by intensive agricultural land use. *Ecology and Evolution*, *5*(13), 2556–2571. Scopus. https://doi.org/10.1002/ece3.1534

Ihuoma, S. O., & Madramootoo, C. A. (2017). Recent advances in crop water stress detection. *Computers and Electronics in Agriculture*, *141*, 267–275. https://doi.org/10.1016/j.compag.2017.07.026

IPCC (Ed.). (2021). *Climate Change 2021 – The Physical Science Basis: Working Group I Contribution to the Sixth Assessment Report of the Intergovernmental Panel on Climate Change*. Cambridge University Press. https://doi.org/10.1017/9781009157896.002

Iqbal, M. A., Shen, Y., Stricevic, R., Pei, H., Sun, H., Amiri, E., Penas, A., & del Rio, S. (2014). Evaluation of the FAO AquaCrop model for winter wheat on the North China Plain under deficit irrigation from field experiment to regional yield simulation. *Agricultural Water Management*, *135*, 61–72. https://doi.org/10.1016/j.agwat.2013.12.012

IRDA. (2021). *Base de Données Hydropédologiques du Québec pour l'horizon de surface des sols agricoles du Québec* (Version 2) [dataset]. Institut de recherche et de développement en agroenvironnement.

IRDA. (2022). *Soil coverage of the province of Quebec.* (2nd digital version) [Complete coverage. Scale 1:20 000]. Produced by AAFC, MAPAQ and IRDA. Distributed by IRDA.

Irmak, S. (2019, July 11). *Soil water content- and soil matric potential-based irrigation trigger values for different soil types*. CropWatch. https://cropwatch.unl.edu/2019/SWC-SMP-irrigation-trigger-values

Irmak, S., Odhiambo, L., Kranz, W. L., & Eisenhauer, D. (2011). Irrigation efficiency and uniformity, and crop water use efficiency. *Biological Systems Engineering: Papers and Publications*. https://digitalcommons.unl.edu/biosysengfacpub/451

Jabet, T., Caron, J., & Lambert, R. (2016). Payback period in cranberry associated with a wireless irrigation technology. *Canadian Journal of Soil Science*, CJSS-2016-0011. https://doi.org/10.1139/CJSS-2016-0011

Jacovides, C. P., & Kontoyiannis, H. (1995). Statistical procedures for the evaluation of evapotranspiration computing models. *Agricultural Water Management*, *27*(3), 365–371. https://doi.org/10.1016/0378-3774(95)01152-9

Jacques, M. M., Gumiere, S. J., Gallichand, J., Celicourt, P., & Gumiere, T. (2020). Impacts of Water Stress Severity and Duration on Potato Photosynthetic Activity and Yields. *Frontiers in Agronomy*, *2*. https://www.frontiersin.org/articles/10.3389/fagro.2020.590312

Jamieson, P. D., Porter, J. R., & Wilson, D. R. (1991). A test of the computer simulation model ARCWHEAT1 on wheat crops grown in New Zealand. *Field Crops Research*, *27*(4), 337–350. https://doi.org/10.1016/0378-4290(91)90040-3

Jarvis, N. j., & Leeds-Harrison, P. b. (1987). Some problems associated with the use of the neutron probe in swelling/shrinkling clay soils. *Journal of Soil Science*, *38*(1), 149–156. https://doi.org/10.1111/j.1365-2389.1987.tb02132.x

Jayawardane, N. S., Meyer, W. S., & Barrs, H. D. (1984). Moisture measurement in a swelling clay soil using neutron moisture meters. *Soil Research*, *22*(2), 109–117. https://doi.org/10.1071/sr9840109

Jean, M., & Létourneau, G. (2011). *Changements dans les milieux humides du fleuve Saint-Laurent de 1970 à 2002*. Environnement Canada, Direction générale des sciences et de la technologie ….

Jégo, G., Sánchez-Pérez, J. M., & Justes, E. (2012). Predicting soil water and mineral nitrogen contents with the STICS model for estimating nitrate leaching under agricultural fields. *Agricultural Water Management*, *107*, 54–65. https://doi.org/10.1016/j.agwat.2012.01.007

Jennings, S. A., Koehler, A.-K., Nicklin, K. J., Deva, C., Sait, S. M., & Challinor, A. J. (2020). Global potato yields increase under climate change with adaptation and CO2 fertilisation. *Frontiers in Sustainable Food Systems*, *4*. https://www.frontiersin.org/articles/10.3389/fsufs.2020.519324

Jensen, M. E., & Allen, R. G. (2016). *Evaporation, Evapotranspiration, and Irrigation Water Requirements* (2nd ed., Vol. 70). American Society of Civil Engineers.

Jeranyama, P., DeMoranville, C. J., & Kennedy, C. D. (2017). Evaluating tensiometers and moisture sensors for cranberry irrigation. *Acta Horticulturae*, *1180*, 369–372. https://doi.org/10.17660/ActaHortic.2017.1180.50

Jia, Z., Wu, Z., Luo, W., Xi, W., Tang, S., Liu, W. L., & Fang, S. (2013). The impact of improving irrigation efficiency on wetland distribution in an agricultural landscape in the upper reaches of the Yellow River in China. *Agricultural Water Management*, *121*, 54–61. https://doi.org/10.1016/j.agwat.2013.01.003

Jiang, Y., Xiong, L., Yao, F., & Xu, Z. (2019). Optimizing regional irrigation water allocation for multi-stage pumping-water irrigation system based on multi-level optimization-coordination model. *Journal of Hydrology X*, *4*, 100038. https://doi.org/10.1016/j.hydroa.2019.100038

Jin, X., Li, Z., Nie, C., Xu, X., Feng, H., Guo, W., & Wang, J. (2018). Parameter sensitivity analysis of the AquaCrop model based on extended fourier amplitude sensitivity under different agro-meteorological conditions and application. *Field Crops Research*, *226*, 1–15. https://doi.org/10.1016/j.fcr.2018.07.002

Jin, X., Li, Z., Yang, G., Yang, H., Feng, H., Xu, X., Wang, J., Li, X., & Luo, J. (2017). Winter wheat yield estimation based on multi-source medium resolution optical and radar imaging data and the AquaCrop model using the particle swarm optimization algorithm. *ISPRS Journal of Photogrammetry and Remote Sensing*, *126*, 24–37. https://doi.org/10.1016/j.isprsjprs.2017.02.001

Jing, Q., Qian, B., Bélanger, G., VanderZaag, A., Jégo, G., Smith, W., Grant, B., Shang, J., Liu, J., He, W., Boote, K., & Hoogenboom, G. (2020). Simulating alfalfa regrowth and biomass in eastern Canada using the CSM-CROPGRO-perennial forage model. *European Journal of Agronomy*, *113*, 125971. https://doi.org/10.1016/j.eja.2019.125971

Joly, M., Primeay, S., Sager, M., & Bazoge, A. (2008). *Guide d'élaboration d'un plan de conservation des milieux humides* (p. 68). ministère du Développement durable, de l'Environnement et des Parcs, Direction du patrimoine écologique et des parcs. https://belsp.uqtr.ca/id/eprint/1179/1/Joly%20et%20al_2008_Guide_plan_conservation_milieux-humides_A.pdf

Jones, J. W., Hoogenboom, G., Porter, C. H., Boote, K. J., Batchelor, W. D., Hunt, L. A., Wilkens, P. W., Singh, U., Gijsman, A. J., & Ritchie, J. T. (2003). The DSSAT cropping system model. *European Journal of Agronomy*, *18*(3), 235–265. https://doi.org/10.1016/S1161-0301(02)00107-7

Jones, P. G., & Thornton, P. K. (2003). The potential impacts of climate change on maize production in Africa and Latin America in 2055. *Global Environmental Change*, *13*(1), 51–59. https://doi.org/10.1016/S0959-3780(02)00090-0

Joy, K. J., & Paranjape, S. (2007). Understanding water conflicts in South Asia. *Contemporary Perspectives*, *1*(2), 29–57. https://doi.org/10.1177/223080750700100202

Kang, Y., Khan, S., & Ma, X. (2009). Climate change impacts on crop yield, crop water productivity and food security – A review. *Progress in Natural Science*, *19*(12), 1665–1674. https://doi.org/10.1016/j.pnsc.2009.08.001

Kapfer, J., Grytnes, J.-A., Gunnarsson, U., & Birks, H. J. B. (2011). Fine-scale changes in vegetation composition in a boreal mire over 50 years. *Journal of Ecology*, *99*(5), 1179–1189. https://doi.org/10.1111/j.1365-2745.2011.01847.x

Kelleners, T. J., Soppe, R. W. O., Ayars, J. E., & Skaggs, T. H. (2004). Calibration of capacitance probe sensors in a saline silty clay soil. *Soil Science Society of America Journal*, *68*(3), 770–778. https://doi.org/10.2136/sssaj2004.7700

Khordadi, M. J., Olesen, J. E., Alizadeh, A., Nassiri Mahallati, M., Ansari, H., & Sanaeinejad, H. (2019). climate change impacts and adaptation for crop management of winter wheat and maize in the semi-arid region of iran. *Irrigation and Drainage*, *68*(5), 841–856. https://doi.org/10.1002/ird.2373

Kim, S., Meki, M. N., Kim, S., & Kiniry, J. R. (2020). Crop modeling application to improve irrigation efficiency in year-round vegetable production in the texas winter garden region. *Agronomy*, *10*(10), Article 10. https://doi.org/10.3390/agronomy10101525

King, B. A., Stark, J. C., & Neibling, H. (2020). *Potato irrigation management*. Springer.

King, M., Altdorff, D., Li, P., Galagedara, L., Holden, J., & Unc, A. (2018). Northward shift of the agricultural climate zone under 21st-century global climate change. *Scientific Reports*, *8*(1), Article 1. https://doi.org/10.1038/s41598-018-26321-8

Kinzli, K., Manana, N., & Oad, R. (2012). Comparison of laboratory and field calibration of a soil-moisture capacitance probe for various soils. *Journal of Irrigation and Drainage Engineering*, *138*, 310–321. https://doi.org/10.1061/(ASCE)IR.1943-4774.0000418

Kisekka, I., DeJonge, K. C., Ma, L., Paz, J., & Douglas-Mankin, K. R. (2017). Crop modeling applications in agricultural water management. *Transactions of the ASABE*, *60*(6), 1959–1964.

Knox, J., Morris, J., & Hess, T. (2010). Identifying future risks to UK agricultural crop production: Putting climate change in context. *Outlook on AGRICULTURE*, *39*(4), 249–256.

Knox, S. H., Sturtevant, C., Matthes, J. H., Koteen, L., Verfaillie, J., & Baldocchi, D. (2015). Agricultural peatland restoration: Effects of land-use change on greenhouse gas (CO2 and CH4) fluxes in the Sacramento-San Joaquin Delta. *Global Change Biology*, *21*(2), 750–765. https://doi.org/10.1111/gcb.12745

Koudahe, K., Djaman, K., & Adewumi, J. (2018). Evaluation of the Penman-Monteith reference evapotranspiration under limited data and its sensitivity to key climatic variables under humid and semiarid conditions. *Modeling Earth Systems and Environment*, *4*. https://doi.org/10.1007/s40808-018-0497-y

Krishnan Kutty, S., Buis, S., Sekhar, M., Ruiz, L., Tomer, S.-K., & Guerif, M. (2017). Estimation of available water capacity components of two-layered soils using crop model inversion: Effect of crop type and water regime. *Journal of Hydrology*, *546*, 166–178. https://doi.org/10.1016/j.jhydrol.2016.12.049

Kroetsch, D., & Wang, C. (2008). Particle Size Distribution. In M. Carter & E. Gregorich (Eds.), *Soil Sampling and Methods of Analysis* (Second). CRC Press. https://doi.org/10.1201/9781420005271.ch55

Kumar, N., Adeloye, A. J., Shankar, V., & Rustum, R. (2020). Neural computing modelling of the crop water stress index. *Agricultural Water Management*, *239*, 106259. https://doi.org/10.1016/j.agwat.2020.106259

Kumar, S., & Dey, P. (2011). Effects of different mulches and irrigation methods on root growth, nutrient uptake, water-use efficiency and yield of strawberry. *Scientia Horticulturae*, *127*(3), 318–324. Scopus. https://doi.org/10.1016/j.scienta.2010.10.023

Kumudini, S. (2004). Effect of radiation and temperature on cranberry photosynthesis and characterization of diurnal change in photosynthesis. *Journal of the American Society for Horticultural Science*, *129*(1), 106–111. https://doi.org/10.21273/JASHS.129.1.0106

Lamm, F. R., Bordovsky, J. P., & Howell Sr., T. A. (2019). A review of in-canopy and near-canopy sprinkler irrigation concepts. *Transactions of the ASABE*, *62*(5), 1355–1364. https://doi.org/10.13031/trans.13229

Lee, J., De Gryze, S., & Six, J. (2011). Effect of climate change on field crop production in California's Central Valley. *Climatic Change*, *109*(1), 335–353. https://doi.org/10.1007/s10584-011-0305-4

Legates, D. R., & McCabe Jr., G. J. (1999). Evaluating the use of "goodness-of-fit" Measures in hydrologic and hydroclimatic model validation. *Water Resources Research*, *35*(1), 233–241. https://doi.org/10.1029/1998WR900018

Létourneau, G., & Caron, J. (2019). Irrigation management scale and water application method to improve yield and water productivity of field-grown strawberries. *Agronomy*, *9*(6), Article 6. https://doi.org/10.3390/agronomy9060286

Létourneau, G., Caron, J., Anderson, L., & Cormier, J. (2015). Matric potential-based irrigation management of field-grown strawberry: Effects on yield and water use efficiency. *Agricultural Water Management*, *161*, 102–113. https://doi.org/10.1016/j.agwat.2015.07.005

Li, F., Zhang, M., Zhao, Y., & Jiang, R. (2020). Multi-target planting structure adjustment under different hydrologic years using AquaCrop model. *Theoretical and Applied Climatology*, *142*(3), 1343–1357. https://doi.org/10.1007/s00704-020-03381-3

Li, R., Wei, C., Afroz, M. D., Lyu, J., & Chen, G. (2021). A GIS-based framework for local agricultural decision-making and regional crop yield simulation. *Agricultural Systems*, *193*, 103213. https://doi.org/10.1016/j.agsy.2021.103213

Liao, X., Su, Z., Liu, G., Zotarelli, L., Cui, Y., & Snodgrass, C. (2016). Impact of soil moisture and temperature on potato production using seepage and center pivot irrigation. *Agricultural Water Management*, *165*, 230–236. https://doi.org/10.1016/j.agwat.2015.10.023

Licker, R., Johnston, M., Foley, J. A., Barford, C., Kucharik, C. J., Monfreda, C., & Ramankutty, N. (2010). Mind the gap: How do climate and agricultural management explain the 'yield gap' of croplands around the world? *Global Ecology and Biogeography*, *19*(6), 769–782. https://doi.org/10.1111/j.1466-8238.2010.00563.x

Linker, R., Ioslovich, I., Sylaios, G., Plauborg, F., & Battilani, A. (2016). Optimal model-based deficit irrigation scheduling using AquaCrop: A simulation study with cotton, potato and tomato. *Agricultural Water Management*, *163*, 236–243. https://doi.org/10.1016/j.agwat.2015.09.011

Liu, H. L., Yang, J. Y., Tan, C. S., Drury, C. F., Reynolds, W. D., Zhang, T. Q., Bai, Y. L., Jin, J., He, P., & Hoogenboom, G. (2011). Simulating water content, crop yield and nitrate-N loss under free and controlled tile drainage with subsurface irrigation using the DSSAT model. *Agricultural Water Management*, *98*(6), 1105–1111. https://doi.org/10.1016/j.agwat.2011.01.017

Liu, W. (2021). Risk management potential of supplemental irrigation for cotton in a sub-humid climate under climate change. *Masters Theses*. https://trace.tennessee.edu/utk_gradthes/6119

Lu, X., Ju, Y., Wu, L., Fan, J., Zhang, F., & Li, Z. (2018). Daily pan evaporation modeling from local and cross-station data using three tree-basedmachine learning models. *Journal of Hydrology*, *566*, 668–684. https://doi.org/10.1016/j.jhydrol.2018.09.055

L'union des producteurs agricoles de Lanaudière. (2022). *Base de données des parcelles et productions agricoles déclarées* [dataset]. Produced by FADQ. Modified and distributed by UPA. https://www.fadq.qc.ca/documents/donnees/base-de-donnees-des-parcelles-et-productions-agricoles-declarees/

Lunt, P., Allot, T., Anderson, P., Buckler, M., Coupar, A., Jones, P., Labadz, J., Worrall, P., & Evans, E. M. (2010). Impacts of Peatland Restoration. *Draft Scientific Review of the IUCN U.K. Peatland Programme's Commission of Inquiry into Peatland Restoration*.

Madramootoo, C., Broughton, S., & Dodds, G. (1995). Watertable management strategies for soybean production on a sandy loam soil. *Canadian Agricultural Engineering*, *37*(1), 1–8.

Maguire, D. J. (1991). An overview and definition of GIS. *Geographical Information Systems: Principles and Applications*, *1*(1), 9–20.

Malik, W., Isla, R., & Dechmi, F. (2019). DSSAT-CERES-maize modelling to improve irrigation and nitrogen management practices under Mediterranean conditions. *Agricultural Water Management*, *213*, 298–308. https://doi.org/10.1016/j.agwat.2018.10.022

Manevski, K., Børgesen, C. D., Li, X., Andersen, M. N., Zhang, X., Shen, Y., & Hu, C. (2019). Modelling agro-environmental variables under data availability limitations and scenario managements in an alluvial region of the North China Plain. *Environmental Modelling & Software*, *111*, 94–107. https://doi.org/10.1016/j.envsoft.2018.10.001

Marx, A., Kumar, R., Thober, S., Zink, M., Wanders, N., Wood, E. F., Ming, P., Sheffield, J., & Samaniego, L. (2017). *Climate change alters low flows in Europe under a 1.5, 2, and 3 degree global warming* [Preprint]. Catchment hydrology/Modelling approaches. https://doi.org/10.5194/hess-2017-485

Matteau, J.-P. (2019). Irrigation, potatoes and unintended consequences of optimizing water management. *The Canadian Agri-Food Policy Institute*. https://capi-icpa.ca/wp-content/uploads/2019/11/2019-10-30-CAPI-Doctoral-Fellows-2017-19-paper-J-P-Matteau_WEB.pdf

Matteau, J.-P., Célicourt, P., Létourneau, G., Gumiere, T., & Gumiere, S. J. (2022). Effects of irrigation thresholds and temporal distribution on potato yield and water productivity in sandy soil. *Agricultural Water Management*, *264*, 107483. https://doi.org/10.1016/j.agwat.2022.107483

Maughan, T., Drost, D., & Allen, L. N. (n.d.). *Vegetable Irrigation: Squash and Pumpkin*.

Maulé, C., Helgason, W., McGinn, S., & Cutforth, H. (2006). Estimation of standardized reference evapotranspiration on the Canadian Prairies using simple models with limited weather data. *Canadian Biosystems Engineering*, *48*, 1.

Maurer, E. P., Hidalgo, H. G., Das, T., Dettinger, M. D., & Cayan, D. R. (2010). The utility of daily large-scale climate data in the assessment of climate change impacts on daily streamflow in California. *Hydrology and Earth System Sciences*, *14*(6), 1125–1138. https://doi.org/10.5194/hess-14-1125-2010

McClymont, E. L., Mauquoy, D., Yeloff, D., Broekens, P., van Geel, B., Charman, D. J., Pancost, R. D., Chambers, F. M., & Evershed, R. P. (2008). The disappearance of Sphagnum imbricatum from Butterburn Flow, UK. *The Holocene*, *18*(6), 991–1002. https://doi.org/10.1177/0959683608093537

McCown, R. L., Hammer, G. L., Hargreaves, J. N. G., Holzworth, D. P., & Freebairn, D. M. (1996). APSIM: A novel software system for model development, model testing and simulation in agricultural systems research. *Agricultural Systems*, *50*(3), 255–271. https://doi.org/10.1016/0308-521X(94)00055-V

Mebane, V. J., Day, R. L., Hamlett, J. M., Watson, J. E., & Roth, G. W. (2013). Validating the FAO AquaCrop model for rainfed maize in Pennsylvania. *Agronomy Journal*, *105*(2), 419–427. https://doi.org/10.2134/agronj2012.0337

Medellín-Azuara, J., Harou, J. J., Olivares, M. A., Madani, K., Lund, J. R., Howitt, R. E., Tanaka, S. K., Jenkins, M. W., & Zhu, T. (2008). Adaptability and adaptations of California's water supply system to dry climate warming. *Climatic Change*, *87*(1), 75–90. https://doi.org/10.1007/s10584-007-9355-z

Mehata, M., Datta, S., Taghvaeian, S., Ochsner, T., Mirchi, A., & Moriasi, D. N. (2023). Performance of a Multi-Sensor Capacitance Probe in Estimating Soil Water Content and Field Capacity. *Journal of Agricultural Safety and Health*, *66*(2), 253–261. https://doi.org/10.13031/ja.15416

Mehdizadeh, S. (2018). Estimation of daily reference evapotranspiration (ETo) using artificial intelligence methods: Offering a new approach for lagged ETo data-based modeling. *Journal of Hydrology*, *559*, 794–812. https://doi.org/10.1016/j.jhydrol.2018.02.060

Menzel, A., Sparks, T. H., Estrella, N., Koch, E., Aaasa, A., Ahas, R., Alm-Kübler, K., Bissolli, P., Braslavská, O., Briede, A., Chmielewski, F. M., Crepinsek, Z., Curnel, Y., Dahl, Å., Defila, C., Donnelly, A., Filella, Y., Jatczak, K., Måge, F., … Zust, A. (2006). European phenological response to climate change matches the warming pattern. *Global Change Biology*, *12*(10), 1969–1976. Scopus. https://doi.org/10.1111/j.1365-2486.2006.01193.x

Minguez, M. I., Ruiz-Ramos, M., Diaz-Ambrona, C. H., Quemada, M., & Sau, F. (2007). First-order impacts on winter and summer crops assessed with various high-resolution climate models in the Iberian Peninsula. *Climatic Change*, *81*, 343–355. https://doi.org/10.1007/s10584-006-9223-2

Ministère de l'Environnement, de la Lutte contre les changements climatiques, de la Faune et des Parcs. (2023). *Québec's Water: A Resource To Be Protected*. https://www-environnement-gouv-qc-ca.proxy3.library.mcgill.ca/eau/inter_en.htm#:%7E:text%3DFreshwater%20covers%2010%25%20of%20the,Lawrence%20River%20watershed

Mirsafi, Z.-S., Sepaskhah, A. R., Ahmadi, S. H., & Kamgar-Haghighi, A. A. (2016). Assessment of AquaCrop model for simulating growth and yield of saffron (Crocus sativus L.). *Scientia Horticulturae*, *211*, 343–351. https://doi.org/10.1016/j.scienta.2016.09.020

Mirzaei, A., & Zibaei, M. (2021). Water conflict management between agriculture and wetland under climate change: application of economic-hydrological-behavioral modelling. *Water Resources Management*, *35*(1), 1–21. https://doi.org/10.1007/s11269-020-02703-4

Mitsch, W. J., & Gosselink, J. G. (2015). *Wetlands* (5th ed.). John Wiley & Sons, Incorporated. http://ebookcentral.proquest.com/lib/mcgill/detail.action?docID=1895927

Mittelbach, H., Lehner, I., & Seneviratne, S. I. (2012). Comparison of four soil moisture sensor types under field conditions in Switzerland. *Journal of Hydrology*, *430–431*, 39–49. https://doi.org/10.1016/j.jhydrol.2012.01.041

Mkhabela, M. S., & Bullock, P. R. (2012). Performance of the FAO AquaCrop model for wheat grain yield and soil moisture simulation in Western Canada. *Agricultural Water Management*, *110*, 16–24. https://doi.org/10.1016/j.agwat.2012.03.009

Montoya, F., Camargo, D., Ortega, J. F., Córcoles, J. I., & Domínguez, A. (2016). Evaluation of Aquacrop model for a potato crop under different irrigation conditions. *Agricultural Water Management*, *164*, 267–280. https://doi.org/10.1016/j.agwat.2015.10.019

Montoya, F., García, C., Pintos, F., & Otero, A. (2017). Effects of irrigation regime on the growth and yield of irrigated soybean in temperate humid climatic conditions. *Agricultural Water Management*, *193*, 30–45. https://doi.org/10.1016/j.agwat.2017.08.001

Moriasi, D. N., Arnold, J. G., Van Liew, M. W., Bingner, R. L., Harmel, R. D., & Veith, T. L. (2007). Model Evaluation Guidelines for Systematic Quantification of Accuracy in Watershed Simulations. *Transactions of the ASABE*, *50*(3), 885–900. https://doi.org/10.13031/2013.23153

Morillo, J. G., Martín, M., Camacho, E., Díaz, J. A. R., & Montesinos, P. (2015). Toward precision irrigation for intensive strawberry cultivation. *Agricultural Water Management*, *151*, 43–51. https://doi.org/10.1016/j.agwat.2014.09.021

Mualem, Y. (1976). A new model for predicting the hydraulic conductivity of unsaturated porous media. *Water Resources Research*, *12*(3), 513–522.

Mwendwa, S. (2022). Revisiting soil texture analysis: Practices towards a more accurate Bouyoucos method. *Heliyon*, *8*(5), e09395. https://doi.org/10.1016/j.heliyon.2022.e09395

Nand, V., & Qi, Z. (2023). Potential of implementing irrigation in rainfed agriculture in Quebec: A review of climate change-induced challenges and adaptation strategies. *Irrigation and Drainage*, *72*(4), 1165–1187. https://doi.org/10.1002/ird.2840

Nash, J. E., & Sutcliffe, J. V. (1970). River flow forecasting through conceptual models part I — A discussion of principles. *Journal of Hydrology*, *10*(3), 282–290. https://doi.org/10.1016/0022-1694(70)90255-6

Nasta, P., Vrugt, J. A., & Romano, N. (2013). Prediction of the saturated hydraulic conductivity from Brooks and Corey's water retention parameters. *Water Resources Research*, *49*(5), 2918–2925. https://doi.org/10.1002/wrcr.20269

National Aeronautics and Space Administration. (2022). *Prediction of Worldwide Energy Resource (POWER) Project funded through the NASA Earth Science Program* (2.0.10) [dataset].

Navrátilová, J., Hájek, M., Navrátil, J., Hájková, P., & Frazier, R. J. (2017). Convergence and impoverishment of fen communities in a eutrophicated agricultural landscape of the Czech Republic. *Applied Vegetation Science*, *20*(2), 225–235. Scopus. https://doi.org/10.1111/avsc.12298

Nguyen, H. H., Dargusch, P., Moss, P., & Aziz, A. A. (2017). Land-use change and socio-ecological drivers of wetland conversion in Ha Tien Plain, Mekong Delta, Vietnam. *Land Use Policy*, *64*, 101–113. https://doi.org/10.1016/j.landusepol.2017.02.019

Noborio, K. (2001). Measurement of soil water content and electrical conductivity by time domain reflectometry: A review. *Computers and Electronics in Agriculture*, *31*(3), 213–237. https://doi.org/10.1016/S0168-1699(00)00184-8

Nyathi, M. K., Mabhaudhi, T., Van Halsema, G. E., Annandale, J. G., & Struik, P. C. (2019). Benchmarking nutritional water productivity of twenty vegetables—A review. *Agricultural Water Management*, *221*, 248–259. https://doi.org/10.1016/j.agwat.2019.05.008

Ojo, E. R., Bullock, P. R., & Fitzmaurice, J. (2015). Field performance of five soil moisture instruments in heavy clay soils. *Soil Science Society of America Journal*, *79*(1), 20–29. https://doi.org/10.2136/sssaj2014.06.0250

Olden, J. (2008). Biotic Homogenization. In *Ecology* (Vol. 83). https://doi.org/10.1002/9780470015902.a0020471

Olesen, J. E., Børgesen, C. D., Elsgaard, L., Palosuo, T., Rötter, R. P., Skjelvåg, A. O., Peltonen-Sainio, P., Börjesson, T., Trnka, M., Ewert, F., Siebert, S., Brisson, N., Eitzinger, J., van Asselt, E. D., Oberforster, M., & van der Fels-Klerx, H. J. (2012). Changes in time of sowing, flowering and maturity of cereals in Europe under climate change. *Food Additives & Contaminants: Part A*, *29*(10), 1527–1542. https://doi.org/10.1080/19440049.2012.712060

OMAFRA. (2022). *Pumpkin and squash production | ontario.ca*. Ontario Ministry of Agriculture, Food and Rural Affairs. http://www.ontario.ca/page/pumpkin-and-squash-production

Ontario Federation of Agriculture (OFA). (2004). Irrigation Systems. In *Irrigation Systems – Best Management Practices* (2nd ed.). Ontario Federation of Agriculture. https://bmpbooks.com/publications/irrigation-management/irrigation-systems/

Opena, G. B., & Porter, G. A. (1999). Soil management and supplemental irrigation effects on potato: II. root growth. *Agronomy Journal*, *91*(3), 426–431. https://doi.org/10.2134/agronj1999.00021962009100030011x

Ouranos. (2015). *Vers l'adaptation. Synthèse des connaissances sur les changements climatiques au Québec*. https://www.ouranos.ca/sites/default/files/2022-12/proj-201419-synthese2015-rapportcomplet.pdf

Pan, T., Hou, S., Liu, Y., & Tan, Q. (2019). Comparison of three models fitting the soil water retention curves in a degraded alpine meadow region. *Scientific Reports*, *9*(1), Article 1. https://doi.org/10.1038/s41598-019-54449-8

Paquette, S., Poullaouec-Gonidec, P., & Domon, G. (2008). *Guide de gestion des paysages au Québec: Lire, comprendre et valoriser le paysage*. Culture, communications et condition féminine Québec.

Paredes, P., D'Agostino, D., Assif, M., Todorovic, M., & Pereira, L. S. (2018). Assessing potato transpiration, yield and water productivity under various water regimes and planting dates using the FAO dual Kc approach. *Agricultural Water Management*, *195*, 11–24. https://doi.org/10.1016/j.agwat.2017.09.011

Paredes, P., de Melo-Abreu, J. P., Alves, I., & Pereira, L. S. (2014). Assessing the performance of the FAO AquaCrop model to estimate maize yields and water use under full and deficit irrigation with focus on model parameterization. *Agricultural Water Management*, *144*, 81–97. https://doi.org/10.1016/j.agwat.2014.06.002

Parvin, N., & Degré, A. (2016). Soil-specific calibration of capacitance sensors considering clay content and bulk density. *Australian Journal of Soil Research*. https://doi.org/10.1071/SR15036

Pasquet, S., Pellerin, S., & Poulin, M. (2015). Three decades of vegetation changes in peatlands isolated in an agricultural landscape. *Applied Vegetation Science*, *18*(2), 220–229. Scopus. https://doi.org/10.1111/avsc.12142

Pavlista, A. D. (1995). EC95-1249 potato production stages: Scheduling key practices. *Historical Materials from University of Nebraska-Lincoln Extension*, 1584.

Pawar, G. S., Kale, M. U., & Lokhande, J. N. (2017). Response of AquaCrop Model to Different Irrigation Schedules for Irrigated Cabbage. *Agricultural Research*, *6*(1), 73–81. https://doi.org/10.1007/s40003-016-0238-2

Paz, J. O., Fraisse, C. W., Hatch, L. U., Garcia y Garcia, A., Guerra, L. C., Uryasev, O., Bellow, J. G., Jones, J. W., & Hoogenboom, G. (2007). Development of an ENSO-based irrigation decision support tool for peanut production in the southeastern US. *Computers and Electronics in Agriculture*, *55*(1), 28–35. https://doi.org/10.1016/j.compag.2006.11.003

Peacock, M., Gauci, V., Baird, A. J., Burden, A., Chapman, P. J., Cumming, A., Evans, J. G., Grayson, R. P., Holden, J., Kaduk, J., Morrison, R., Page, S., Pan, G., Ridley, L. M., Williamson, J., Worrall, F., & Evans, C. D. (2019). The full carbon balance of a rewetted cropland fen and a conservation-managed fen. *Agriculture, Ecosystems and Environment*, *269*, 1–12. Scopus. https://doi.org/10.1016/j.agee.2018.09.020

Pellerin, S., & Lavoie, C. (2003). reconstructing the recent dynamics of mires using a multitechnique approach. *Journal of Ecology*, *91*(6), 1008–1021.

Pellerin, S., Lavoie, M., Boucheny, A., Larocque, M., & Garneau, M. (2016). Recent vegetation dynamics and hydrological changes in bogs located in an agricultural landscape. *Wetlands*, *36*(1), 159–168. Scopus. https://doi.org/10.1007/s13157-015-0726-3

Pelletier, V., Gallichand, J., Caron, J., Jutras, S., & Marchand, S. (2015). Critical irrigation threshold and cranberry yield components. *Agricultural Water Management*, *148*, 106–112. https://doi.org/10.1016/j.agwat.2014.09.025

Pelletier, V., Gallichand, J., Gumiere, S., Pepin, S., & Caron, J. (2015). Water table control for increasing yield and saving water in cranberry production. *Sustainability*, *7*(8), Article 8. https://doi.org/10.3390/su70810602

Pelletier, V., Pepin, S., Gallichand, J., & Caron, J. (2016). Reducing cranberry heat stress and midday depression with evaporative cooling. *Scientia Horticulturae*, *198*, 445–453. https://doi.org/10.1016/j.scienta.2015.12.028

Pereira, L. S., & Allen, R. G. (1999). Chapter 5 Irrigation and drainage, part 5.1 crop water requirements. In *CIGR Handbook of Agricultural Engineering, Volume I Land and Water Engineering*. ASAE. https://doi.org/10.13031/2013.36302

Pereira, L. S., & Alves, I. (2005). Crop Water Requirements. In D. Hillel (Ed.), *Encyclopedia of Soils in the Environment* (pp. 322–334). Elsevier. https://doi.org/10.1016/B0-12-348530-4/00255-1

Pereira, L. S., Paredes, P., Hunsaker, D. J., López-Urrea, R., & Mohammadi Shad, Z. (2021). Standard single and basal crop coefficients for field crops. Updates and advances to the FAO56 crop water requirements method. *Agricultural Water Management*, *243*, 106466. https://doi.org/10.1016/j.agwat.2020.106466

Pinceloup, N., Poulin, M., Brice, M.-H., & Pellerin, S. (2020). Vegetation changes in temperate ombrotrophic peatlands over a 35 year period. *PLoS ONE*, *15*(2). Scopus. https://doi.org/10.1371/journal.pone.0229146

Post, W. M., Emanuel, W. R., Zinke, P. J., & Stangenberger, A. G. (1982). Soil carbon pools and world life zones. *Nature*, *298*(5870), 156–159. https://doi.org/10.1038/298156a0

Priestley, C. H. B., & Taylor, R. J. (1972). On the assessment of surface heat flux and evaporation using large-scale parameters. *Monthly Weather Review*, *100*(2), 81–92. https://doi.org/10.1175/1520-0493(1972)100<0081:OTAOSH>2.3.CO;2

Raes, D., Steduto, P., Hsiao, T. C., & Fereres, E. (2009). AquaCrop—The FAO crop model to simulate yield response to water: ii. main algorithms and software description. *Agronomy Journal*, *101*(3), 438–447. https://doi.org/10.2134/agronj2008.0140s

Rallo, G., Paço, T., Paredes, P., Puig-Sirera, À., Massai, R., Provenzano, G., & Pereira, L. (2021). Updated single and dual crop coefficients for tree and vine fruit crops. *Agricultural Water Management*, *250*, 106645.

Rawls, W. J., Pachepsky, Y., & Shen, M. H. (2001). Testing soil water retention estimation with the MUUF pedotransfer model using data from the southern United States. *Journal of Hydrology*, *251*(3), 177–185. https://doi.org/10.1016/S0022-1694(01)00467-X

Razzaghi, F., Zhou, Z., Andersen, M. N., & Plauborg, F. (2017). Simulation of potato yield in temperate condition by the AquaCrop model. *Agricultural Water Management*, *191*, 113–123. https://doi.org/10.1016/j.agwat.2017.06.008

Resop, J. P., Fleisher, D. H., Wang, Q., Timlin, D. J., & Reddy, V. R. (2012). Combining explanatory crop models with geospatial data for regional analyses of crop yield using field-scale modeling units. *Computers and Electronics in Agriculture*, *89*, 51–61. https://doi.org/10.1016/j.compag.2012.08.001

Richard, M., Jose, A., Mark, G., & Keith, M. (2002). Spring squash production in California. *Vegetable Research and Information Center, Vegetable Reproduction Series, California, Publication*, *7245*.

Robertson, D., Zhang, H., Palta, J. A., Colmer, T., & Turner, N. C. (2009). Waterlogging affects the growth, development of tillers, and yield of wheat through a severe, but transient, N deficiency. *Crop and Pasture Science*, *60*(6), 578–586. Scopus. https://doi.org/10.1071/CP08440

Robinson, D. A., Campbell, C. S., Hopmans, J. W., Hornbuckle, B. K., Jones, S. B., Knight, R., Ogden, F., Selker, J., & Wendroth, O. (2008). Soil moisture measurement for ecological and hydrological watershed-scale observatories: a review. *Vadose Zone Journal*, *7*(1), 358–389. https://doi.org/10.2136/vzj2007.0143

Robinson, M., & Dean, T. J. (1993). Measurement of near surface soil water content using a capacitance probe. *Hydrological Processes*, *7*(1), 77–86. https://doi.org/10.1002/hyp.3360070108

Rohini, K., & Singh, D. N. (2004). Methodology for determination of electrical properties of soils. *Journal of Testing and Evaluation*, *32*(1), 62–68. https://doi.org/10.1520/JTE11884

Rötter, R. P., Tao, F., Höhn, J. G., & Palosuo, T. (2015). Use of crop simulation modelling to aid ideotype design of future cereal cultivars. *Journal of Experimental Botany*, *66*(12), 3463–3476.

Rouge, C., Ge, Y., & Cai, X. (2013). Detecting gradual and abrupt changes in hydrological records. *Advances in Water Resources*, *53*, 33–44. https://doi.org/10.1016/j.advwatres.2012.09.008

Rowlandson, T. L., Berg, A. A., Bullock, P. R., Ojo, E. R., McNairn, H., Wiseman, G., & Cosh, M. H. (2013). Evaluation of several calibration procedures for a portable soil moisture sensor. *Journal of Hydrology*, *498*, 335–344. https://doi.org/10.1016/j.jhydrol.2013.05.021

Sadras, V. O., Lawson, C., Hooper, P., & McDonald, G. K. (2012). Contribution of summer rainfall and nitrogen to the yield and water use efficiency of wheat in Mediterranean-type environments of South Australia. *European Journal of Agronomy*, *36*(1), 41–54. https://doi.org/10.1016/j.eja.2011.09.001

Salman, M. (2021). *The AquaCrop model – Enhancing crop water productivity: Ten years of development, dissemination and implementation 2009–2019*. FAO. https://doi.org/10.4060/cb7392en

Sandhu, R., & Irmak, S. (2019). Performance of AquaCrop model in simulating maize growth, yield, and evapotranspiration under rainfed, limited and full irrigation. *Agricultural Water Management*, *223*, 105687. https://doi.org/10.1016/j.agwat.2019.105687

Sandler, H. A., & DeMoranville, C. J. (2008). *Cranberry Production Guide*.

Sandler, H. A., DeMoranville, C. J., & Lampinen, B. (2004). *Cranberry Irrigation Management*.

Satterfield, Z. (2010). Fundamentals of Hydraulics: Flow. In *Tech Brief—Fundamentals of Hydraulics* (1st ed., Vol. 10, p. 4). The National Environmental Services Center. https://wcwc.ca/wp-content/uploads/2021/01/NESC-Tech-Brief_Fundamentals-of-Hydraulics-Flow.pdf

Satti, S. R., Jacobs, J. M., & Irmak, S. (2004). Agricultural water management in a humid region: Sensitivity to climate, soil and crop parameters. *Agricultural Water Management*, *70*(1), 51–65. https://doi.org/10.1016/j.agwat.2004.05.004

Saxton, K. E., & Rawls, W. J. (2006). Soil water characteristic estimates by texture and organic matter for hydrologic solutions. *Soil Science Society of America Journal*, *70*(5), 1569–1578. https://doi.org/10.2136/sssaj2005.0117

Saxton, K. E., Rawls, W. J., Romberger, J. S., & Papendick, R. I. (1986). estimating generalized soil-water characteristics from texture. *Soil Science Society of America Journal*, *50*(4), 1031–1036. https://doi.org/10.2136/sssaj1986.03615995005000040039x

Schaap, M. G., Leij, F. J., & van Genuchten, M. Th. (2001). rosetta: A computer program for estimating soil hydraulic parameters with hierarchical pedotransfer functions. *Journal of Hydrology*, *251*(3), 163–176. https://doi.org/10.1016/S0022-1694(01)00466-8

Schewe, J., Heinke, J., Gerten, D., Haddeland, I., Arnell, N. W., Clark, D. B., Dankers, R., Eisner, S., Fekete, B. M., Colon-Gonzalez, F. J., Gosling, S. N., Kim, H., Liu, X., Masaki, Y., Portmann, F. T., Satoh, Y., Stacke, T., Tang, Q., Wada, Y., … Kabat, P. (2014). Multimodel assessment of water scarcity under climate change. *Proceedings of the National Academy of Sciences of the United States of America*, *111*(9), 3245–3250. https://doi.org/10.1073/pnas.1222460110

Selig, E. T., & Mansukhani, S. (1975). Relationship of soil moisture to the dielectric property. *Journal of the Geotechnical Engineering Division*, *101*(8), 755–770. https://doi.org/10.1061/AJGEB6.0000184

Sentelhas, P. C., Gillespie, T. J., & Santos, E. A. (2010). Evaluation of FAO Penman–Monteith and alternative methods for estimating reference evapotranspiration with missing data in Southern Ontario, Canada. *Agricultural Water Management*, *97*(5), 635–644. https://doi.org/10.1016/j.agwat.2009.12.001

Sharma, A., Deepa, R., Sankar, S., Pryor, M., Stewart, B., Johnson, E., & Anandhi, A. (2021). Use of growing degree indicator for developing adaptive responses: A case study of cotton in Florida. *Ecological Indicators*, *124*, 107383. https://doi.org/10.1016/j.ecolind.2021.107383

Sharma, V. (2019). *Basics of irrigation scheduling*. University of Minnesota Extension. https://extension.umn.edu/irrigation/basics-irrigation-scheduling

Shen, H., Tolson, B. A., & Mai, J. (2022). Time to Update the Split-Sample Approach in Hydrological Model Calibration. *Water Resources Research*, *58*(3), e2021WR031523. https://doi.org/10.1029/2021WR031523

Shiri, J., Marti, P., Karimi, S., & Landeras, G. (2019). Data splitting strategies for improving data driven models for reference evapotranspiration estimation among similar stations. *Computers and Electronics in Agriculture*, *162*, 70–81. https://doi.org/10.1016/j.compag.2019.03.030

Shock, C. C., Pereira, A. B., & Eldredge, E. P. (2007). Irrigation best management practices for potato. *American Journal of Potato Research*, *84*(1), 29–37. https://doi.org/10.1007/BF02986296

Shortt, R., Pate, E., & Handyside, P. (2022). Factsheet: Irrigation for frost protection of strawberries. *Ontario Ministry of Agriculture, Food and Rural Affairs*, *22*(043). http://www.ontario.ca/page/irrigation-frost-protection-strawberries

Sica, Y. V., Quintana, R. D., Radeloff, V. C., & Gavier-Pizarro, G. I. (2016). Wetland loss due to land use change in the Lower Paraná River Delta, Argentina. *Science of The Total Environment*, *568*, 967–978. https://doi.org/10.1016/j.scitotenv.2016.04.200

Singh, A. K., Tripathy, R., & Chopra, U. K. (2008). Evaluation of CERES-Wheat and CropSyst models for water–nitrogen interactions in wheat crop. *Agricultural Water Management*, *95*(7), 776–786. https://doi.org/10.1016/j.agwat.2008.02.006

Singh, G. (1969). A review of the soil-moisture relationship in potatoes. *American Potato Journal*, *46*, 398–403.

Soil Classification WorkingGroup. (1998). *The Canadian System of Soil Classification*. National Research Council of Canada.

Sommer, R., & Stöckle, C. (2010). Correspondence between the Campbell and van Genuchten Soil-Water-Retention Models. *Journal of Irrigation and Drainage Engineering*, *136*(8), 559–562. https://doi.org/10.1061/(ASCE)IR.1943-4774.0000204

Song, L., Chen, S., Yao, N., Feng, H., Zhang, T., & He, J. (2015). Parameter estimation and verification of CERES-maize model with GLUE and PEST methods. *Nongye Jixie Xuebao/Transactions of the Chinese Society for Agricultural Machinery*, *46*(11), 95–111. Scopus. https://doi.org/10.6041/j.issn.1000-1298.2015.11.015

Songara, J. C., & Patel, J. N. (2022). Calibration and comparison of various sensors for soil moisture measurement. *Measurement*, *197*, 111301. https://doi.org/10.1016/j.measurement.2022.111301

Souza, G., de Faria, B. T., Gomes Alves, R., Lima, F., Aquino, P. T., & Soininen, J.-P. (2020). Calibration equation and field test of a capacitive soil moisture sensor. *2020 IEEE International Workshop on Metrology for Agriculture and Forestry (MetroAgriFor)*, 180–184. https://doi.org/10.1109/MetroAgriFor50201.2020.9277634

Spinoni, J., Vogt, J., Naumann, G., Carrao, H., & Barbosa, P. (2015). Towards identifying areas at climatological risk of desertification using the Köppen–Geiger classification and FAO aridity index. *International Journal of Climatology*, *35*(9), 2210–2222. https://doi.org/10.1002/joc.4124

Sreedeep, S., Reshma, A. C., & Singh, D. N. (2004). Measuring Soil Electrical Resistivity Using a Resistivity Box and a Resistivity Probe. *Geotechnical Testing Journal*, *27*(4), 411–415. https://doi.org/10.1520/GTJ11199

Stark, J. C., Thornton, M., & Nolte, P. (2020). *Potato Production Systems*. Springer Nature.

Statistics Canada. (2017). *Quebec leads in dairy, maple, pigs, and fruits, berries and nuts* (p. 8). https://publications.gc.ca/collections/collection_2017/statcan/95-640-x/14804-eng.pdf

Statistics Canada. (2023). *Total area that received irrigation by crop type Table 38-10-0241-01*. https://www150.statcan.gc.ca/t1/tbl1/en/tv.action?pid=3810024101

Steduto, P., Hsiao, T. C., Raes, D., & Fereres, E. (2009). AquaCrop—The FAO crop model to simulate yield response to water: i. concepts and underlying principles. *Agronomy Journal*, *101*(3), 426–437. https://doi.org/10.2134/agronj2008.0139s

Steduto, P., Raes, D., Hsiao, T. C., Fereres, E., Heng, L. K., Howell, T. A., Evett, S. R., Rojas-Lara, B. A., Farahani, H. J., Izzi, G., Oweis, T. Y., Wani, S. P., Hoogeveen, J., & Geerts, S. (2009). Concepts and applications of aquacrop: the fao crop water productivity model. In W. Cao, J. W. White, & E. Wang (Eds.), *Crop Modeling and Decision Support* (pp. 175–191). Springer. https://doi.org/10.1007/978-3-642-01132-0_19

Stockle, C. O., Martin, S. A., & Campbell, G. S. (1994). CropSyst, a cropping systems simulation model: Water/nitrogen budgets and crop yield. *Agricultural Systems*, *46*(3), 335–359. https://doi.org/10.1016/0308-521X(94)90006-2

Stricevic, R., Cosic, M., Djurovic, N., Pejic, B., & Maksimovic, L. (2011). Assessment of the FAO AquaCrop model in the simulation of rainfed and supplementally irrigated maize, sugar beet and sunflower. *Agricultural Water Management*, *98*(10), 1615–1621. https://doi.org/10.1016/j.agwat.2011.05.011

Stricevic, R., Simic, A., Kusvuran, A., & Cosic, M. (2017). Assessment of AquaCrop model in the simulation of seed yield and biomass of Italian ryegrass. *Archives of Agronomy and Soil Science*, *63*(9), 1301–1313. https://doi.org/10.1080/03650340.2016.1275580

Surendran, U., Sushanth, C. M., Mammen, G., & Joseph, E. J. (2015). modelling the crop water requirement using fao-cropwat and assessment of water resources for sustainable water resource management: a case study in palakkad district of humid tropical kerala, india. *Aquatic Procedia*, *4*, 1211–1219. https://doi.org/10.1016/j.aqpro.2015.02.154

Susha Lekshmi, S. U., Singh, D. N., & Shojaei Baghini, M. (2014). A critical review of soil moisture measurement. *Measurement*, *54*, 92–105. https://doi.org/10.1016/j.measurement.2014.04.007

Tabari, H., Grismer, M. E., & Trajkovic, S. (2013). Comparative analysis of 31 reference evapotranspiration methods under humid conditions. *Irrigation Science*, *31*(2), 107–117. https://doi.org/10.1007/s00271-011-0295-z

Talbot, J., Roulet, N. T., Sonnentag, O., & Moore, T. R. (2014). Increases in aboveground biomass and leaf area 85 years after drainage in a bog. *Botany*, *92*(10), 713–721. https://doi.org/10.1139/cjb-2013-0319

Tao, F., & Zhang, Z. (2013). Climate change, wheat productivity and water use in the North China Plain: A new super-ensemble-based probabilistic projection. *Agricultural and Forest Meteorology*, *170*, 146–165. https://doi.org/10.1016/j.agrformet.2011.10.003

Tarboton, D. G. (2003). Rainfall-runoff processes. *Utah State University*, *1*(2).

Tatsumi, K. (2017). Integrated assessment of climate change impacts on corn yield in the u.s. using a crop model. *Transactions of the ASABE*, *60*(6), 2123–2136.

Taylor, R. G., Scanlon, B., Doell, P., Rodell, M., van Beek, R., Wada, Y., Longuevergne, L., Leblanc, M., Famiglietti, J. S., Edmunds, M., Konikow, L., Green, T. R., Chen, J., Taniguchi, M., Bierkens, M. F. P., MacDonald, A., Fan, Y., Maxwell, R. M., Yechieli, Y., … Treidel, H. (2013). Ground water and climate change. *Nature Climate Change*, *3*(4), 322–329. https://doi.org/10.1038/NCLIMATE1744

Tedeschi, A., Huang, C. H., Zong, L., You, Q. G., & Xue, X. (2014). Calibration equations for Diviner 2000 capacitance measurements of volumetric soil water content in salt-affected soils. *Soil Research*, *52*(4), 379–387. Scopus. https://doi.org/10.1071/SR13172

ten Brink, P., Russi, D., Farmer, A., Badura, T., Coates, D., Förster, J., Kumar, R., & Davidson, N. (2013). *The economics of ecosystems and biodiversity for water and wetlands. Executive summary.* https://www.teebweb.org/wp-content/uploads/2013/04/TEEB_WaterWetlands_ExecSum_2013.pdf

Terán-Chaves, C. A., García-Prats, A., & Polo-Murcia, S. M. (2022). Calibration and validation of the fao aquacrop water productivity model for perennial ryegrass (Lolium perenne L.). *Water*, *14*(23), Article 23. https://doi.org/10.3390/w14233933

Tian, H., Lu, C., Melillo, J., Ren, W., Huang, Y., Xu, X., Liu, M., Zhang, C., Chen, G., & Pan, S. (2012). Food benefit and climate warming potential of nitrogen fertilizer uses in China. *Environmental Research Letters*, *7*(4), 044020.

Tichoux, H. (1999). *Model comparison of three irrgation systems for potato production in Quebec*.

Tolomio, M., & Casa, R. (2020). Dynamic crop models and remote sensing irrigation decision support systems: a review of water stress concepts for improved estimation of water requirements. *Remote Sensing*, *12*(23), Article 23. https://doi.org/10.3390/rs12233945

Topp, G. c., Zegelin, S., & White, I. (2000). Impacts of the real and imaginary components of relative permittivity on time domain reflectometry measurements in soils. *Soil Science Society of America Journal*, *64*(4), 1244–1252. https://doi.org/10.2136/sssaj2000.6441244x

Tousignant, M. Ê., Pellerin, S., & Brisson, J. (2010). The relative impact of human disturbances on the vegetation of a large wetland complex. *Wetlands*, *30*(2), 333–344.

Tsakmakis, I. D., Kokkos, N. P., Gikas, G. D., Pisinaras, V., Hatzigiannakis, E., Arampatzis, G., & Sylaios, G. K. (2019). Evaluation of AquaCrop model simulations of cotton growth under deficit irrigation with an emphasis on root growth and water extraction patterns. *Agricultural Water Management*, *213*, 419–432. https://doi.org/10.1016/j.agwat.2018.10.029

Tubiello, F. N., & Ewert, F. (2002). Simulating the effects of elevated CO2 on crops: Approaches and applications for climate change. *European Journal of Agronomy*, *18*(1), 57–74. https://doi.org/10.1016/S1161-0301(02)00097-7

Tubiello, F. N., Soussana, J.-F., & Howden, S. M. (2007). Crop and pasture response to climate change. *Proceedings of the National Academy of Sciences of the United States of America*, *104*(50), 19686–19690. https://doi.org/10.1073/pnas.0701728104

Turral, H., Burke, J., & Faurès, J.-M. (2011). *Climate change, water and food security*. Food and Agriculture Organization of the United Nations.

United States Department of Agriculture. (2005). New Jersey Irrigation Guide. In *NRCS National Engineering Handbook, Part 652 Irrigation Guide*. USDA. https://www.nrcs.usda.gov/sites/default/files/2022-09/NRCS_NJ_Irrigation_Guide_May_2020_0.pdf

United States Department of Agriculture. (2021). Part 634 Hydraulics—Chapter 4 Pipe Flow. In *National Engineering Handbook* (1st ed.). United States Department of Agriculture.

Vaasma, T. (2008). Grain-size analysis of lacustrine sediments: A comparison of pre-treatment methods. *Estonian Journal of Ecology*, *57*(4), 231. https://doi.org/10.3176/eco.2008.4.01

van Genuchten, M. Th. (1980). A closed-form equation for predicting the hydraulic conductivity of unsaturated soils. *Soil Science Society of America Journal*, *44*(5), 892–898. https://doi.org/10.2136/sssaj1980.03615995004400050002x

van Ittersum, M. K., & Cassman, K. G. (2013). Yield gap analysis—Rationale, methods and applications—Introduction to the Special Issue. *Field Crops Research*, *143*, 1–3. https://doi.org/10.1016/j.fcr.2012.12.012

Van Looy, K., Bouma, J., Herbst, M., Koestel, J., Minasny, B., Mishra, U., Montzka, C., Nemes, A., Pachepsky, Y. A., Padarian, J., Schaap, M. G., Tóth, B., Verhoef, A., Vanderborght, J., van der Ploeg, M. J., Weihermüller, L., Zacharias, S., Zhang, Y., & Vereecken, H. (2017). Pedotransfer functions in earth system science: challenges and perspectives. *Reviews of Geophysics*, *55*(4), 1199–1256. https://doi.org/10.1002/2017RG000581

Vanderleest, C. P. L., & Bland, W. L. (2017). Evapotranspiration from cranberry compared with the equilibrium rate. *Canadian Journal of Soil Science*, *97*(1), 5–10. https://doi.org/10.1139/cjss-2015-0093

Vanderleest, C. P. L., Caron, J., & Bland, W. L. (2017). Water table level management as an irrigation strategy for cranberry (Vaccinium macrocarpon Aiton). *Canadian Journal of Soil Science*, *97*(1), 11–19. https://doi.org/10.1139/cjss-2016-0001

Vanuytrecht, E., Raes, D., Steduto, P., Hsiao, T. C., Fereres, E., Heng, L. K., Garcia Vila, M., & Mejias Moreno, P. (2014). AquaCrop: FAO's crop water productivity and yield response model. *Environmental Modelling & Software*, *62*, 351–360. https://doi.org/10.1016/j.envsoft.2014.08.005

Verhoeven, J. T. A., Beltman, B., Bobbink, R., & Whigham, D. F. (2006). *Wetlands and Natural Resource Management*. Springer Science & Business Media.

Vincent, L. A., Zhang, X., Mekis, É., Wan, H., & Bush, E. J. (2018). Changes in Canada's climate: trends in indices based on daily temperature and precipitation data. *Atmosphere-Ocean*, *56*(5), 332–349. https://doi.org/10.1080/07055900.2018.1514579

Wada, Y., Van Beek, L. P., Wanders, N., & Bierkens, M. F. (2013). Human water consumption intensifies hydrological drought worldwide. *Environmental Research Letters*, *8*(3), 034036.

Wadoux, A. M. J.-C., Odeh, I. O. A., & McBratney, A. B. (2023). Overview of pedometrics. In M. J. Goss & M. Oliver (Eds.), *Encyclopedia of Soils in the Environment (Second Edition)* (pp. 471–485). Academic Press. https://doi.org/10.1016/B978-0-12-822974-3.00001-X

Wale, A., Dessie, M., & Kendie, H. (2022). Evaluating the performance of AquaCrop model for potato production under deficit irrigation. *Air, Soil and Water Research*, *15*, 11786221221108216. https://doi.org/10.1177/11786221221108216

Wang, E., Cresswell, H., Xu, J., & Jiang, Q. (2009). Capacity of soils to buffer impact of climate variability and value of seasonal forecasts. *Agricultural and Forest Meteorology*, *149*(1), 38–50. https://doi.org/10.1016/j.agrformet.2008.07.001

Wang, H., Cheng, M., Liao, Z., Guo, J., Zhang, F., Fan, J., Feng, H., Yang, Q., Wu, L., & Wang, X. (2023). Performance evaluation of AquaCrop and DSSAT-SUBSTOR-Potato models in simulating potato growth, yield and water productivity under various drip fertigation regimes. *Agricultural Water Management*, *276*, 108076. https://doi.org/10.1016/j.agwat.2022.108076

Wang, J., Wang, E., Feng, L., Yin, H., & Yu, W. (2013). Phenological trends of winter wheat in response to varietal and temperature changes in the North China Plain. *Field Crops Research*, *144*, 135–144. Scopus. https://doi.org/10.1016/j.fcr.2012.12.020

Wanniarachchi, S., & Sarukkalige, R. (2022). A review on evapotranspiration estimation in agricultural water management: past, present, and future. *Hydrology*, *9*(7), Article 7. https://doi.org/10.3390/hydrology9070123

Weigel, A. P., Knutti, R., Liniger, M. A., & Appenzeller, C. (2010). Risks of model weighting in multimodel climate projections. *Journal of Climate*, *23*(15), 4175–4191. https://doi.org/10.1175/2010JCLI3594.1

Wellens, J., Raes, D., Fereres, E., Diels, J., Coppye, C., Adiele, J. G., Ezui, K. S. G., Becerra, L.-A., Selvaraj, M. G., Dercon, G., & Heng, L. K. (2022). Calibration and validation of the FAO AquaCrop water productivity model for cassava (Manihot esculenta Crantz). *Agricultural Water Management*, *263*, 107491. https://doi.org/10.1016/j.agwat.2022.107491

Wesseling, J. G., & Feddes, R. A. (2006). Assessing crop water productivity from field to regional scale. *Agricultural Water Management*, *86*(1), 30–39. https://doi.org/10.1016/j.agwat.2006.06.011

Whalley, W. R., Dean, T. J., & Izzard, P. (1992). Evaluation of the capacitance technique as a method for dynamically measuring soil water content. *Journal of Agricultural Engineering Research*, *52*, 147–155. https://doi.org/10.1016/0021-8634(92)80056-X

Wilby, R. L., Charles, S. P., Zorita, E., Timbal, B., Whetton, P., & Mearns, L. O. (2004). Guidelines for use of climate scenarios developed from statistical downscaling methods. *Supporting Material of the Intergovernmental Panel on Climate Change, Available from the DDC of IPCC TGCIA*, *27*.

Williams, J. R., Jones, C. A., Kiniry, J. R., & Spanel, D. A. (1989). EPIC crop growth model. *Transactions of the American Society of Agricultural Engineers*, *32*(2), 497–511. Scopus.

Willmott, C. J. (1982). Some comments on the evaluation of model performance. *Bulletin of the American Meteorological Society*, *63*(11), 1309–1313. https://doi.org/10.1175/1520-0477(1982)063<1309:SCOTEO>2.0.CO;2

Wood, A. P., & Halsema, G. E. van (Eds.). (2008). *Scoping agriculture, wetland interactions: towards a sustainable multiple-response strategy*. Food and Agriculture Organization of the United Nations.

Workmaster, B. A. A., & Palta, J. P. (2006). Shifts in bud and leaf hardiness during spring growth and development of the cranberry upright: regrowth potential as an indicator of hardiness. *Journal of the American Society for Horticultural Science*, *131*(3), 327–337. https://doi.org/10.21273/JASHS.131.3.327

Wu, L., & Fan, J. (2019). Comparison of neuron-based, kernel-based, tree-based and curve-based machine learning models for predicting daily reference evapotranspiration. *PLOS ONE*, *14*(5), e0217520. https://doi.org/10.1371/journal.pone.0217520

Xiao, D., Liu, D. L., Wang, B., Feng, P., Bai, H., & Tang, J. (2020). Climate change impact on yields and water use of wheat and maize in the North China Plain under future climate change scenarios. *Agricultural Water Management*, *238*, 106238. https://doi.org/10.1016/j.agwat.2020.106238

Xu, J., Morris, P. J., Liu, J., & Holden, J. (2018). PEATMAP: Refining estimates of global peatland distribution based on a meta-analysis. *CATENA*, *160*, 134–140. https://doi.org/10.1016/j.catena.2017.09.010

Yagouti, A., Boulet, G., Vincent, L., Vescovi, L., & Mekis, É. (2008). Observed changes in daily temperature and precipitation indices for southern Québec, 1960–2005. *Atmosphere-Ocean*, *46*(2), 243–256. https://doi.org/10.3137/ao.460204

Yan, S., Wu, L., Fan, J., Zhang, F., Zou, Y., & Wu, Y. (2021). A novel hybrid WOA-XGB model for estimating daily reference evapotranspiration using local and external meteorological data: Applications in arid and humid regions of China. *Agricultural Water Management*, *244*, 106594. https://doi.org/10.1016/j.agwat.2020.106594

Yang, G., Guo, P., Huo, L., & Ren, C. (2015). Optimization of the irrigation water resources for Shijin irrigation district in north China. *Agricultural Water Management*, *158*, 82–98. https://doi.org/10.1016/j.agwat.2015.04.006

Yang, J. M., Yang, J. Y., Liu, S., & Hoogenboom, G. (2014). An evaluation of the statistical methods for testing the performance of crop models with observed data. *Agricultural Systems*, *127*, 81–89. https://doi.org/10.1016/j.agsy.2014.01.008

Yavuz, D., Yavuz, N., Seymen, M., & Türkmen, O. (2015). Evapotranspiration, crop coefficient and seed yield of drip irrigated pumpkin under semi-arid conditions. *Scientia Horticulturae*, *197*, 33–40. Scopus. https://doi.org/10.1016/j.scienta.2015.11.010

Yost, J. L., Huang, J., & Hartemink, A. E. (2019). Spatial-temporal analysis of soil water storage and deep drainage under irrigated potatoes in the Central Sands of Wisconsin, USA. *Agricultural Water Management*, *217*, 226–235. https://doi.org/10.1016/j.agwat.2019.02.045

Yu, Z. C. (2012). Northern peatland carbon stocks and dynamics: A review. *Biogeosciences*, *9*(10), 4071–4085. https://doi.org/10.5194/bg-9-4071-2012

Yudina, A. V., Fomin, D. S., Kotelnikova, A. D., & Milanovskii, E. Yu. (2018). From the notion of elementary soil particle to the particle-size and microaggregate-size distribution analyses: a review. *Eurasian Soil Science*, *51*(11), 1326–1347. https://doi.org/10.1134/S1064229318110091

Zazueta, F. S., & Xin, J. (1994). Soil moisture sensors. *Soil Science*, *73*, 391–401.

Zedler, J. B., & Kercher, S. (2005). WETLAND RESOURCES: Status, Trends, Ecosystem Services, and Restorability. *Annual Review of Environment and Resources*, *30*(1), 39–74. https://doi.org/10.1146/annurev.energy.30.050504.144248

Zhai, Z., Martínez, J. F., Beltran, V., & Martínez, N. L. (2020). Decision support systems for agriculture 4.0: Survey and challenges. *Computers and Electronics in Agriculture*, *170*, 105256. https://doi.org/10.1016/j.compag.2020.105256

Zhang, B., Feng, G., Ahuja, L. R., Kong, X., Ouyang, Y., Adeli, A., & Jenkins, J. N. (2018). Soybean crop-water production functions in a humid region across years and soils determined with APEX model. *Agricultural Water Management*, *204*, 180–191. https://doi.org/10.1016/j.agwat.2018.03.024

Zhang, L., Cheng, L., Chiew, F., & Fu, B. (2018). Understanding the impacts of climate and landuse change on water yield. *Current Opinion in Environmental Sustainability*, *33*, 167–174. https://doi.org/10.1016/j.cosust.2018.04.017

Zhang, X., & Cai, X. (2013). Climate change impacts on global agricultural water deficit. *Geophysical Research Letters*, *40*(6), 1111–1117. https://doi.org/10.1002/grl.50279

Zhao, C., Stockle, C. O., Karimi, T., Nelson, R. L., Evert, F. K. van, Pronk, A. A., Riddle, A. A., Marshall, E., Raymundo, R., Li, Y., Guan, K., Gustafson, D., Hoogenboom, G., Wang, X., Cong, J., & Asseng, S. (2022). Potential benefits of climate change for potatoes in the United States. *Environmental Research Letters*, *17*(10), 104034. https://doi.org/10.1088/1748-9326/ac9242

Zhao, G., Siebert, S., Enders, A., Rezaei, E. E., Yan, C., & Ewert, F. (2015). Demand for multi-scale weather data for regional crop modeling. *Agricultural and Forest Meteorology*, *200*, 156–171. https://doi.org/10.1016/j.agrformet.2014.09.026

Zhao, T., Wang, Q. J., Schepen, A., & Griffiths, M. (2019). Ensemble forecasting of monthly and seasonal reference crop evapotranspiration based on global climate model outputs. *Agricultural and Forest Meteorology*, *264*, 114–124. https://doi.org/10.1016/j.agrformet.2018.10.001

Zhao, Z. L., Li, B., Feng, X., Yao, M. Z., Xie, Y., Xing, J. W., & Li, C. X. (2018). [Parameter estimation and verification of DSSAT-CROPGRO-Tomato model under different irrigation levels in greenhouse. *Ying yong sheng tai xue bao = The journal of applied ecology*, *29*(6), 2017–2027. https://doi.org/10.13287/j.1001-9332.201806.012

Zhou, G., & Wang, Y. (2000). Global change and climate-vegetation classification. *Chinese Science Bulletin*, *45*(7), 577–585. https://doi.org/10.1007/BF02886031

Zou, Y., Duan, X., Xue, Z., E, M., Sun, M., Lu, X., Jiang, M., & Yu, X. (2018). Water use conflict between wetland and agriculture. *Journal of Environmental Management*, *224*, 140–146. https://doi.org/10.1016/j.jenvman.2018.07.052

APPENDIX

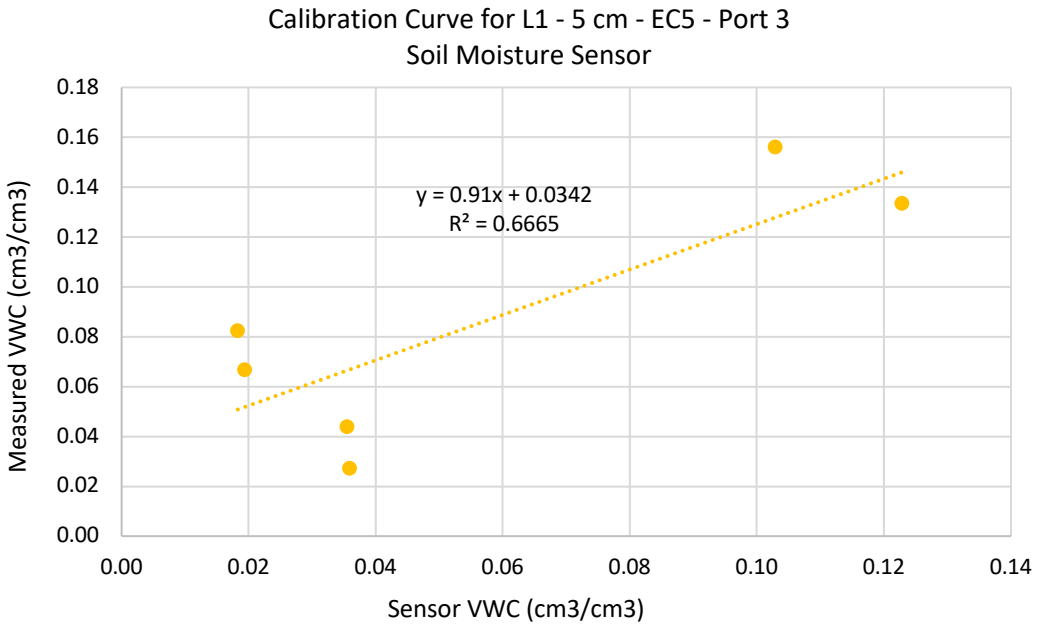

Figure A1. Calibration curve for EC5 sensor placed at a depth of 5 cm at L1.

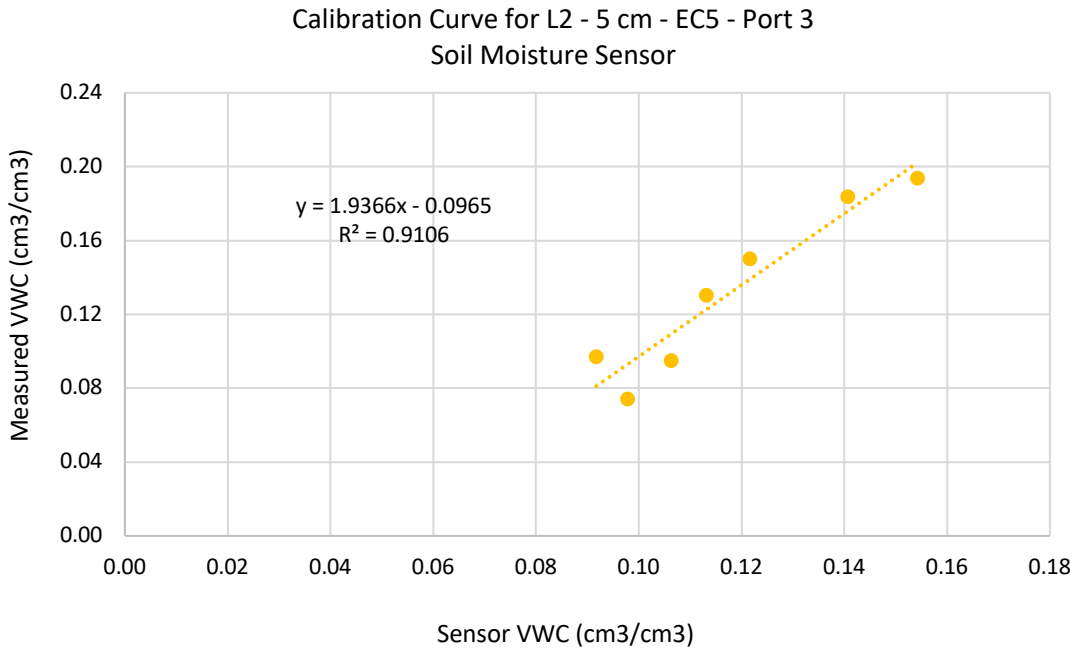

Figure A2. Calibration curve for EC5 sensor placed at a depth of 5 cm at L2.

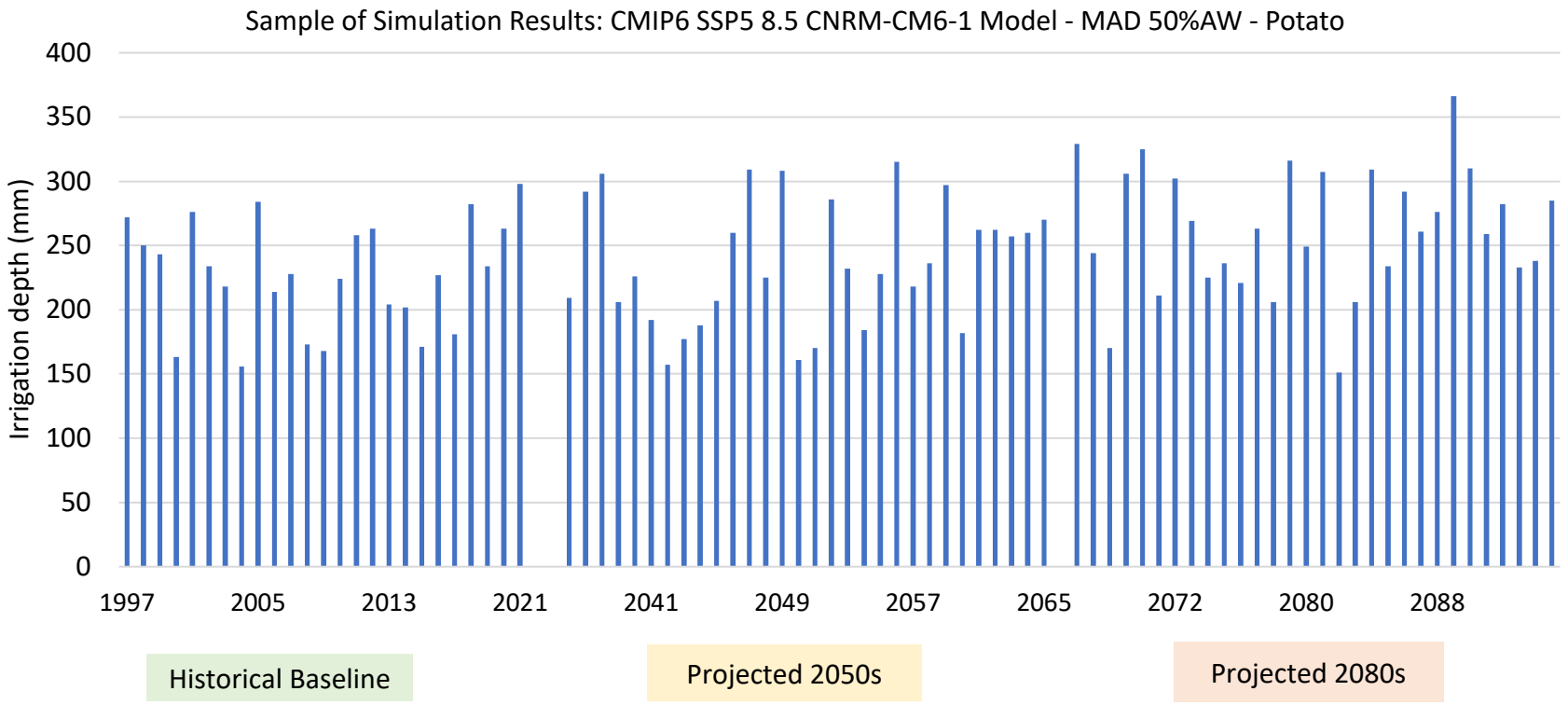

Figure A3. Simulated net irrigation requirements of CNRM-CM6-1 model of the ensemble for potato under MAD set at 50% AW under SSP5-8.5.